

**ACTIVATION ENERGY OF DOUGLAS FIR CHAR  
GASIFICATION BY CARBON DIOXIDE**

by

Eric V. B. Albright

Thesis submitted to the Faculty of the  
Virginia Polytechnic Institute and State University  
in partial fulfillment of the requirements for the degree of  
Master of Science  
in  
Mechanical Engineering

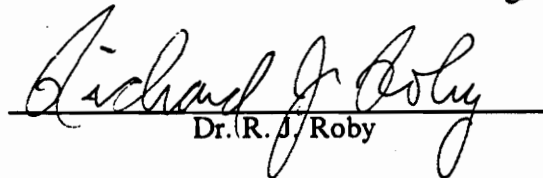
APPROVED:



Dr. C. H. Stern, Co-chairman



Dr. D. R. Jaasma, Co-chairman



Dr. R. J. Roby

June 29, 1992

Blacksburg, Virginia

C.2

LD  
5655  
V855  
1992  
A427  
C.2

**ACTIVATION ENERGY OF DOUGLAS FIR CHAR  
GASIFICATION BY CARBON DIOXIDE**

by

Eric V. B. Albright

Dr. C. H. Stern, Co-chairman

Dr. D. R. Jaasma, Co-chairman

Mechanical Engineering

(ABSTRACT)

The activation energy of Douglas fir wood char gasified in carbon dioxide was determined. Activation energies were found for chars that had been pyrolyzed in nitrogen at 600, 750, and 900°C. A thermogravimetric analyzer provided the weight versus temperature data used to obtain the activation energies. The Coats-Redfern integral method of kinetic analysis was used to extract the activation energies from the data. This method can be used to obtain an activation energy from a single weight versus temperature trace for a constant heating rate. An overall apparent activation energy of  $723 \pm 60$  kJ/mole and a natural log of the preexponential factor of  $68.8 \pm 6.2$  was determined from the data collected for all three chars. The different char preparation temperatures did not appear to affect the activation energy.

# Acknowledgements

First, I would like to thank my parents for their support and patience over the last few years. I would also like to thank Dr. Curtis H. Stern, Dr. Dennis R. Jaasma, and Dr. Richard J. Roby for all the advice, guidance, and support they have provided throughout this project. From the Chemical Engineering Department I would especially like to thank David Rodriguez and all the people in Dr. Wilkes' lab who helped me with the TGA. I would like to thank Ron Dodd from the Center for Advanced Ceramic Materials in the Materials Engineering Department for all his help with the tube furnace and Dr. Hirschfeld for letting me use it. I would like to thank Jeff Stastny from the Center for Intelligent Materials Systems and Structures in the Mechanical Engineering Department for his help in producing the figures in this thesis. For his help with almost anything, I would like to thank Mark Champion of the combustion lab in the Mechanical Engineering Department. Finally, I would like to thank all the other graduate students, technicians, and professors too numerous to mention who helped in some way with this project.

# Table of Contents

<b>1.0 Introduction</b>	<b>1</b>
1.1 Wood as Fuel	1
1.2 Gasification	4
1.3 Present Study	6
<b>2.0 Literature Review</b>	<b>8</b>
2.1 The Boudouard Reaction	8
2.2 Analysis of Thermogravimetric Data	13
2.2.1 Coats-Redfern Method	13
2.2.2 Limitations of Kinetic Parameters Obtained from TGA Curves	16
<b>3.0 Materials and Methods</b>	<b>18</b>
3.1 Experimental Apparatus	18
3.2 Experimental Procedure	23
<b>4.0 Results and Discussion</b>	<b>25</b>
4.1 Thermogravimetric Results and Analysis	25

4.1.1 Pyrolysis of Douglas Fir. ....	25
4.1.2 Gasification of Douglas Fir Char ....	27
4.2 Apparent Activation Energies ....	32
4.2.1 Kinetic Analysis ....	32
4.2.2 Uncertainty in the Apparent Activation Energies ....	37
<b>5.0 Conclusions</b> ....	<b>40</b>
<b>References</b> ....	<b>43</b>
<b>Appendix A. Thermogravimetric Plots</b> ....	<b>46</b>
<b>Appendix B. Coats-Redfern Kinetic Plots</b> ....	<b>65</b>
<b>Appendix C. Numerical Data</b> ....	<b>83</b>
<b>Appendix D. Effect of Reaction Order on Kinetic Parameters</b> ....	<b>89</b>
<b>Appendix E. Verification of TGA</b> ....	<b>93</b>
<b>Appendix F. Approximate Kinetic Analysis</b> ....	<b>96</b>
<b>Vita</b> ....	<b>99</b>

## List of Illustrations

Figure 1. Updraft gasifier processes and temperatures .....	5
Figure 2. Modified double-film theory .....	10
Figure 3. Top view of TGA .....	19
Figure 4. Thermogravimetric plot of Run 23 .....	26
Figure 5. Gasification of Douglas fir HTT 600°C char .....	28
Figure 6. Gasification of Douglas fir HTT 750°C char .....	29
Figure 7. Gasification of Douglas fir HTT 900°C char .....	30
Figure 8. Coats-Redfern kinetic plot of Run 23 .....	34
Figure 9. Activation energies for three chars. ....	36
Figure 10. Thermogravimetric plot of Run 9 .....	47
Figure 11. Thermogravimetric plot of Run 10 .....	48
Figure 12. Thermogravimetric plot of Run 11 .....	49
Figure 13. Thermogravimetric plot of Run 13 .....	50
Figure 14. Thermogravimetric plot of Run 15 .....	51
Figure 15. Thermogravimetric plot of Run 16 .....	52
Figure 16. Thermogravimetric plot of Run 17 .....	53
Figure 17. Thermogravimetric plot of Run 18 .....	54
Figure 18. Thermogravimetric plot of Run 19 .....	55
Figure 19. Thermogravimetric plot of Run 20 .....	56
Figure 20. Thermogravimetric plot of Run 21 .....	57
Figure 21. Thermogravimetric plot of Run 22 .....	58

Figure 22. Thermogravimetric plot of Run 23 .....	59
Figure 23. Thermogravimetric plot of Run 24 .....	60
Figure 24. Thermogravimetric plot of Run A1 .....	61
Figure 25. Thermogravimetric plot of Run A2 .....	62
Figure 26. Thermogravimetric plot of Run A3 .....	63
Figure 27. Thermogravimetric plot of Run A4 .....	64
Figure 28. Coats-Redfern kinetic plot of Run 9 .....	66
Figure 29. Coats-Redfern kinetic plot of Run 10 .....	67
Figure 30. Coats-Redfern kinetic plot of Run 11 .....	68
Figure 31. Coats-Redfern kinetic plot of Run 13 .....	69
Figure 32. Coats-Redfern kinetic plot of Run 15 .....	70
Figure 33. Coats-Redfern kinetic plot of Run 16 .....	71
Figure 34. Coats-Redfern kinetic plot of Run 17 .....	72
Figure 35. Coats-Redfern kinetic plot of Run 18 .....	73
Figure 36. Coats-Redfern kinetic plot of Run 19 .....	74
Figure 37. Coats-Redfern kinetic plot of Run 20 .....	75
Figure 38. Coats-Redfern kinetic plot of Run 21 .....	76
Figure 39. Coats-Redfern kinetic plot of Run 22 .....	77
Figure 40. Coats-Redfern kinetic plot of Run 24 .....	78
Figure 41. Coats-Redfern kinetic plot of Run A1 .....	79
Figure 42. Coats-Redfern kinetic plot of Run A2 .....	80
Figure 43. Coats-Redfern kinetic plot of Run A3 .....	81
Figure 44. Coats-Redfern kinetic plot of Run A4 .....	82
Figure 45. Coats-Redfern plot of Run 23 (reaction order of 2/3) .....	91
Figure 46. Coats-Redfern plot of Run 23 (reaction order of 1/2) .....	92
Figure 47. Pyrolysis of Monterey pine .....	94
Figure 48. Pyrolysis of Monterey pine .....	95

# List of Tables

Table 1. Ultimate analysis data for coals and Douglas fir (Reed, 1981). . . . .	3
Table 2. Ultimate analysis of sample chars. . . . .	22
Table 3. Effect of Reaction Order on Kinetic Parameters. . . . .	90
Table 4. Comparison of Apparent Activation Energies from Approximate and C-R Analysis Methods. . . . .	98

# 1.0 Introduction

## *1.1 Wood as Fuel*

Wood as an alternative energy source has become an increasingly popular concept in recent years. Wood is used by many homeowners for home heating, and the wood products industry has long used production residues for power and process steam. Wood and other biomass resources such as agricultural and wood industry residues and solid organic municipal waste ("garbage" without metal or glass) have become attractive principally due to their renewability and low cost. This interest has increased because traditional energy sources - coal, oil, and natural gas - have all begun to show their shortcomings in recent years.

Coal and oil both currently present large scale environmental concerns as air pollution becomes more of a problem in large cities as well as on a global scale. In recent decades, dependence on oil has been demonstrated to be a political liability. Natural gas, the most environmentally attractive of the three, is currently abundant, but will inevitably experience availability problems similar to those of oil. It is becoming apparent that these economic, political, and environmental concerns

will require industry and government to develop a diversified energy portfolio, which will probably include wood and biomass resources.

That wood is renewable is obvious, since trees can be grown as long as there is land, water, and sunlight available. Coal, natural gas, and oil are not renewable resources, since when they are collected and used they are gone forever. Wood, if the growth and collection of trees is managed properly, can become a lasting energy resource. To accomplish this, schemes for more intensive forestry are being developed. Limiting this potential is the availability of land. Every year more forest land is being lost as the population and size of urban areas increase. Also, other demands on wood, especially the need for furniture and building products, will increase greatly as the population increases (Tillman, 1978). Balancing these demands will present a challenge in the future as the population grows and wood is developed as an energy source.

Wood's potential for being a low emission energy source has been well documented. Table 1 presents ultimate analysis data for several coals and Douglas fir wood and bark (Reed, 1981). Though the wood has a lower heating value than coal, it has markedly lower amounts of nitrogen, sulfur, and ash, which would result in lower NO<sub>x</sub>, SO<sub>x</sub>, and particulate emissions than coal if properly burned (Tillman et al., 1981). In solid form, however, biomass fuels are difficult and expensive to transport, store, and burn cleanly on an industrial scale. In order to make the energy accessible and cost-effective, a gasification process is used to convert solid fuel to gaseous or liquid fuels. In gaseous or liquid form fuel can be easily piped or stored and, when burned, the flame can be controlled for reduced emissions.

Despite their merits, biomass fuels have not been industrially important in the recent past. Consequently, investigations into the thermochemical behavior of these fuels have focused on fire safety rather than energy production. In the late 19th and early 20th centuries local "gasworks" pyrolyzed biomass and coal to produce manufactured gases, but the installation of large natural gas pipelines in the 1930's led to the closing of nearly all of these regional gas producers (Reed, 1981). These extensive natural gas pipelines are supplied by underground deposits often found on top of or near

**Table 1. Ultimate analysis data for coals and Douglas fir (Reed, 1981).**

<b>Material</b>	<b>C (%)</b>	<b>H (%)</b>	<b>N (%)</b>	<b>S (%)</b>	<b>O (%)</b>	<b>Ash (%)</b>	<b>Higher Heating Value (Btu/lb)</b>
Pittsburgh seam coal	75.5	5.0	1.2	3.1	4.9	10.3	13,650
West Kentucky No. 11 coal	74.4	5.1	1.5	3.8	7.9	7.3	13,460
Utah coal	77.9	6.0	1.5	0.6	9.9	4.1	14,170
Wyoming Elkol coal	71.5	5.3	1.2	0.9	16.9	4.2	12,710
Douglas fir	52.3	6.3	0.1	0.0	40.5	0.8	9,050
Douglas fir bark	56.2	5.9	0.0	0.0	36.7	1.2	9,500

oil deposits. Converting this system to deliver another gas would be expensive because the fixtures are designed specifically for use with natural gas. Still, interest in using wood to produce fuels is increasing, and the small volume of thermochemical biomass knowledge (when compared to the extensive database of information on coal and oil) must be expanded for wood to be developed as a viable energy resource. This thesis addresses one phenomenon which occurs during wood gasification.

## *1.2 Gasification*

The gasification of wood or other biomass can produce various "manufactured" gases which contain varying amounts of hydrogen, carbon monoxide, carbon dioxide, methane, heavier hydrocarbons, and usually nitrogen (Antal, 1979). In the gasification process, wood is dried and then pyrolyzed, which releases gases and tars, leaving a carbonaceous residue called char (Sekiguchi et al., 1983). This char is gasified by several heterogeneous reactions involving carbon dioxide, steam, and hydrogen to produce synthesis gas (carbon monoxide and hydrogen) which is collected for use as fuel or further processing to produce other fuels. The gasification process is divided into four zones as shown in Figure 1: drying, pyrolysis, reduction, and oxidation (Reed, 1981). An updraft gasifier is shown in Figure 1.

In the lowest zone, char is oxidized by introduced oxygen or air with (or without) steam which produces heat for processes above it. The next zone up is the reduction zone where char is gasified by the  $\text{CO}_2$  and steam produced (water is generally introduced with the air blast) in the oxidation zone below. The high temperature of the reduction zone favors the highly endothermic Boudouard ( $\text{C} + \text{CO}_2 \rightleftharpoons 2\text{CO}$ ) and water-gas ( $\text{C} + \text{H}_2\text{O} \rightleftharpoons \text{CO} + \text{H}_2$ ) reactions that produce CO and  $\text{H}_2$  gases which rise into the upper zones. In the pyrolysis zone, the rising hot gases come in contact with the solid feedstock of processed wood or biomass and produce char, tars, CO,  $\text{CO}_2$ ,  $\text{H}_2$ ,

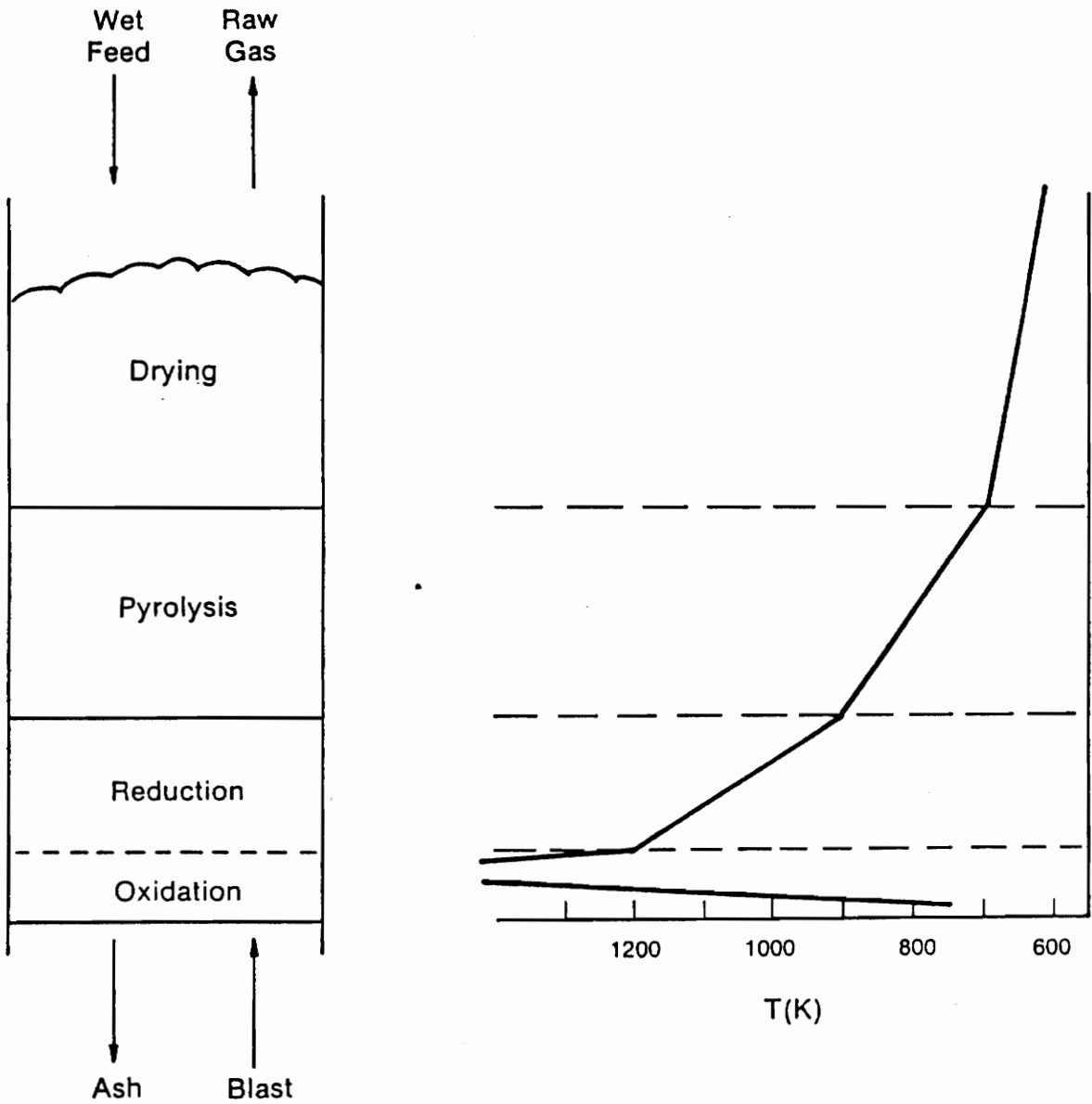


**Figure 1. Updraft gasifier processes and temperatures:** (Reed, 1981).

H<sub>2</sub>O, and CH<sub>4</sub>. This feedstock is introduced to the gasifier in the drying zone, where the material is heated and dried by the rising heat from the pyrolysis zone below.

### *1.3 Present Study*

This thesis deals with one of the reactions in a gasifier's reduction zone, namely the gasification of char with carbon dioxide. The thermochemical behavior of wood char in this zone is of interest because it is a rate-limiting step in the overall gasification process and 30-40% of the wood's original chemical energy remains after pyrolysis (DeGroot et al., 1988). This reaction is also of concern in the study of any high temperature wood burning application such as wood stoves or boilers where carbon dioxide reduction serves as an oxygen transport mechanism in the combustion of wood char. This reaction must be isolated in order to be studied.

The dilemma presented by a reaction that occurs at a high temperature and high heating rate, is to accurately represent the reaction in a laboratory setting while remaining within the equipment's capabilities. Beyond this, differences in laboratory equipment and analysis methods can lead to significant differences in parameters determined for the same reaction. International round-robin testing of biomass materials is being performed in order to provide reliable and useful information to researchers and industry (Chum et al., 1992). The activation energies of the reactions of wood and wood char and methods used to obtain them are part of this information. Widely available and easy to reproduce methods would facilitate the development of standards.

The intention of this study is to add to this database of biomass material testing and information. The study's goal is the determination of some kinetic parameters for the gasification of wood char in carbon dioxide using thermogravimetry, a widely used technique, and an integral method of

kinetic analysis. Also the effect of char pyrolysis temperature on the activation energy will be investigated.

Experimentation was done using high temperature treated Douglas fir wood char prepared by pyrolysis under flowing nitrogen at three different treatment temperatures. A thermogravimetric balance was used to prepare the char as well as to gather the activation energy data. Dynamic thermogravimetric analysis (TGA) was used to analyze the data and obtain the activation energy.

The next chapter presents a brief history of research on wood char reactions and the carbon-carbon dioxide reaction in particular. The following chapter provides the details of the actual experimental equipment used and procedures followed. The thermogravimetric data and kinetic analysis are presented along with the activation energies in the fourth chapter, and finally, some conclusions are presented in the last chapter.

## 2.0 Literature Review

### *2.1 The Boudouard Reaction*

Carbon is a major constituent of virtually all fuels of industrial importance. During the industrial revolution of the 19th century many processes involving combustion were studied in order to improve them or make them more efficient. During this time, because of its significant role in these processes, the combustion of carbon, generally in the form of graphite, began to receive attention from the scientific community. Carbon combustion continues to be an area of importance and study to this day.

The reaction  $\text{CO}_2 + \text{C(s)} \rightleftharpoons 2\text{CO}$  was originally confirmed to be reversible by H. Sainte-Claire Deville in 1864 and is sometimes called the "Boudouard reaction" after O. Boudouard, who studied its equilibrium at different temperatures around the turn of the century (Rhead and Wheeler, 1910). In 1910, Rhead and Wheeler apparently were the first to apply Le Chatelier's equilibrium principle to the reaction (Timnat, 1982). In a later paper, they concluded that neither carbon monoxide nor carbon dioxide was the sole product of the combustion of carbon, rather, that they were both produced simultaneously (Rhead and Wheeler, 1913). In the years preceding and following World

War I, many noted scientists were involved in developing theories, conducting experiments, and constructing mathematical models related to carbon combustion (Tu et al., 1934).

In a paper published in the Proceedings of the International Conference on Bituminous Coal in 1932, Burke and Schumann described a "modified double-film theory" as shown in Figure 2. This theory described a mechanism in which practically all oxygen reaching the carbon particle surface was in the form of carbon dioxide made from supplied oxygen reacting with carbon monoxide from the carbon particle. The carbon dioxide reaching the carbon particle surface creates the carbon monoxide by the Boudouard reaction which diffuses out to react with the oxygen, creating more carbon dioxide (Fendell, 1969). This theory was confirmed by Hougen and Watson in 1947, who also determined that the reaction was most significant at temperatures around 900°C (Avedesian and Davidson, 1973). This prompted experiments to find the activation energy of the carbon-carbon dioxide reaction at high temperatures (Wicke, 1955; Khitrin, 1956; Golovina and Khaustovich, 1960; and Gray and Kimber, 1967). In 1959, Walker, Rusinko, and Austin published their "Gas Reactions of Carbon," a review which became the standard reference for kinetics of carbon reactions and listed the activation energy of the Boudouard reaction as 170.8 kJ/mole.

Interest in applying advances in carbon combustion to coal combustion began to develop in earnest in the 1960's and became widespread in the 1970's due to the energy crisis early in that decade. To design more efficient coal-fired power plants and gasifiers, more information was needed concerning the kinetics of coal combustion and the effects of temperature, pressure, environment, and type of coal on the kinetic rates (Essenhigh, 1977). The high temperatures involved in these newly developed processes made it necessary to find the activation energies of various reactions, such as the reduction of coals, coal chars, and coke in a carbon dioxide atmosphere (Dutta et al., 1977; Laurendeau, 1978; Kasuoka et al., 1985; Huttinger and Nill, 1990).

To develop working systems of wood and biomass gasification, a knowledge of activation energies and other kinetic parameters is needed in the same way that it was needed for coal. Wood and other biomass chars are quite similar to coal and coal char in composition, and both experience similar

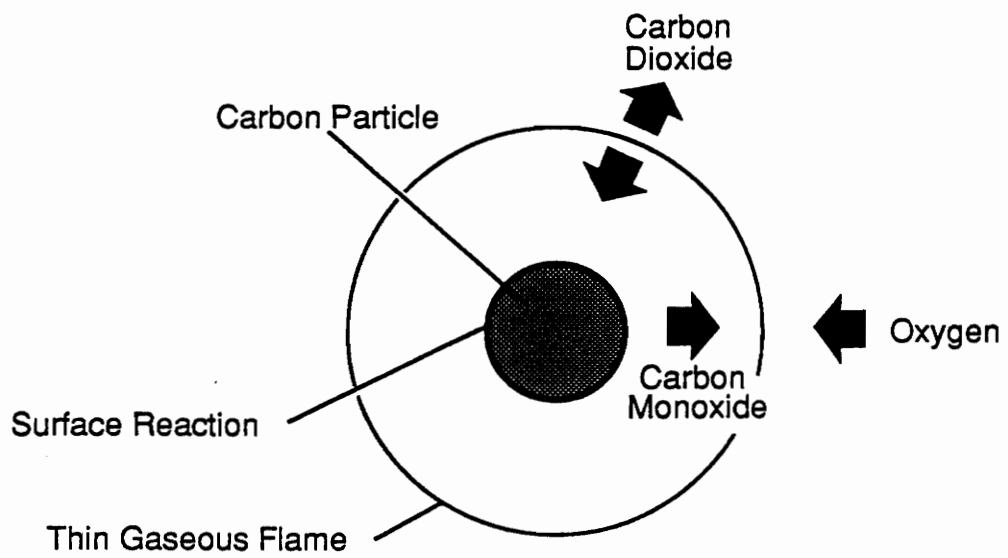


**Figure 2. Modified double-film theory:** (Fendell, 1969).

reactions when gasified. Other biomass materials and their chars have been and are still being investigated to determine their kinetics, emissions, and general potential as an energy source. These materials include: agricultural residues (DeGroot et al., 1990), wood industry wastes such as black liquor (Frederick et al., 1992) and bark (Clements and McMahon, 1980), and lignin, hemicellulose, and cellulose - the constituent materials of wood (Sadakata et al., 1987; DeGroot and Richards, 1989). Some of the chars of these materials have been gasified in carbon dioxide and had activation energies determined for the reaction. A study of the gasification of black liquor char (pyrolyzed in nitrogen at temperatures of 600 to 900°C) in carbon dioxide, reports an activation energy of 204 kJ/mole (Frederick et al., 1992). Another study reports an activation energy of 51 kJ/mole for coconut shell char (pyrolyzed in nitrogen at 1000°C) gasified in carbon dioxide at temperatures of 760, 900, 1090, and 1290°C (Van Deventer and Renter, 1989).

Only a few studies concerning the gasification of wood char in carbon dioxide are known to the author, and all have occurred since the middle 1980's. One study (Nandi and Onischak, 1985) used chars of maple and jack pine prepared at temperatures between 649 and 927°C. These chars were gasified at elevated and reduced pressures in atmospheres containing CO<sub>2</sub>, hydrogen, and steam at temperatures between 649 and 927°C. A thermobalance was used to obtain sample weights at certain times during the gasification process. The weight loss fractions were then used to determine overall rate constants, which then gave activation energies. No tests were done using only CO<sub>2</sub> as the gasifier, and no activation energies were given for tests using CO<sub>2</sub> mixed with steam and hydrogen. The activation energy given for stabilized (no more weight loss observed at pyrolysis temperature) jack pine char gasified in a half-steam, half-nitrogen atmosphere was 170.5 kJ/mole. The addition of 5% hydrogen raised the activation energy to 177.9 kJ/mole.

The Wood Chemistry Laboratory at the University of Montana performed a series of studies that used only carbon dioxide to gasify chars of both Douglas fir and cottonwood chars. The ultimate goal was to investigate the effect of catalysts on the kinetics of gasification of wood chars by carbon dioxide. The chars were prepared under nitrogen at a constant temperature of 1000°C. These chars were gasified by CO<sub>2</sub> at temperatures between 600 and 900°C. Gasification rates were determined

using evolved gas analysis (EGA), a method which detects the amount of H<sub>2</sub> and CO produced during a reaction, but does not differentiate between the two. The rates of production of CO (in the case of gasification of char) were correlated to the rates of sample weight loss, which were analyzed to give apparent activation energies. The kinetic parameters reported for Douglas fir char were an activation energy of  $221.1 \pm 11.7$  kJ/mole and a natural log of the preexponential factor of  $21.4 \pm 1.3$ . This study led to investigations into the influence of natural and added catalysts on chars gasified by CO<sub>2</sub> (DeGroot and Shafizadeh, 1985; DeGroot et al., 1988; DeGroot and Richards, 1988; Van Deventer and Renter, 1989).

The same laboratory later studied the relative rates of carbon gasification in oxygen, steam, and carbon dioxide. The carbon used was produced by pyrolyzing filter papers (100% cellulose) at 1000°C in nitrogen. The char samples gasified by carbon dioxide were carried out at a reactant gas pressure of 0.1 atm and a mixture of 10% in helium. The gases from the reaction were swept into a combustible gas detector based on a zirconium oxide oxygen sensor. This sensor was used to determine the quantity of oxygen used to combust the combustible gases produced by the gasification reaction. The amount of oxygen depletion was equivalent to the extent of carbon gasification, which gives the rate of gasification. The kinetic parameters reported for the gasification of carbon by carbon dioxide were an activation energy of 280 kJ/mole and a natural log of the preexponential factor of 22.5. The activation energy for carbon gasified by steam was 160 kJ/mole and the natural log of the preexponential factor was 12.0. For the reaction of carbon and oxygen, the activation energy was 117 kJ/mole and the natural log of the preexponential factor was 14.0 (DeGroot and Richards, 1989).

The University of Montana study is the only study known to the author which has reported the activation energy of wood char gasified solely by carbon dioxide. The University of Montana study differs from this study in its use of evolved gas detection rather than TGA. An EGA system has advantages over a TGA system in several areas. Pyrolysis reactions that take place concurrently with gasification can be readily detected by EGA, whereas this is much more difficult when using TGA. Also, EGA systems are generally more sensitive, less noisy, and generally have a smaller

furnace tube, which allows for quicker changes of atmosphere. TGA systems however are more widely available and can be purchased whole, while EGA systems must be built using purchased and laboratory built components. This can result in an apparatus that only the actual builders can use successfully (DeGroot, 1992).

International round-robin testing of biomass materials (including wood char) is proceeding using a variety of procedures, equipment, and analysis methods towards establishing standards (Chum et al., 1992). This ongoing effort should result in a survey of test methods and values that has been lacking for biomass materials.

The study described here presents the activation energy and preexponential constant of Douglas fir wood char gasified in carbon dioxide at 900°C. A common piece of laboratory equipment, a TGA, was used to obtain weight loss versus temperature data from which the desired kinetic parameters were found using an integral method of kinetic analysis. Samples were pyrolyzed at temperatures of 600, 750, and 900°C in order to investigate the effect on activation energy.

## ***2.2 Analysis of Thermogravimetric Data***

### **2.2.1 Coats-Redfern Method**

The various methods of kinetic analysis can be divided into five categories (Flynn and Wall, 1966): (1) "Integral" methods utilizing weight loss versus temperature data directly, (2) "Differential" methods utilizing the rate of weight loss, (3) "Difference-Differential" methods involving differences in rate, (4) Methods specially applicable to initial rates and (5) Nonlinear or cyclic rate methods.

The method developed by Coats and Redfern is an integral method, and is well suited for obtaining activation energies from data gathered by a thermogravimetric analyzer (TGA).

A TGA basically consists of a microbalance and a controllable furnace. While the microbalance measures the instantaneous weight of the sample, the furnace maintains a constant temperature or heating rate, which is monitored by a thermocouple placed close to the sample. By recording the output of both the microbalance and the thermocouple, a curve of the changing weight of the sample versus the temperature of the sample is obtained.

Most kinetic analysis methods begin by postulating the following form for the rate of weight loss of a solid involved in a reaction:

$$\frac{d\alpha}{dt} = k f(\alpha) \quad [2.2.1]$$

where  $\alpha$  is the fraction of solid decomposed at time  $t$ ,  $k$  is the rate constant, and  $f(\alpha)$  is the conversion function which describes the rate at which the solid disappears. The rate constant is given by

$$k = A e^{-E/RT} \quad [2.2.2]$$

where  $A$  is the preexponential factor,  $E$  is the activation energy,  $R$  is the universal gas constant, and  $T$  is the absolute temperature (Coats and Redfern, 1964). By analogy to simple cases in homogeneous reaction kinetics, the conversion function can be expressed by

$$f(\alpha) = (1 - \alpha)^n \quad [2.2.3]$$

where  $n$  is the order of the reaction (Flynn and Wall, 1966).

For a linear heating rate of  $a$  degrees per minute,

$$a = \frac{dT}{dt} \quad [2.2.4]$$

Equations 2.2.1-2.2.4 can be combined to give

$$a \frac{d\alpha}{dT} = A e^{-E/RT} (1 - \alpha)^n \quad [2.2.5]$$

Rearranging and integrating gives

$$\int_0^\alpha \frac{d\alpha}{(1 - \alpha)^n} = \frac{A}{a} \int_0^T e^{-E/RT} dT \quad [2.2.6]$$

Performing the integration and taking the log (base ten) of both sides,

$$\log \left\{ \frac{1 - (1 - \alpha)^{1-n}}{T^2(1-n)} \right\} = \log \left\{ \frac{AR}{aE} \left[ 1 - \frac{2RT}{E} \right] \right\} - \frac{E}{2.3RT} \quad [2.2.7]$$

for all values of  $n$  except  $n = 1$  in which case Equation 2.2.6 after integrating and taking logs (base ten) becomes

$$\log \left[ \frac{-\log(1 - \alpha)}{T^2} \right] = \log \left\{ \frac{AR}{aE} \left[ 1 - \frac{2RT}{E} \right] \right\} - \frac{E}{2.3RT} \quad [2.2.8]$$

Equations 2.2.7 and 2.2.8 are both linear equations of the form  $y = mx + b$  where

$$y = \log \left\{ \frac{1 - (1 - \alpha)^{1-n}}{T^2(1-n)} \right\} \quad (n \neq 1) \quad [2.2.9]$$

or

$$y = \log \left\{ \frac{-\log(1 - \alpha)}{T^2} \right\} \quad (n = 1) \quad [2.2.10]$$

$$x = \frac{1}{T} \quad [2.2.11]$$

$$m = \frac{-E}{2.3R} \quad [2.2.12]$$

$$b = \log \left\{ \frac{AR}{aE} \left[ 1 - \frac{2RT}{E} \right] \right\} \quad [2.2.13]$$

Thus a plot of  $y$  versus  $x$  should give a straight line of slope  $m$  for the correct value of  $n$  since it can be shown that  $b$  is reasonably constant over the temperature range in which most reactions generally occur (Coats and Redfern, 1964).

To calculate  $x$  and  $y$  only a set of decomposed weight fractions,  $\alpha$ , and temperatures,  $T$ , are needed over a specified range of  $\alpha$ . The value of  $n$  must be chosen based on the assumption that the reaction order remains constant throughout the reaction (Fritsky, 1991). Coats and Redfern (1964) stated that there was theoretical justification for orders of reaction of 0, 1/2, 2/3, and 1 in solid-state kinetics. This study will assume the order of the Boudouard reaction to be one, as has been done in the past for global reactions such as this (Wicke, 1955; Khitrin, 1956; Khaustovich, 1968; Dutta et al., 1977; Laurendeau, 1978). Reaction orders of 2/3 and 1/2 will also be used to determine their effect on the results.

## 2.2.2 Limitations of Kinetic Parameters Obtained from TGA Curves

Activation energies can be obtained from weight loss versus temperature curves generated by a TGA by several methods; the Coats-Redfern method is employed in this study. All methods, including Coats-Redfern, have drawbacks associated with them that must be understood both when obtaining and using the parameters found by means of these methods. There are three factors reported by Sestak (1966) which influence the error of computed kinetic data: the accuracy of determining directly measured data, the accuracy of maintaining controlled conditions during the reaction, and the accuracy of mathematical evaluation of experimental curves.

The first factor is dependent on the quality of the apparatus used and the placement of the thermocouple relative to the sample. Sestak reports differences between measured and correct

temperatures ranging from 5 to 20 K using a thermocouple placed only 2 mm from the crucible. The most significant effects of the second type involve the heat and mass transfer. A furnace is used to heat the sample at a desired rate to a given temperature. The thermal properties and geometry of the furnace used, the atmosphere in the furnace around the sample, and the non-infinite thermal conductivity of the sample itself all cause temperature gradients. These gradients can be limited by using a low heating rate (between 3 and 6 K/min is recommended by Sestak), and using a thin sample layer in the crucible. Mass transfer effects involve the diffusion of the gas to the sample and the influence of the environment on the sample. The former is addressed by keeping the sample in a thin layer, and the latter by maintaining an adequate flow of constant composition gas. The third source of error, the accuracy of the mathematical evaluation of curves, was examined by Sestak using theoretical thermogravimetric curves and six different methods: one differential, three integral, and two approximate. The activation energies computed by the various methods were all within 10% of the originally chosen value, and the Coats-Redfern method was deemed more accurate, but considerably more time consuming (Sestak, 1966). While it does provide a simple method for calculating apparent activation energies and preexponential factors from thermogravimetric data, the method loses some of the physics of the reaction and becomes difficult to interpret.

Evaluation of kinetic parameters still has inherent limitations even after all possible precautions have been taken. In fact, parameters obtained in this way are strictly only good for describing the reaction in exactly the conditions that they were obtained, and are sometimes referred to as "apparent" kinetic parameters (Fritsky, 1991). Experimentally determined parameters will always be affected by the heating rates used, the extent of conversion of sample, and the general method employed (DeGroot and Richards, 1989).

## 3.0 Materials and Methods

This chapter will present details of the experimental apparatus and materials used in obtaining the desired kinetic parameters. Sources of error in the apparatus will be identified and their magnitudes estimated. A general overview of the procedure will be presented at the end of the chapter.

### *3.1 Experimental Apparatus*

The testing of the char was performed on a Seiko TG/DTA 200 TGA and the data was stored by a Seiko SSC5000 Series TA Disk Station. The TGA data gathering system, shown in Figure 3, is comprised of a microbalance which measures the sample weight using a horizontal differential balance mechanism, and a thermocouple to measure the temperature of the sample in the furnace. Sample weight changes are measured by a sample balance beam and a reference balance beam, each independently supported by a driving coil/pivot, and each with sample pans at one end and optical position sensors at the other. Movement in either the sample or reference balance is detected by the optical sensors, which provide a feedback current to the driving coil so that the balance beams return to the balanced position. The currents running to the driving coils are detected and con-

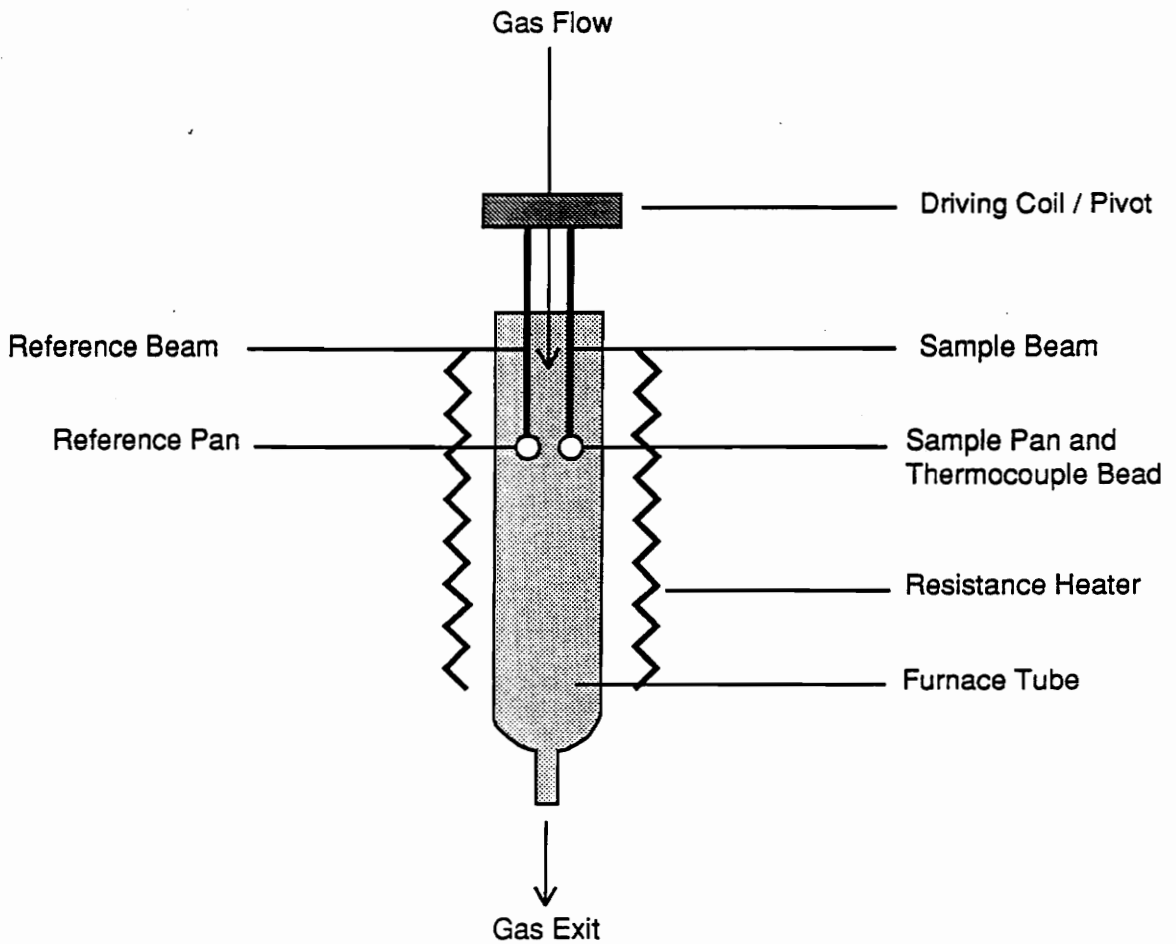


**Figure 3. Top view of TGA:** (Seiko Instruments, Inc.).

verted to weight signals. The platinum-platinum rhodium 13% (R type) thermocouple is incorporated in the alumina tube balance beam and welded to the sample pan holder.

The balance reads 19.995 mg when a supplied 20.00 mg mass is placed on the measuring arm. The balance can be read to the nearest 1  $\mu\text{g}$  when the weight is under 9.999 mg, but due to noise it can practically only be read to the nearest 2 or 3  $\mu\text{g}$ . Any buoyancy effects the gas flow would introduce are compensated for by the design of the TGA. Since both the sample and reference balance beams are in the furnace tube together, they experience the same buoyant force, thus negating any bias. Any potential errors caused by thermal effects on the balance arm are prevented in the same way.

The temperature controller precision was tested by measuring the time for a given temperature change while the TGA furnace was heating at a programmed rate of 3°C/min. The programmed temperature rise was from 600°C to 900°C, and ten measured intervals were taken from one run. The intervals were six minutes each with two minutes between intervals starting at 618°C and ending at  $\approx 852^\circ\text{C}$ . Dividing the observed temperature rise by the time it takes for the rise gives the actual heating rate. Ten runs were made, resulting in an experimental heating rate of  $2.96 \pm 0.04^\circ\text{C}/\text{min}$  using the "student's t" distribution for a 95% confidence interval.

In order to have an ultimate (carbon-hydrogen-oxygen-nitrogen-sulfur) analysis performed on the char, larger amounts of char than could be made in the TGA were needed ( $\approx 2$  g). Therefore, a large tube furnace was used to char  $\approx 6$  g of sample for each of the three heat treatment temperatures (HTT's) used (600, 750, and 900°C). These temperatures were selected because they cover the range of temperatures that typically occur in a biomass gasifier (Section 1.2).

Each sample was heated to the desired HTT while being monitored with a K type thermocouple. The two alumina sample boats used to pyrolyze the wood were  $\approx 1$  cm deep and were packed tightly with the sample. To eliminate top to bottom differences in the sample, the sample was left at the HTT for 30 minutes to ensure that the entire sample was equally charred. Nitrogen was continuously fed through the tube furnace while the char was made, and after cooling the char was stored

in glass jars under nitrogen until the analysis was performed. The results of the ultimate analysis are presented in Table 2 along with analyses from other studies of similar substances all pyrolyzed under nitrogen (DeGroot and Shafizadeh, 1984; Nandi and Onischak, 1985; Richard et al., 1985; DeGroot and Richards, 1989). Char made in this manner was not used for the kinetic analysis because it would have resulted in char being exposed to air for long periods of time while the proper sample weight was established. The chars that were gasified for the kinetic analysis were pyrolyzed in the TGA immediately before gasification.

Thus, the conditions under which the chars for ultimate analysis were produced were slightly different. The larger tube furnace heating system increased the temperature at a decreasing rate until reaching the HTT and then remained at that temperature for 30 minutes. The tube furnace heating rate varied from an initial rate of  $\approx 30^{\circ}\text{C}/\text{min}$  to a rate of  $\approx 2^{\circ}\text{C}/\text{min}$  upon reaching the HTT. The chars made in the TGA experienced a constant temperature increase of  $20^{\circ}\text{C}/\text{min}$  to the HTT after which they were ramped at  $50^{\circ}\text{C}/\text{min}$  to the gasification temperature of  $900^{\circ}\text{C}$ .

As expected, the chars are principally composed of carbon with higher HTT's having larger percentages of carbon. All other constituents decrease with increasing HTT except for nitrogen which experiences an enrichment as the treatment temperature rises. The analyses of the Douglas fir samples of this study are consistent with those of the other studies listed in Table 2.

## ***3.2 Experimental Procedure***

Samples for the tests were taken from a single Douglas fir 4X4 avoiding visible knots and concentrations of sap. The wood was cut up and then ground in a Wiley mill and the 14/28 mesh fraction was retained for analysis. The ground wood samples were stored in an airtight glass container.

**Table 2. Ultimate analysis of sample chars.**

Substance	Char HTT (°C)	C (%)	H (%)	N (%)	S (%)	O (%)	Ash (%)	Source
Douglas fir	600	92.95	2.31	0.67	0.01	3.54	0.52	This study
" "	750	95.92	0.95	0.95	0.00	1.66	0.52	" "
" "	900	97.09	0.32	1.19	0.00	0.92	0.48	" "
" "	1000	94.7	0.6			3.8	0.9	a
Fir	800-920	90	1.2	0.3		6.0	2.5	b
Cellulose	1000	96.12	0.58			1.58	0.6	c
Jack pine	732	94.10	1.09		4.04 <sup>1</sup>		0.77	d
" "	774	95.00	0.97		2.84 <sup>1</sup>		1.19	d
" "	816	95.20	0.82		2.88 <sup>1</sup>		1.10	d
" "	871	95.80	0.71		2.41 <sup>1</sup>		1.08	d
" "	927	95.20	0.60		2.58 <sup>1</sup>		1.62	d

<sup>1</sup> These are the combined percentages of O, N, and S.

a DeGroot and Shafizadeh, 1984.

b Richard et al., 1985.

c DeGroot and Richards, 1989.

d Nandi and Onischak, 1985.

Before the test could be started, the balance had to be zeroed and allowed an hour to reach steady state, then rezeroed if any drift had occurred. A small amount of sample ( $\approx 8$  mg) was placed in the platinum sample pan (used for temperatures over  $600^{\circ}\text{C}$ ) on the sample pan holder in the furnace tube of the TGA. To purge the system and allow the sample weight to stabilize, a nitrogen flow of  $100\text{ml}/\text{min}$  was passed through the furnace tube at ambient temperature ( $\approx 30^{\circ}\text{C}$ ) until the weight reached steady state (around two hours or more). This was done to ensure that there was no oxygen in the tube or on the sample which would cause direct oxidation, and to provide an accurate initial weight.

The pyrolysis phase was begun by heating the sample at a rate of  $20^{\circ}\text{C}/\text{min}$  to  $110^{\circ}\text{C}$  and holding it at that temperature for two minutes to allow all of the moisture in the sample to evaporate. The nitrogen flow rate was  $100\text{ ml}/\text{min}$  throughout the pyrolysis phase. After the moisture was driven off, the pyrolysis was continued by heating at the same rate of  $20^{\circ}\text{C}/\text{min}$  to the desired HTT. Upon reaching HTT's of  $600$  and  $750^{\circ}\text{C}$ , the sample was heated at a rate of  $50^{\circ}\text{C}/\text{min}$  to  $900^{\circ}\text{C}$  at which time the gasification was begun. For an HTT of  $900^{\circ}\text{C}$ , the gasification was begun immediately upon reaching  $900^{\circ}\text{C}$ . The highest available heating rate was used between the lower HTT's and the initial gasification temperature in an attempt to bring the char to the  $900^{\circ}\text{C}$  gasification temperature as quickly as possible. Despite this there was a short period of time (six minutes for  $600^{\circ}\text{C}$  HTT chars and 3 minutes for  $750^{\circ}\text{C}$  HTT chars) during which the char continued to pyrolyze under nitrogen at temperatures higher than the HTT.

The gasification was begun when the temperature reached  $900^{\circ}\text{C}$ , provided the weight remaining was consistent with past pyrolysis runs (10 to 20% of the original sample weight). The initial char weight before gasification was recorded for calculating weight percentages. The  $\text{CO}_2$  (99.999% pure, 2 ppm  $\text{O}_2$ ) was switched on (a flow rate of  $100\text{ ml}/\text{min}$  was used) and the nitrogen was switched off while the sample was heated from  $900^{\circ}\text{C}$  to  $1000^{\circ}\text{C}$  at a rate of  $3^{\circ}\text{C}/\text{min}$ . The flow rate of  $\text{CO}_2$  filled the furnace tube in approximately one minute, which resulted in a complete  $\text{CO}_2$  atmosphere surrounding the sample by the time the temperature reached  $\approx 904^{\circ}\text{C}$ . The low heating rate was necessary to provide a range of temperatures and decomposed weight fractions

while ensuring accurate and uniform heating of the sample. If gasification of the sample was complete (no more weight loss was occurring, meaning only ash remained) before the temperature reached 1000°C, the test was ended in order to conserve the high purity CO<sub>2</sub>. Between runs the sample pan was cleaned using a propane torch.

## **4.0 Results and Discussion**

This chapter presents results from tests performed on the Douglas fir wood char using a TGA. The thermogravimetric data from the pyrolysis of the wood and the gasification of the resultant char are presented and analyzed. Following this is the presentation and analysis of the kinetic parameters.

### ***4.1 Thermogravimetric Results and Analysis***

#### **4.1.1 Pyrolysis of Douglas Fir.**

Data from a thermogravimetric analyzer is generally presented as weight (or weight percentage) versus time or temperature (for a constant heating rate). A typical weight and temperature versus time curve of the pyrolysis of a sample at an HTT of 900°C and its subsequent gasification is shown in Figure 4. The weight loss and temperature versus time curves are all presented in Appendix A.

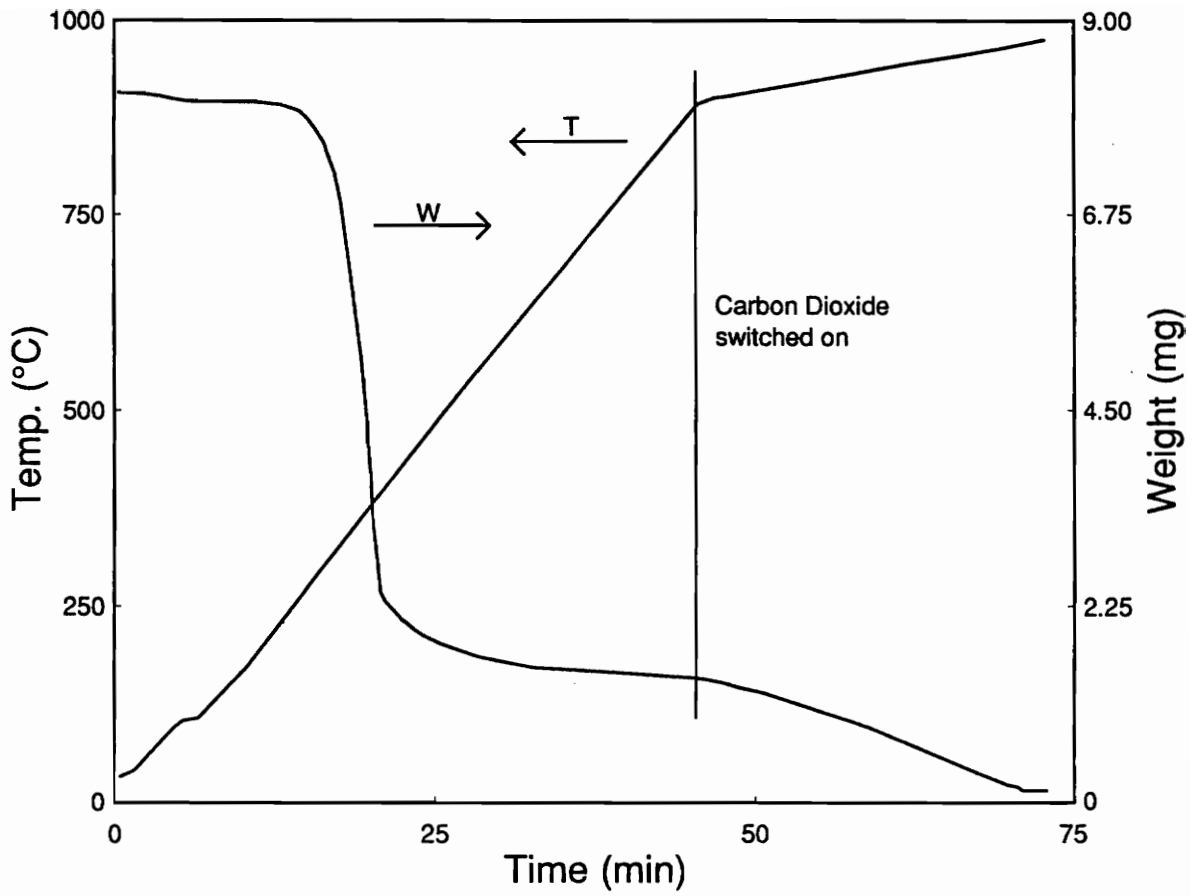


**Figure 4. Thermogravimetric plot of Run 23: HTT 900°C.**

Wood samples were pyrolyzed at HTT's of 600, 750, and 900°C to provide the char for the gasification tests.

The first weight loss is the result of the moisture in the wood chips being vaporized and driven off until the sample has been heated to above 100°C. The weight then remains constant until the temperature reaches  $\approx 300^\circ\text{C}$  where the devolatilization of the wood begins. This devolatilization continues until  $\approx 400^\circ\text{C}$  where the slope of the weight loss curve changes. At this point, most of the volatiles have been driven off, leaving only carbon, ash, and some trace nitrogen, hydrogen, and oxygen. After this point, the carbon itself is slowly driven off. After reaching the treatment temperature the charred sample is generally between 10 and 20% of the initial sample weight, the average being around 16%. The curves resulting from HTT's of 600 and 750°C are all similar in shape to the 900°C HTT runs, with the lower HTT's taking a shorter time. The final region of weight loss is the gasification region which is discussed in detail in the following section.

#### 4.1.2 Gasification of Douglas Fir Char

Weight percent versus temperature plots of 14 gasification tests are shown in Figure 5 through Figure 7. The first shows gasifications of four chars pyrolyzed under nitrogen at an HTT of 600°C, the second of four chars made at an HTT of 750°C, and the final plot of six chars made at an HTT of 900°C. The initial weight of the char samples used for gasification was controlled by using a constant initial sample weight and a constant pyrolysis treatment method. The initial sample weights were  $8028 \pm 83 \mu\text{g}$ , which resulted in initial char weights of  $1282 \pm 139 \mu\text{g}$  for an average char yield of 16.1% of the initial sample weight. This char yield is of the same order as the value of 11.7% given in the University of Montana study using Douglas fir pyrolyzed in nitrogen at an HTT of 1000°C (DeGroot and Shafizadeh, 1984). There is no apparent correlation between char yield and activation energy.

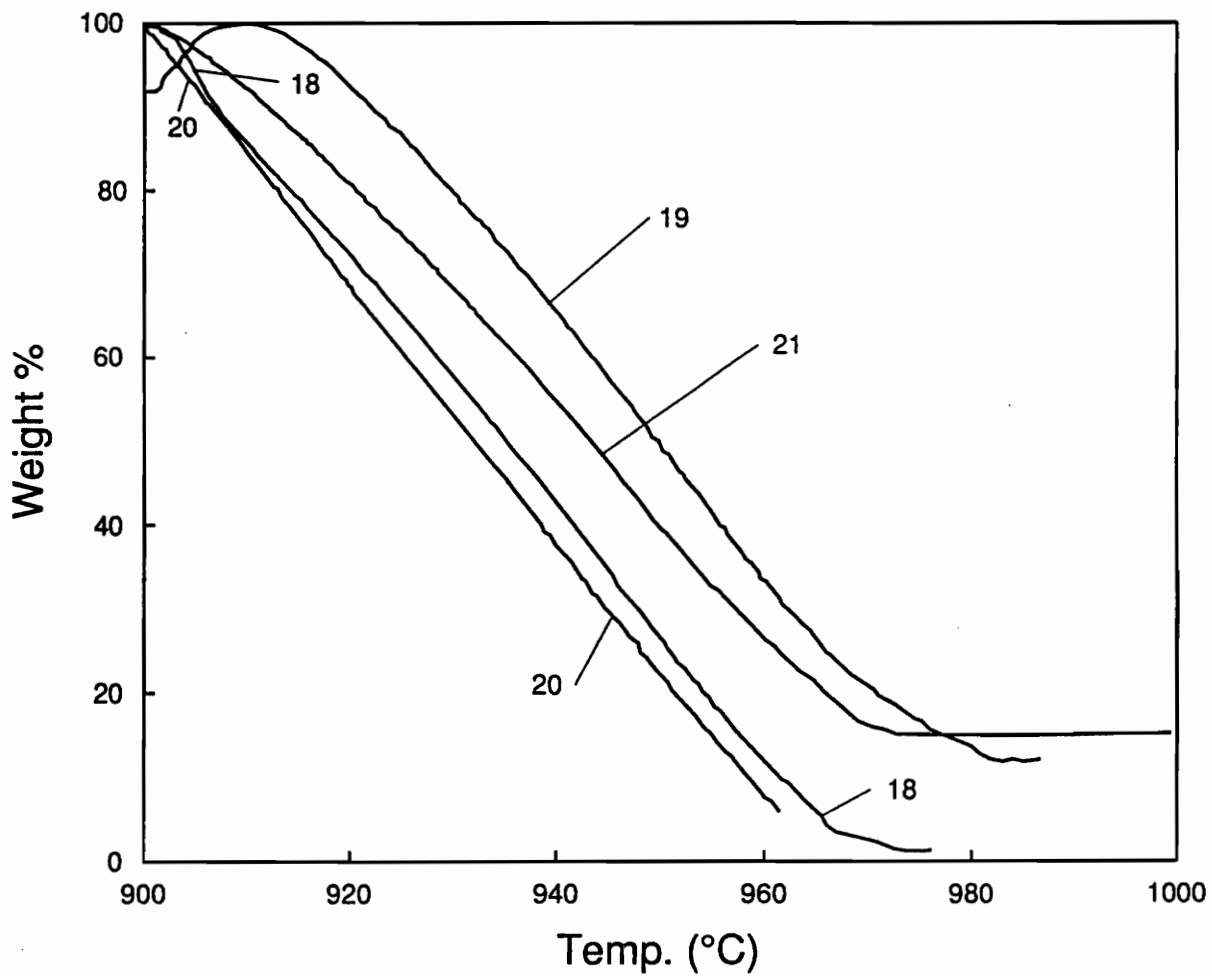


**Figure 5. Gasification of Douglas fir HTT 600°C char: Runs 18-21.**

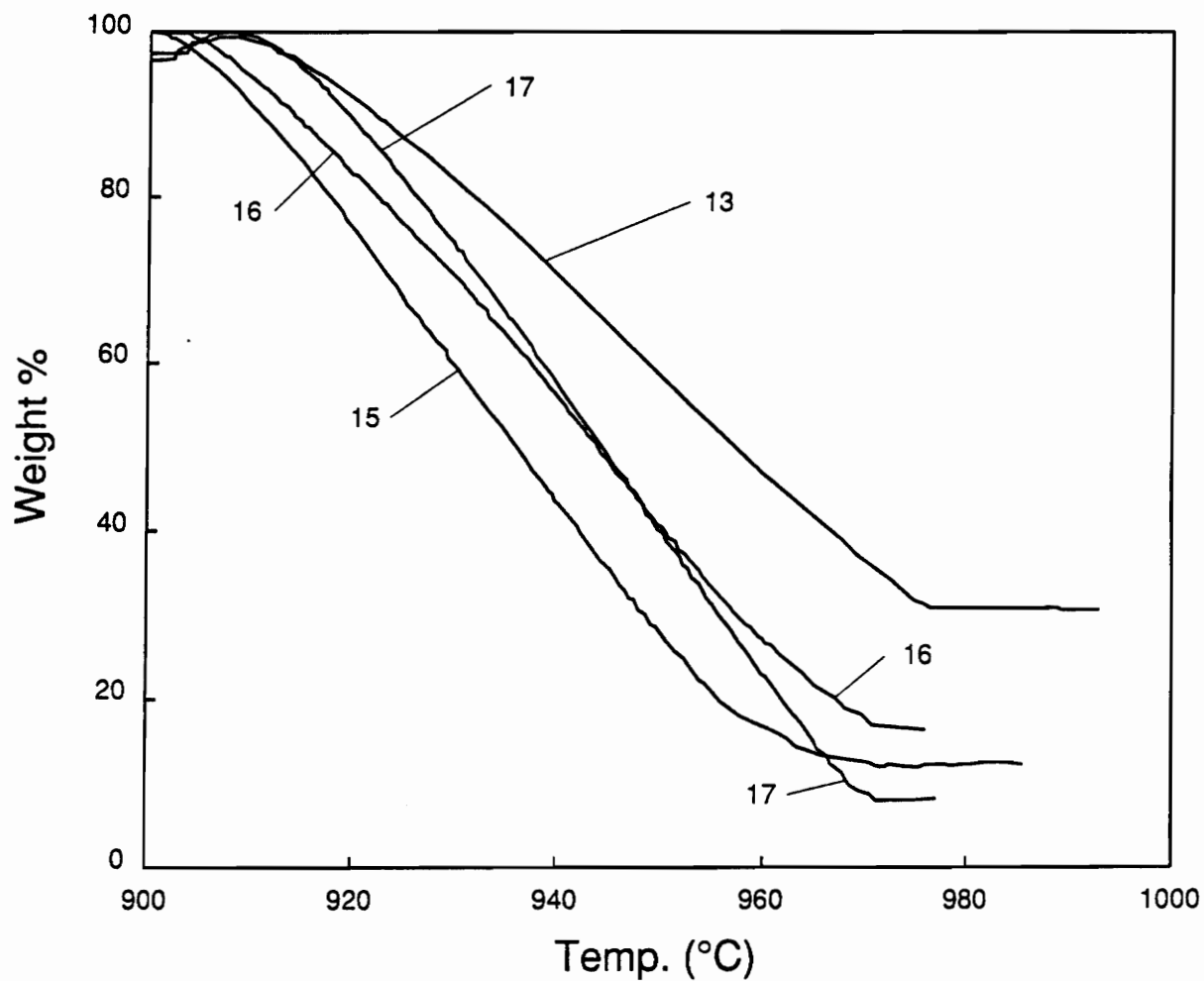


**Figure 6. Gasification of Douglas fir HTT 750°C char: Runs 13, 15-17.**

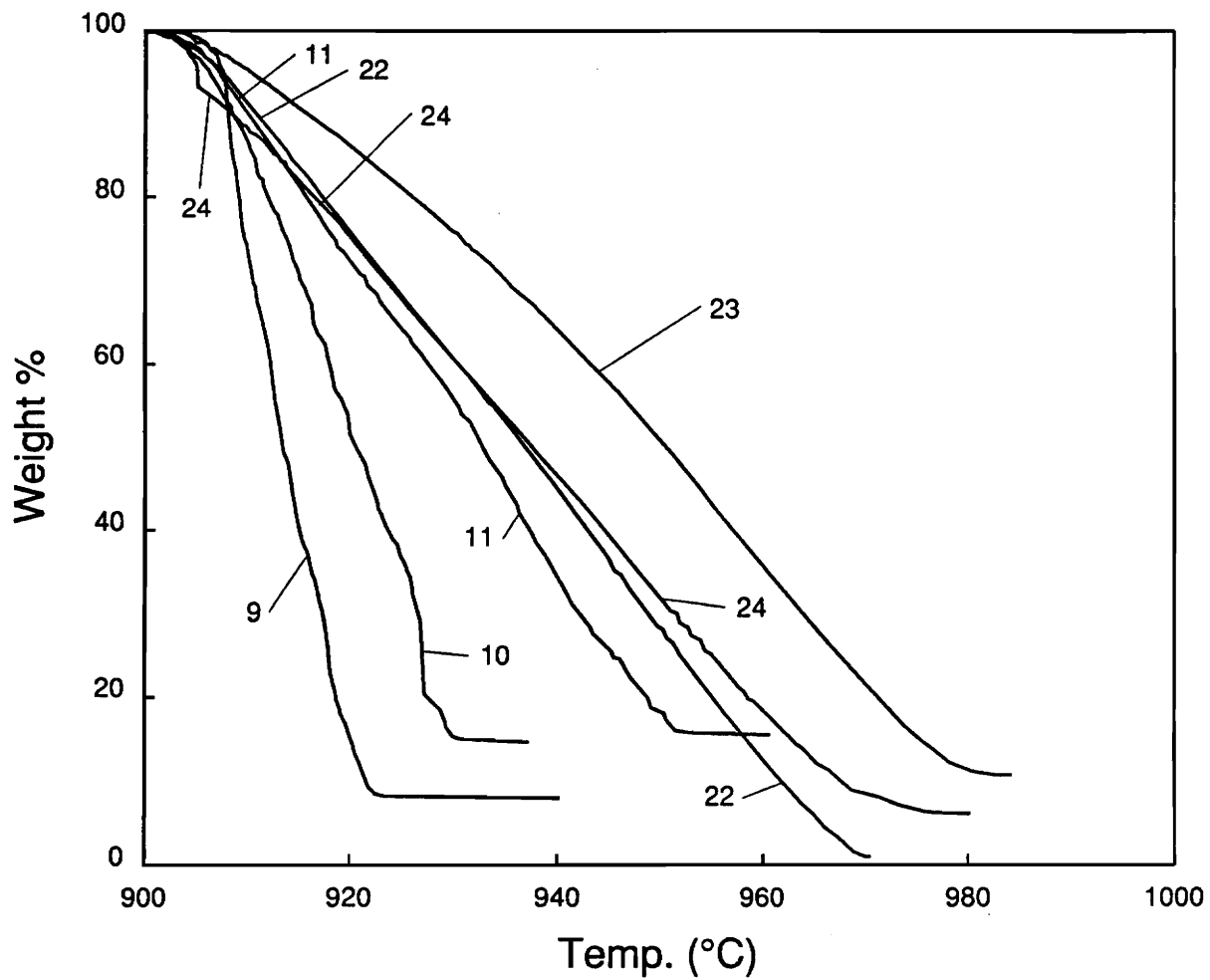


**Figure 7. Gasification of Douglas fir HTT 900°C char: Runs 9-11, 22-24.**

The gasification plots are all similar in shape, irrespective of char treatment temperature. Immediately after the carbon dioxide is introduced the weight sometimes increases slightly as the gas adsorbs onto the char. The phenomenon of weight increase after introduction of carbon dioxide has been observed in another investigation, but no mention was made of its consistency from run to run (Frederick et al., 1992). This could be due to the different surface conditions of the char at the introduction of carbon dioxide, some of which would greatly favor the adsorption of carbon dioxide over the gasification reaction at first. During the first few minutes of gasification the rate of weight loss increases as the carbon dioxide replaces the nitrogen and the temperature increases. After this period the rate of weight loss becomes steady, resulting in a constant slope. This constant slope continues until 30-40% of the char remains when the slope begins to fluctuate and then flatten out to a lower rate of weight loss. The fluctuation and final flattening of the slope occurs due to the depletion of carbon causing the reaction to become diffusion limited. The gasification ends abruptly when the gas has reacted with all the carbon it can reach.

The amount of sample left after the reaction has stopped varies considerably from run to run. The "ash" left in the sample pan was generally grey and/or black in color. Ideally, only the ash would be left at the end, which, based on the ultimate analysis, would be around 0.5%. Based on the average initial char weight of the samples, the ash left after the gasification should weigh  $\approx 6 \mu\text{g}$ . The average measured final sample weight was  $\approx 145 \mu\text{g}$ , and the weight percentage of initial char was between 2 and 32%. This could be attributed to a number of possibilities.

One possibility is an offset error in the balance which would cause all of the measured weights to be higher by a fixed amount, thus making the final weight appear higher than it really is. Another explanation for the higher final weight samples could be that the sample contained large pieces of wood that gasified to ash on the outside, effectively coating the char particle with nonreactive ash which the carbon dioxide could not penetrate. Any of these effects would result in higher than expected final weights as seen in the actual experiments.

It should be mentioned that a total of 24 runs were made. The 14 runs presented here are all relatively consistent in appearance. The initial eight runs were used to develop a workable and adequate heating and gas-switching scheme. The initial two runs (9 and 10) at an HTT of 900°C are shown in Figure 7 with the other runs using the same HTT. Although these two runs had identical pyrolysis and gasification conditions as the other runs, both exhibited markedly higher gasification rates. These very steep weight-loss curves give apparent activation energies of 3410 and 1667 kJ/mole, respectively, much higher than all the other runs. These runs were excluded from the average apparent activation energies and preexponential factors presented based on the fact that the rest of the runs were comparatively consistent and were closer to the expected range. Runs 12 and 14 were also excluded from the averages: Run 12 used a heating rate of 6°C/min (as opposed to 3°C/min for all the other runs) and Run 14 had to be aborted.

## ***4.2 Apparent Activation Energies***

### **4.2.1 Kinetic Analysis**

The Coats-Redfern integral method of kinetic analysis is used to determine the activation energy of the three chars. Each weight versus temperature plot gives an activation energy. Four plots of each of the three chars were obtained using approximately the same initial char weights and identical heating programs.

The only information needed for a Coats-Redfern analysis is a series of devolatilized weight fractions and their corresponding temperatures over a range of steadily increasing temperatures. Five evenly spaced data points are taken from each plot between devolatilized weight fractions of 0.1 and 0.6. This range was chosen because it is the region with the most constant rate of weight loss in

all cases, indicating that a relatively constant process is occurring. The slope in the region before the 0.1 devolatilized weight fraction was not constant because of the presence of nitrogen and the still changing heating rate. The introduction of the carbon dioxide either began the gasification immediately which is shown by a steadily increasing rate of weight loss, or initially began adsorbing onto the char as shown by curves that increase before showing the expected weight loss. After the 0.6 devolatilized weight fraction, the slope began to waver due to the reduced amount of carbon present in the sample which resulted in a lower surface area. This lower surface area reduced the available sites for the gasification to occur, and began to limit the diffusion of the gas to reaction sites.

A representative Coats-Redfern kinetic plot is shown in Figure 8, and the remaining kinetic plots for the other 13 runs are shown in Appendix B. The plotted points are obtained from the five data points taken from the constant-slope region of the gasification curve using the Coats-Redfern method as described in Section 2.2.1, assuming a reaction order of one. A linear regression is performed on these five plotted points using a least-squares fit, and an apparent activation energy is calculated from the resultant slope then the preexponential factor is calculated from the activation energy and the y-intercept. A sample calculation and the data used as well as the apparent activation energies and preexponential factors are presented in Appendix C.

The points on the Coats-Redfern plots all exhibit a consistent curvature relative to the line calculated to best fit those points. The slope of the line fit through the data is an average slope over that portion of the data, which gives average kinetic parameters. The curvature of the data shows that the higher temperatures (lower  $x$  values) later in the conversion of the sample give a slope that approaches zero which would result in lower activation energies, and that lower temperatures early in the conversion of the sample give steeper slopes approaching one which would give higher activation energies. This shows the dependence of the kinetic parameters on conversion of the sample as suggested in one of the University of Montana studies (DeGroot and Richards, 1989). The same curvature was shown in Coats-Redfern plots of data computed using reaction orders of  $2/3$  and  $1/2$  (typical plots are shown in Appendix D).

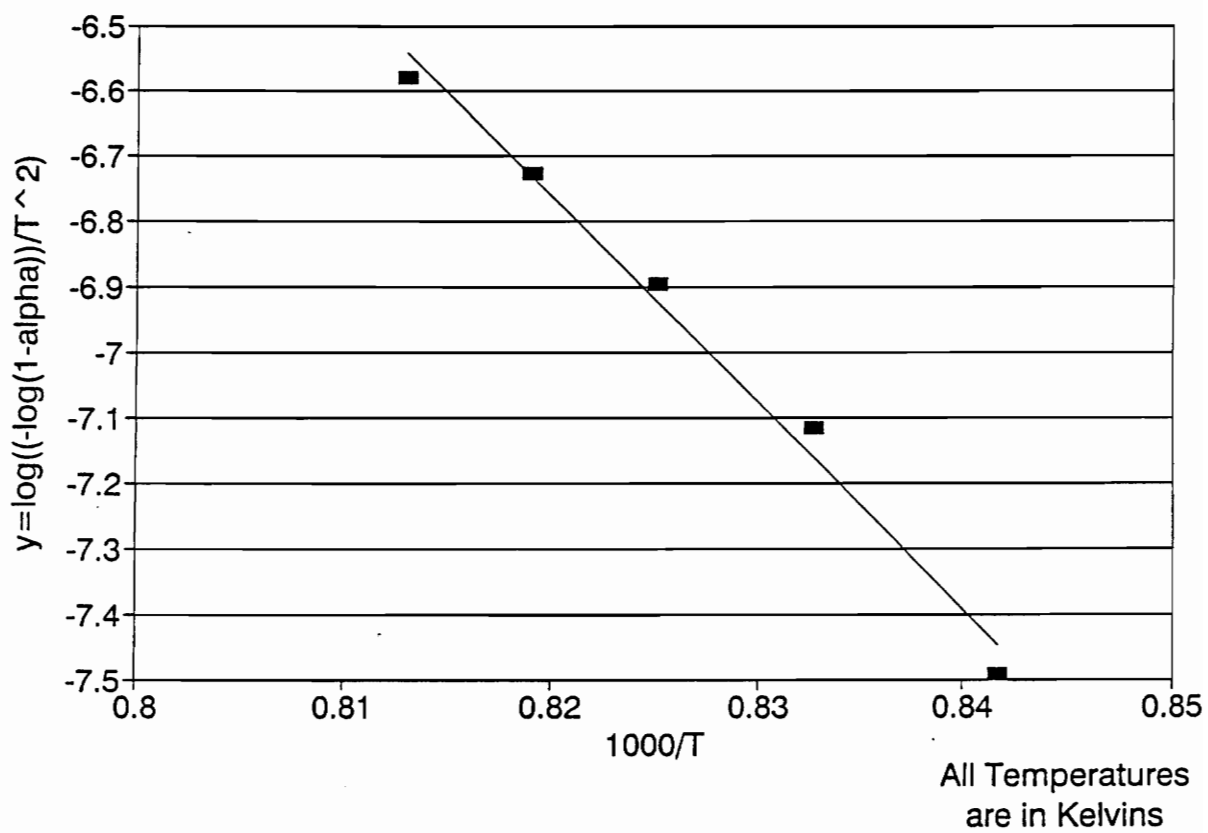


**Figure 8. Coats-Redfern kinetic plot of Run 23: HTT 900°C.**

A variance of ten percent in the slope of the linear fit results in a ten percent variance in the activation energy due to their direct proportionality (Equation 2.2.12). Variation in the natural log of the preexponential factor is more complex due to its dependence on the y-intercept of the line as well as the slope through the activation energy (Equation 2.2.13). The preexponential value increases by 11% for a ten percent increase in the slope, while a decrease of the same amount results in a decrease of 25% in the preexponential factor. These values come from recalculating the y-intercept based on the varied slope and using the average  $x$  and  $y$  values for that particular set of data.

The average apparent activation energies found are  $733.6 \pm 192.0$  kJ/mole for an HTT of 900°C,  $716.3 \pm 198.0$  kJ/mole for an HTT of 750°C, and  $719.3 \pm 72.8$  kJ/mole for an HTT of 600°C. The values for each of the HTT chars are shown in Figure 9. The natural log of the preexponential factors found are  $70.0 \pm 20.0$  for an HTT of 900°C,  $67.9 \pm 20.5$  for an HTT of 750°C, and  $68.5 \pm 7.5$  for an HTT of 600°C. The average values are consistent between the chars, the overall average apparent activation energy is  $723.1 \pm 59.7$  kJ/mole and the natural log of the preexponential factor is  $68.8 \pm 6.2$ . This can be compared to an apparent activation energy of  $221.1 \pm 11.7$  kJ/mole from an EGA study of the gasification of Douglas fir char in carbon dioxide (DeGroot and Shafizadeh, 1984). This value is of the same order as those found in this study but considerably lower and with less scatter. Comparison of the thermogravimetric curves and the resulting apparent activation energies suggests that the slower the reaction, the lower the activation energy.

There is no indication of a dependence of the activation energy on the char's HTT. The only obvious difference between the chars is the reduced scatter associated with the 600°C HTT chars when compared to the wider and similar scatter of both the 750 and 900°C HTT chars.

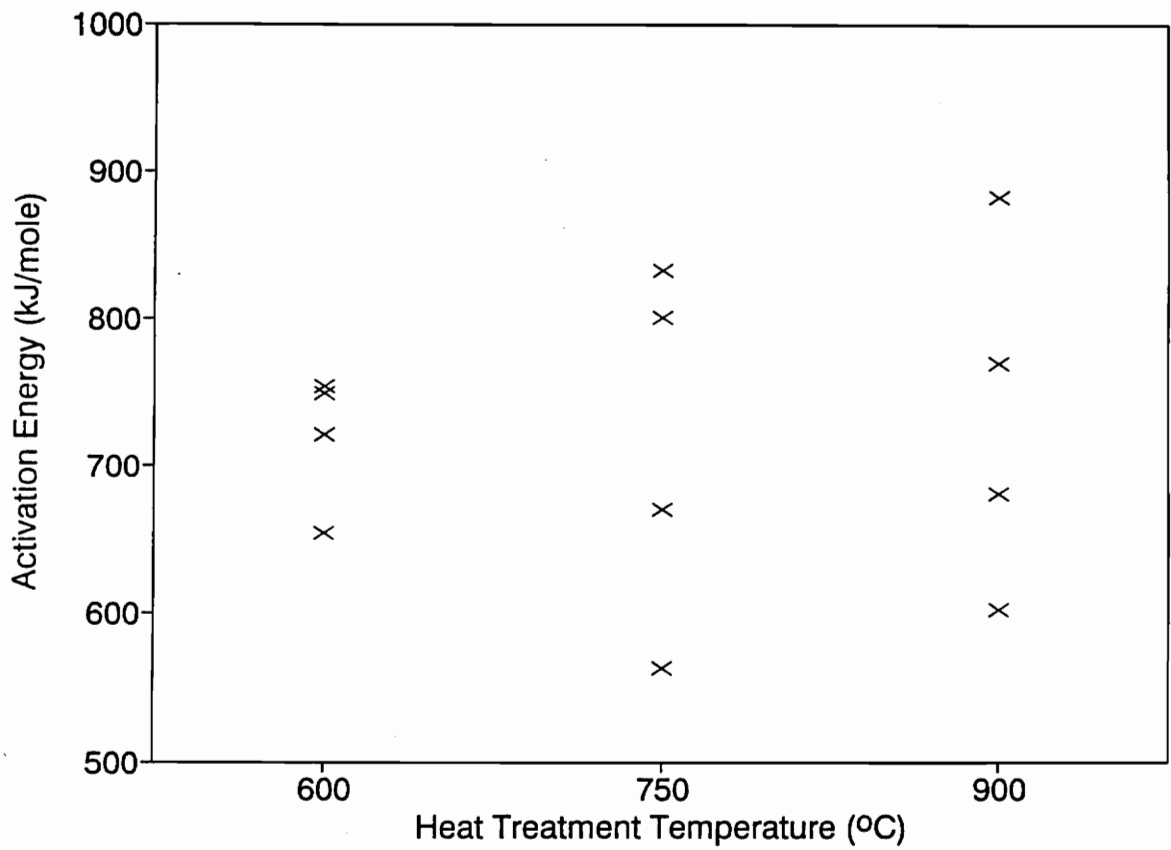


**Figure 9. Activation energies for three chars.**

## 4.2.2 Uncertainty in the Apparent Activation Energies

The uncertainty intervals that accompany the average values are the two-tailed "student's t" distribution at 95% confidence level. The "student's t" distribution accounts for the random error that is inherent in repeated measurements, but a proper uncertainty interval should also have a component that accounts for any systematic error, or bias, associated with the measurements. Most biases are eliminated by calibration of equipment and by using a consistent procedure and environment for each measurement. However, not all biases can be eliminated. The chief way to obtain a value for a bias error is to compare measurements with values obtained elsewhere using the same substance (Abernethy et al., 1973).

A sample of Monterey pine was obtained from NREL (National Renewable Energy Laboratory) in order to have some basis for comparison. These Monterey pine samples were among the biomass materials used in the round-robin testing. Four runs were performed using the Monterey pine charred under nitrogen at an HTT of 900°C. The exact same procedure was used for the Monterey pine as had been used for the Douglas fir. The thermogravimetric curves are shown in Appendix A, the Coats-Redfern kinetic plots are shown in Appendix B, and the data used are shown in Appendix C. The four runs performed gave an average apparent activation energy of  $1724 \pm 102.7$  kJ/mole and an average natural log of the preexponential factor of  $172 \pm 10.5$ . Again, the uncertainty was estimated using the "student's t" distribution at a 95% confidence interval. These values are more than double the average values found for Douglas fir char, and are closer in value and appearance to the earlier runs (Runs 9 and 10) performed using Douglas fir.

The results of the Monterey pine runs shed new light on the earlier, faster reacting runs. It could be that the earlier runs and the Monterey pine runs are valid and the slower later Douglas fir runs are showing some unanticipated and unexpected effect. However, no changes were made in procedure or equipment between these runs to suggest a reason for the existence of two distinct data sets.

Along with the Monterey pine, a thermogram of its pyrolysis under nitrogen was obtained from another laboratory to check for any discrepancies caused by the TGA itself. The thermogram from the Colorado School of Mines and one from the apparatus of this study are shown in Appendix E. No significant differences between TGA's that could help explain the high apparent activation energies are apparent from the plots.

The kinetic parameters found for Douglas fir char were checked to determine their sensitivity to changes in the input variables. An offset in the weight of  $\pm 50 \mu\text{g}$  resulted in only a  $\pm 1.1\%$  change in activation energy and a  $\pm 1.2\%$  change in the natural log of the preexponential factor. A five degree offset in temperature, both negative and positive, resulted in a  $\pm 0.84\%$  change in activation energy and a  $\pm 0.45\%$  change in the natural log of the preexponential factor. These low sensitivities further suggest that the data from the TGA is not responsible for the high apparent activation energies found.

The apparent activation energy values are all positive and large, which indicates an endothermic reaction. A lower, or even negative, activation energy would suggest an exothermic reaction. The values obtained are all an order of magnitude above the diffusion-limited region ( $\approx 40 \text{ kJ/mole}$  and below), assuring that the experiments measured the kinetics of the reaction and not the rate of diffusion of carbon dioxide to the carbon in the char. Of course, this assumes that the kinetic analysis results are accurate.

Since the data from the TGA does not show any discrepancies with similar data from other studies, the search for an explanation for the larger-than-expected apparent activation energies included a closer look at the kinetic method. This prompted the development of another analysis method that could make use of the existing data. The method developed was an approximate one from the differential form of the Arrhenius equation used by the Coats-Redfern method. The development of the approximate method and the results are shown in Appendix F. The apparent activation energies that resulted from this method are all lower than those from the Coats-Redfern method by an average of 49%. While the values were lower (an average of 568.7 kJ/mole as opposed to

723.1 kJ/mole for the C-R method), the scatter was much larger (187.1 kJ/mole as opposed to 59.7 kJ/mole for the C-R method) due to the approximate nature of the method. However, these results do show that the Coats-Redfern method may not be accurately predicting the apparent activation energy of the reaction. The approximate method also continued to predict higher activation energies for quicker reactions, the same trend shown by the Coats-Redfern method.

The choice of reaction order in the kinetic analysis was investigated. The linear regression used to obtain the slope of the Coats-Redfern plot showed that the selection of a reaction order of one was a good one. The linear correlation coefficient is a value between one and negative one which expresses to what extent a set of points supports a linear relation between  $x$  and  $y$ . The closer the coefficient is to one or negative one, the closer the points lie to a straight line. The closer the value is to zero the more uncorrelated the points are (Taylor, 1982). The worst linear correlation coefficient from the twelve regressions performed is 0.98 suggesting that the points do indeed have a linear relation, which in turn confirms the choice of one as the reaction order.

When reaction orders of two-thirds and one half were used the activation energy and natural log of the preexponential factor both dropped. For a reaction order of two-thirds, the activation energy was  $\simeq 6.3\%$  lower and the natural log of the preexponential was  $\simeq 5.7\%$  lower. A reaction order of one-half resulted in values that were  $\simeq 9.3\%$  and  $\simeq 8.9\%$  lower, respectively. However, the linear correlation coefficient was also slightly lower for both, indicating a worse fit to the data. For a reaction order of two-thirds, the coefficient fell by  $\simeq 0.0035$ , and by  $\simeq 0.0054$  for one-half. The complete results are shown in Appendix D.

## 5.0 Conclusions

The activation energies of Douglas fir char gasified in carbon dioxide using chars pyrolyzed at three temperatures have been presented. The activation energies were obtained from thermogravimetric data using the integral Coats-Redfern method of kinetic analysis. A method of pyrolyzing wood was developed to provide a consistent wood char sample for the gasification. The char samples were made and gasified consecutively in a thermogravimetric analyzer. The weight versus temperature data obtained as the char was gasified was used to determine the activation energies by the Coats-Redfern integral method of kinetic analysis. A total of 14 samples were gasified, four of two chars and six of another.

The apparent activation energies show that using different temperatures to produce the char had little effect on its activation energy. This is most likely due to the relatively consistent composition of chars prepared at temperatures greater than 400°C, as evidenced by the ultimate analysis. The activation energy values found were high enough to represent the carbon-carbon dioxide gasification reaction and not the result of the pores of the char particles limiting the diffusion of the gas to the carbon. The range of values, while consistent, did show scatter larger than that reported in other studies.

To the author's knowledge activation energies of char gasified in carbon dioxide have not been previously determined using this method of kinetic analysis. However, kinetic parameters can be compared to studies using a different method. In general, the activation energy reported for the gasification of carbon or chars in carbon dioxide is around 200 kJ/mole, ranging from 51 kJ/mole to 221 kJ/mole, while this study found it to be around 720 kJ/mole.

The average activation energy found for Douglas fir char is approximately three and a half times the generally reported value of  $\approx 200$  kJ/mole. It is likely that a systematic error exists in the kinetic analysis. The consistency and favorable agreement with published data of the pyrolysis process and the chars indicate that the problem does not lie with the sample or the preparation of the sample. The only unusual effect associated with the samples are the two different rates of gasification. The first two runs using Douglas fir rapidly gasified the carbon in the sample, while later runs did so more slowly. When using Monterey pine, the gasification rate appeared to agree more closely with the faster Douglas fir runs. This could suggest that the slower runs are diffusion limited, despite the dubiously high activation energies predicted by the Coats-Redfern analysis. The TGA used in this study was checked by comparing a thermogram to that produced at another lab. The thermograms did not show any significant discrepancies. This leaves the analysis method as the probable source of the problem.

The Coats-Redfern analysis method has given, from data obtained using reliable equipment, apparent activation energies that are much higher than expected. It also predicts lower activation energies for runs that take longer to convert the carbon. However, the activation energies and preexponential factors found using the Coats-Redfern method predict relative reaction rates consistent with the data.

The approximate method developed to check the Coats-Redfern method gave lower apparent activation energies, but showed the same unexpected trend that faster reactions resulted in higher activation energies. This approximate method showed that there could be a problem with the Coats-Redfern method or with integral methods in general.

tivation energies. This approximate method showed that there could be a problem with the Coats-Redfern method or with integral methods in general.

Future work should include a new method that uses constant temperature gasification and a new kinetic analysis method to use with the constant-temperature data. The Monterey pine samples should be used in order to facilitate comparison to other labs participating in the round-robin testing effort. Once the data is collected, a multiple regression analysis should be used to determine the activation energy that gives a best fit to the data. A greater volume of data and a more reliable test method may also lead to an explanation for the different rates of conversion shown by the data in this study. Once a new procedure and analysis method are established, then work can proceed into the effects of varied pyrolysis temperatures as well as other areas of interest.

## References

- Abernethy, R.B., and J.W. Thompson, 1973, *Handbook: Uncertainty in Gas Turbine Measurements*, USAF Arnold Engineering Development Center, Report AEDC-TR-73-5.
- Antal, M.J., 1979, "Thermochemical Conversion of Biomass: the Scientific Aspects," *A Report to the Office of Technology Assessment of the Congress of the United States*, Princeton University.
- Avedesian, M.M., and J.F. Davidson, 1973, "Combustion of Carbon Particles in a Fluidized Bed," *Transactions of the Institute of Chemical Engineering*, Vol. 51, pp. 121-131.
- Burke, S., and T. Schumann, 1932, *Proceedings of the International Conference on Bituminous Coal*, Vol.2, pp. 485-509.
- Chum, Helena L., David K. Johnson, Foster A Agblevor, Robert J. Evans, Bonnie R. Hames, Thomas A. Milne, and Ralph P. Overend, 1992, "Status of the IEA Voluntary Standards Activity - Round Robins on Whole Wood and Lignins," IEA Conference on Advances in Thermochemical Biomass Conversion, Interlaken, Switzerland, May, 11-15, 1992.
- Clements, H.B., and C.K. McMahon, 1980, "Nitrogen Oxides from Burning Forest Fuels Examined by Thermogravimetry and Evolved Gas Analysis," *Thermochemica Acta*, Vol.35, pp. 133-139.
- Coats, A.W., and J.P. Redfern, 1964, "Kinetic Parameters from Thermogravimetric Data," *Nature*, Vol. 201, pp. 68-69.
- DeGroot, W.F., 1992, Private communication to author, June 9, 1992.
- DeGroot, W.F., M.P. Kannan, G.N. Richards, and O. Theander, 1990, "Gasifications of Agricultural Residues (Biomass): Influence of Inorganic Constituents," *Journal of Agricultural and Food Chemistry*, Vol. 38, pp. 320-323.
- DeGroot, W.F., T.H. Osterfeld, and G.N. Richards, 1988, "The Influence of Natural and Added Catalysts in the Gasification of Wood Chars", *Research in Thermochemical Biomass Conversion*, pp. 327-341.

- DeGroot, W.F. and G.N. Richards, 1988, "The Effects of Ion-exchanged Cobalt Catalysts on the Gasification of Wood Chars in Carbon Dioxide," *Fuel*, Vol. 67, pp. 345-351.
- DeGroot, W.F. and G.N. Richards, 1989, "Relative Rates of Carbon Gasification in Oxygen, Steam and Carbon Dioxide," *Carbon*, Vol. 27, No. 2, pp. 247-252.
- DeGroot, W.F., and F. Shafizadeh, 1984, "Kinetics of Gasification of Douglas Fir and Cottonwood Chars by Carbon Dioxide," *Fuel*, Vol. 63, pp. 210-216.
- DeGroot, W.F., and F. Shafizadeh, 1985, "Kinetics of Wood Gasification by Carbon Dioxide and Steam," *Fundamentals of Thermochemical Biomass Conversion*, pp. 275-292.
- Dutta, S., C.Y. Wen, and R.J. Belt, 1977, "Reactivity of Coal and Char. 1. In Carbon Dioxide Atmosphere," *Industrial and Engineering Chemistry, Process Design and Development*, Vol. 16, No.1, pp. 20-30.
- Essenhigh, R.H., 1977, "Combustion and Flame Propagation in Coal Systems: A Review," *Tenth Symposium (International) on Combustion*, pp. 353-372.
- Fendell, F.E., 1969, "The Burning of Spheres Gasified by Chemical Attack," *Combustion Science and Technology*, Vol. 1, pp. 13-24.
- Flynn, J.H., and L.A. Wall, 1966, "General Treatment of the Thermogravimetry of Polymers," *Journal of Research of the National Bureau of Standards - A. Physics and Chemistry*, Vol. 70A, No. 6, pp. 487-523.
- Frederick, W.J., K. Wag, and M. Hupa, 1992, "Pressurized CO<sub>2</sub> Gasification of a High Sodium Content Char from Spent Pulping Liquor," Paper, The Combustion Institute Spring Meeting of the Western States Section, Corvallis, Oregon, March 23-24, 1992.
- Fritsky, K.J., 1991, *Devolatilization Characteristics of Refuse Derived Fuels and Selected Municipal Solid Waste Components*, M.S. Thesis, Department of Mechanical Engineering and Mechanics, Drexel University, Philadelphia, Pennsylvania.
- Golovina, E.S., and G.P. Khaustovich, 1960, "The Interaction of Carbon Dioxide and Oxygen at Temperatures up to 3000°K," *Eighth Symposium (International) on Combustion*, pp. 784-792.
- Gray, M.D., and G.M. Kimber, 1967, "Reaction of Charcoal Particles with Carbon Dioxide and Water at Temperatures up to 2,800°K," *Nature*, Vol. 214, pp. 797-798.
- Huttinger, K.J., and J.S. Nill, 1990, "A Method for the Determination of Active Sites and True Activation Energies in Carbon Gasification: (II) Experimental Results," *Carbon*, Vol. 28, No. 4, pp. 457-465.
- Kasuoka, S., Y. Sakata, M. Shimada, and T. Matsutomi, 1985, "A New Kinetic Model for Temperature Programmed Thermogravimetry and its Applications to the Gasification of Coal Chars with Steam and Carbon Dioxide," *Journal of Chemical Engineering of Japan*, Vol. 18, No. 5, pp. 426-432.
- Khaustovich, G.P., 1968, "Interaction of Carbon with Carbon Dioxide in the Temperature Range 1300-3100 K," *Russian Journal of Physical Chemistry*, Vol. 42, No. 7, pp. 862-864.
- Khitrin, L.N., 1956, "Fundamental Principles of Carbon Combustion and Factors Intensifying the Burning of Solid Fuels," *Sixth Symposium (International) on Combustion*, pp. 565-573.

- Laurendeau, N.M., 1978, "Heterogeneous Kinetics of Coal Char Gasification and Combustion," *Progress in Energy and Combustion Science*, Vol. 4, pp. 221-270.
- Nandi, S.P., and M. Onischak, 1985, "Gasification of Chars Obtained from Maple and Jack Pine Woods," *Fundamentals of Thermochemical Biomass Conversion*, pp. 567-587.
- Reed, T.B., 1981, *Biomass Gasification: Principles and Technology*, Noyes Data Corporation, Park Ridge, New Jersey.
- Rhead, T.F.E., and R.V. Wheeler, 1910, "The Effect of Temperature on the Equilibrium  $2\text{CO} = \text{CO}_2 + \text{C}$ ," *Journal of the Chemical Society*, Vol. 97, pp. 2178-2189.
- Rhead, T.F.E., and R.V. Wheeler, 1913, "The Mode of Combustion of Carbon," *Journal of the Chemical Society*, Vol. 103, pp.461-489.
- Richard, J.R., M. Cathonnet, and J.P. Rouan, 1985, "Gasification of Charcoal: Influence of Water Vapor," *Fundamentals of Thermochemical Biomass Conversion*, pp. 589-599.
- Sadakata, M., K. Takahashi, M. Saito, and T. Sakai, 1987, "Production of Fuel Gas and Char from Wood, Lignin, and Holocellulose by Carbonization," *Fuel*, Vol. 66, pp. 1667-1671.
- Seiko Instruments Inc., 1987, *TG/DTA200, TG/DTA300 Simultaneous Thermo-Gravimetric / Differential Thermal Analyzer Operation Manual*, Version 1.0.
- Sekiguchi, Y., J.S. Frye, and F. Shafizadeh, 1983, "Structure and Formation Cellulosic Chars," *Journal of Applied Polymer Science*, Vol. 28, pp. 3513-3525.
- Sestak, 1966, "Errors of Kinetic Data Obtained From Thermogravimetric Curves at Increasing Temperature," *Talanta*, Vol. 13, pp. 567-579.
- Taylor, John R., 1982, *An Introduction to Error Analysis: The Study of Uncertainties in Physical Measurements*, University Science Books, Mill Valley, California.
- Tillman, David A., 1978, *Wood as an Energy Resource*, Academic Press, New York.
- Tillman, David A., A.J. Rossi, W.D. Kitto, 1981, *Wood Combustion: Principles, Processes, and Economics*, Academic Press, New York.
- Timnat, Y.M., 1982, "Problems of Carbon Oxidation," *Israel Journal of Technology*, Vol. 20, pp. 31-36.
- Tu, C.M., H. Davis, and H.C. Hottel, 1934, "Combustion Rate of Carbon," *Industrial and Engineering Chemistry*, Vol. 26, No. 7, pp.749-757.
- Van Deventer, J.S.J., and M.A. Renter, 1989, "Catalytic Gasification of Activated Carbon by  $\text{CO}_2$ ," *Thermochemica Acta*, Vol. 137, pp. 383-386.
- Walker, P.L., Jr., F. Rusinko, Jr., and L.G. Austin, 1959, "Gas Reactions of Carbon," *Advances in Catalysis*, Vol. 11, pp.133-221.
- Wicke, E., 1955, "Contributions to the Combustion Mechanism of Carbon," *Fifth Symposium (International) on Combustion*, pp. 245-252.

## **Appendix A. Thermogravimetric Plots**

This appendix presents the weight loss versus time curves for Runs 9-11, 13, 15-24, and A1-A4. The curves with an "A" were done using the Monterey pine instead of Douglas fir. The time, temperature, and weight of the initial and final states, the beginning and end of pyrolysis, and the start of gasification are all marked on for each run.

TG/DTA

<Name>  
gas9.900  
<Date>  
92/04/08 20:54

<Sample>	<Comment>	<Temp.program[C]>	[C/min]	[min]
Doug. fir chips	HTT 900	1*	30.0- 110.0	20.00 2.00
8.007 mg	-----	2*	110.0- 900.0	20.00 0.00
( 8.007 mg)	-----	3*	900.0- 900.0	3.00 0.00
<Reference>	-----	4*	900.0- 937.0	3.00 0.00
0.000 mg	<Sampling>	<Gas>		
	1.0 sec	n2	100.0 ml/min	
		co2	100.0 ml/min	

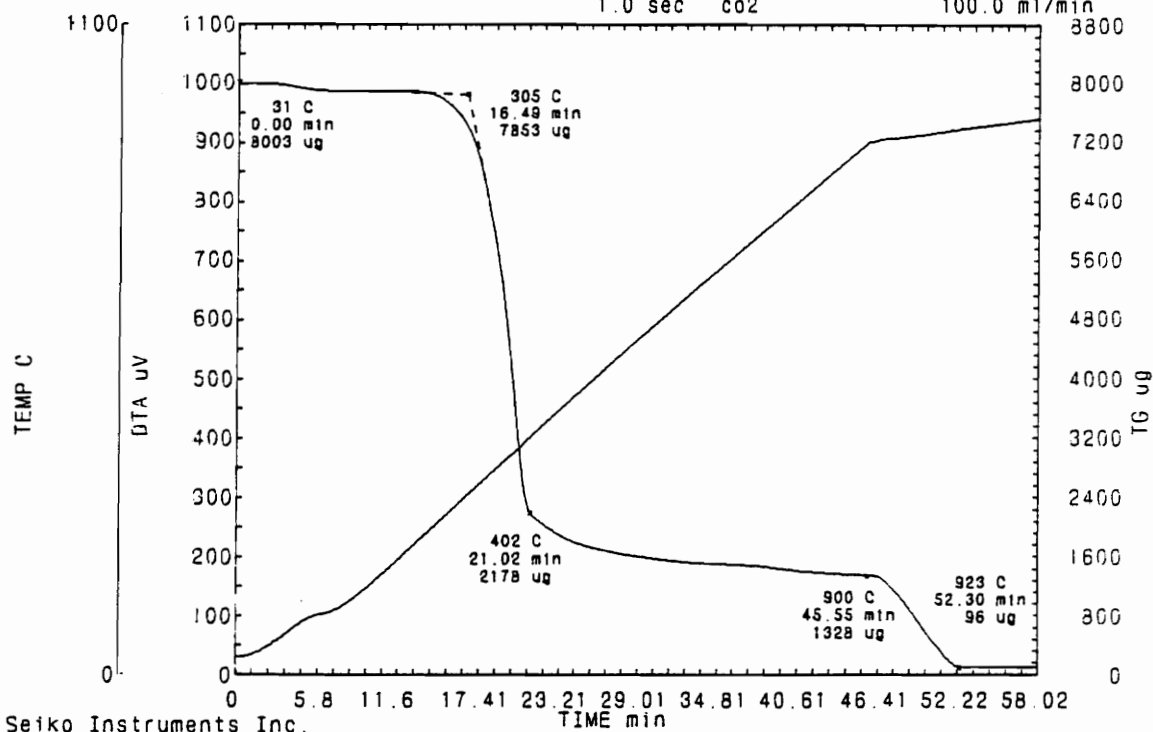


Figure 10. Thermogravimetric plot of Run 9: HTT 900°C.

TG/DTA

<Name>  
gas10.900  
<Date>  
92/04/09 21:25

<Sample>	<Comment>	<Temp.program(C)	[C/min]	[min]
Doug. fir chips	HTT 900	1*	30.0- 110.0	20.00 2.00
8.043 mg	-----	2*	110.0- 900.0	20.00 0.00
( 8.043 mg)	-----	3*	900.0- 900.0	3.00 0.00
<Reference>	-----	4*	900.0- 935.0	3.00 0.00
0.000 mg	<Sampling>	<Gas>		
	1.0 sec	n2	100.0 ml/min	
		co2	100.0 ml/min	

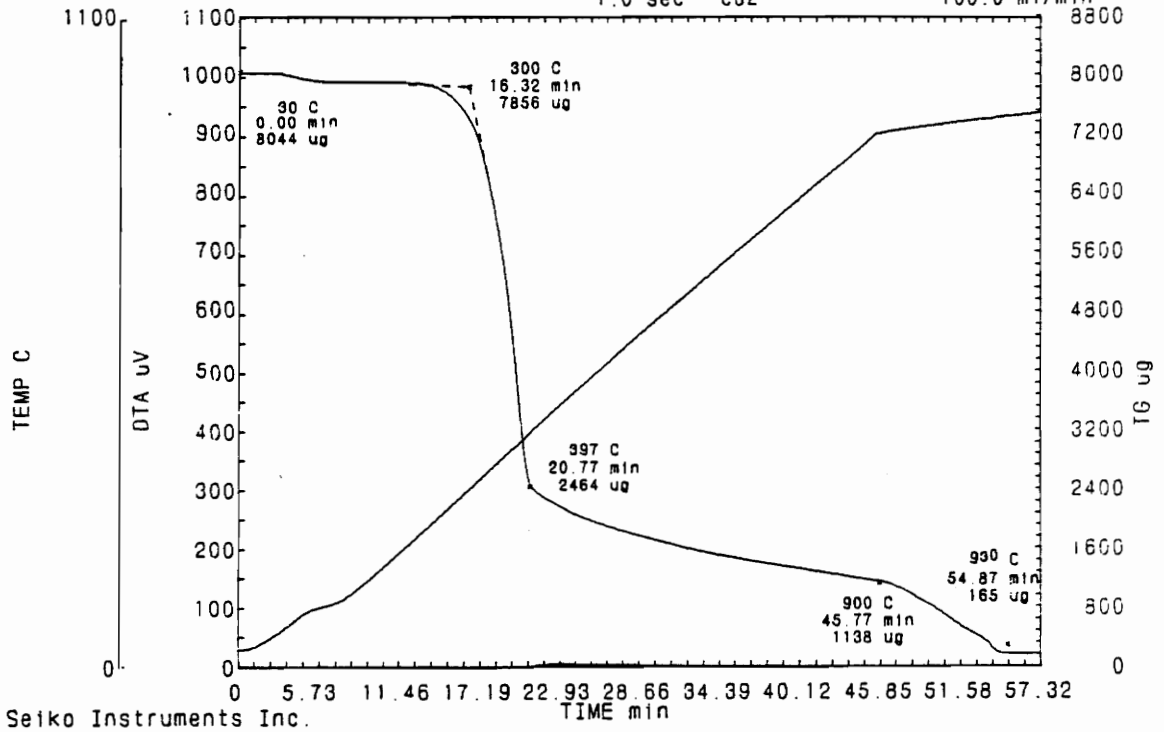


Figure 11. Thermogravimetric plot of Run 10: HTT 900°C.

TG/DTA	<Sample>	<Comment>	<Temp.program[C] (C/min) (min)>
<Name>	Doug. fir chips	HTT 900	1* 30.0- 110.0 20.00 2.00
gas11.900	7.908 mg	-----	2* 110.0- 900.0 20.00 0.00
<Date>	( 7.908 mg)	-----	3* 900.0- 900.0 3.00 0.00
92/04/10 20:56	<Reference>	-----	4* 900.0- 960.0 3.00 0.00
	0.000 mg	<Sampling>	<Gas>
		1.0 sec	n2 100.0 ml/min
			co2 100.0 ml/min

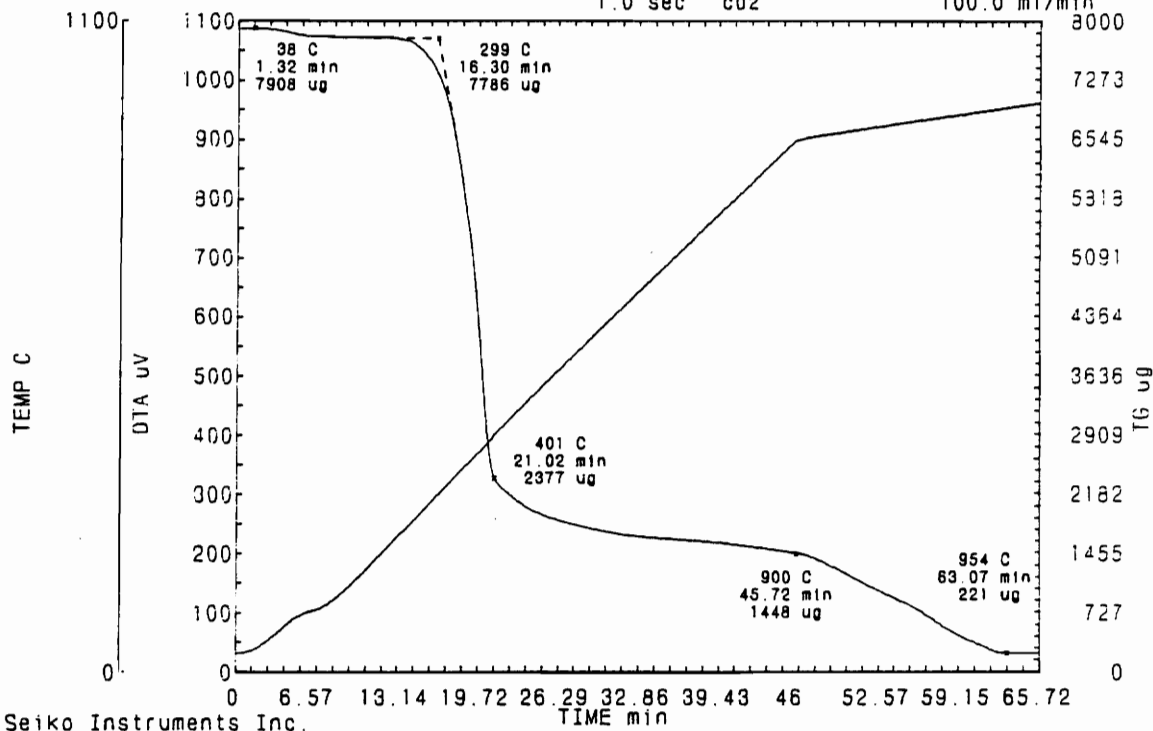


Figure 12. Thermogravimetric plot of Run 11: HTT 900°C.

TG/DTA

<Name>  
gas13.750  
<Date>  
92/04/13 21:43

<Sample>	<Comment>	<Temp.program(C)	[C/min]	[min]
Doug. fir chips	HTT 750	1*	30.0- 110.0	20.00 2.00
8.087 mg	-----	2*	110.0- 750.0	20.00 0.00
( 8.087 mg)	-----	3*	750.0- 900.0	50.00 0.00
<Reference>	-----	4*	900.0- 990.0	3.00 0.00
0.000 mg	<Sampling>	<Gas>		
	1.0 sec	n2	100.0 ml/min	
		co2	100.0 ml/min	

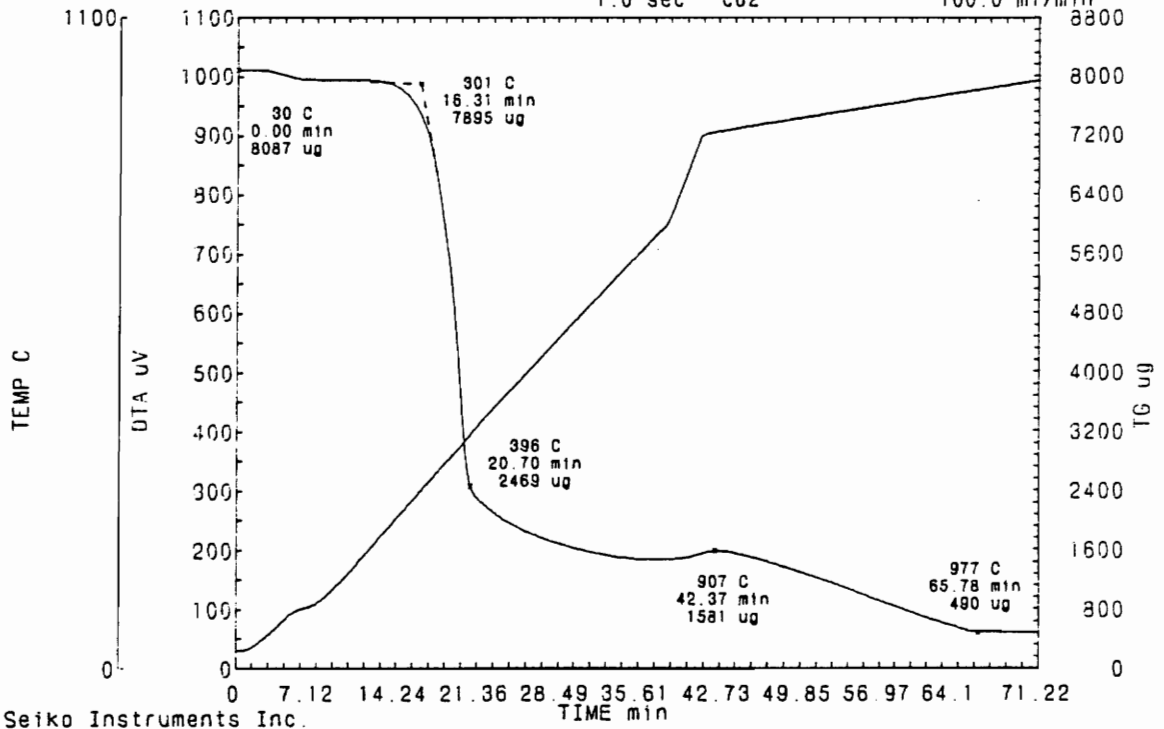


Figure 13. Thermogravimetric plot of Run 13: HTT 750°C.

TG/DTA

<Name>  
gas15.750  
<Date>  
92/04/15 00:25

<Sample>	<Comment>	<Temp.program(C)	[C/min]	[min]
Doug. fir chips	HTT 750	1*	30.0- 110.0	20.00 2.00
8.186 mg	-----	2*	110.0- 750.0	20.00 0.00
( 8.186 mg)	-----	3*	750.0- 900.0	50.00 0.00
<Reference>	-----	4*	900.0- 985.0	3.00 0.00
0.000 mg	<Sampling>	<Gas>		
	1.0 sec	n2	100.0 ml/min	
		air	100.0 ml/min	

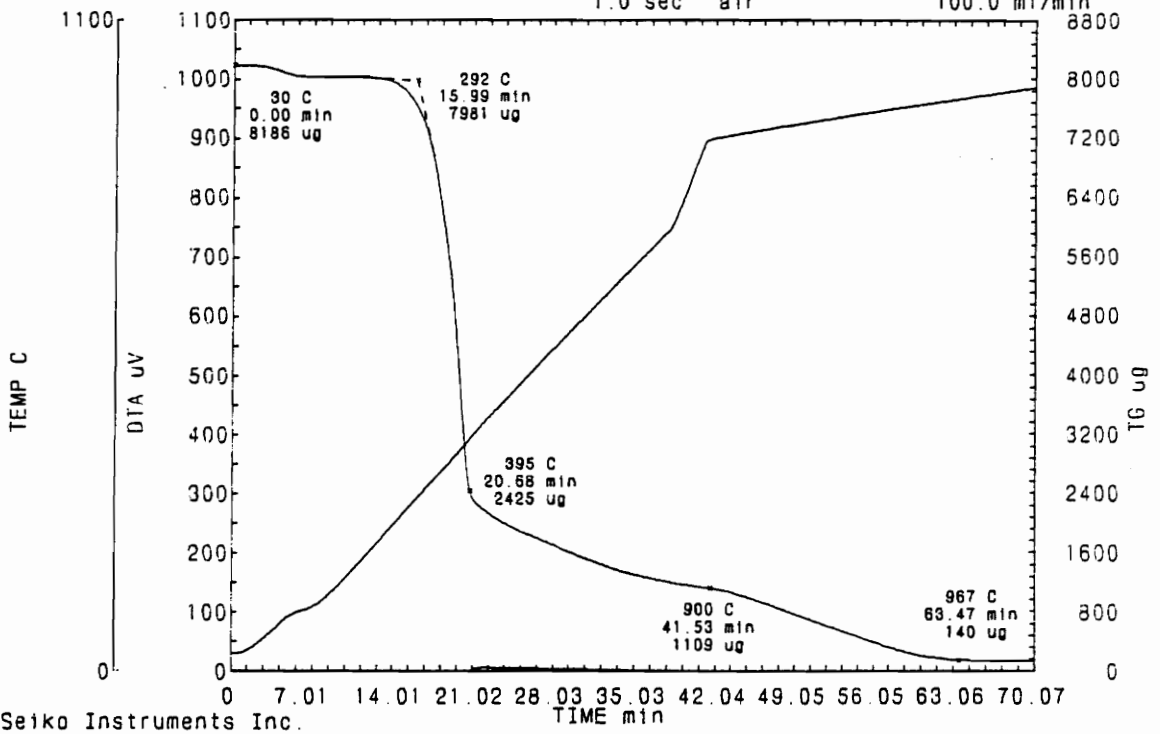


Figure 14. Thermogravimetric plot of Run 15: HTT 750°C.

TG/DTA

<Name>  
gas16.750  
<Date>  
92/04/15 19:22

<Sample>  
Doug. fir chips  
7.984 mg  
( 7.984 mg)  
<Reference>  
-----  
0.000 mg

<Comment>  
HTT 750  
-----  
<Sampling>  
1.0 sec

<Temp.program(C) [C/min] [min]>  
1\* 30.0- 110.0 20.00 2.00  
2\* 110.0- 750.0 20.00 0.00  
3\* 750.0- 900.0 50.00 0.00  
4\* 900.0- 975.0 3.00 0.00  
<Gas>  
n2 100.0 ml/min  
air 100.0 ml/min

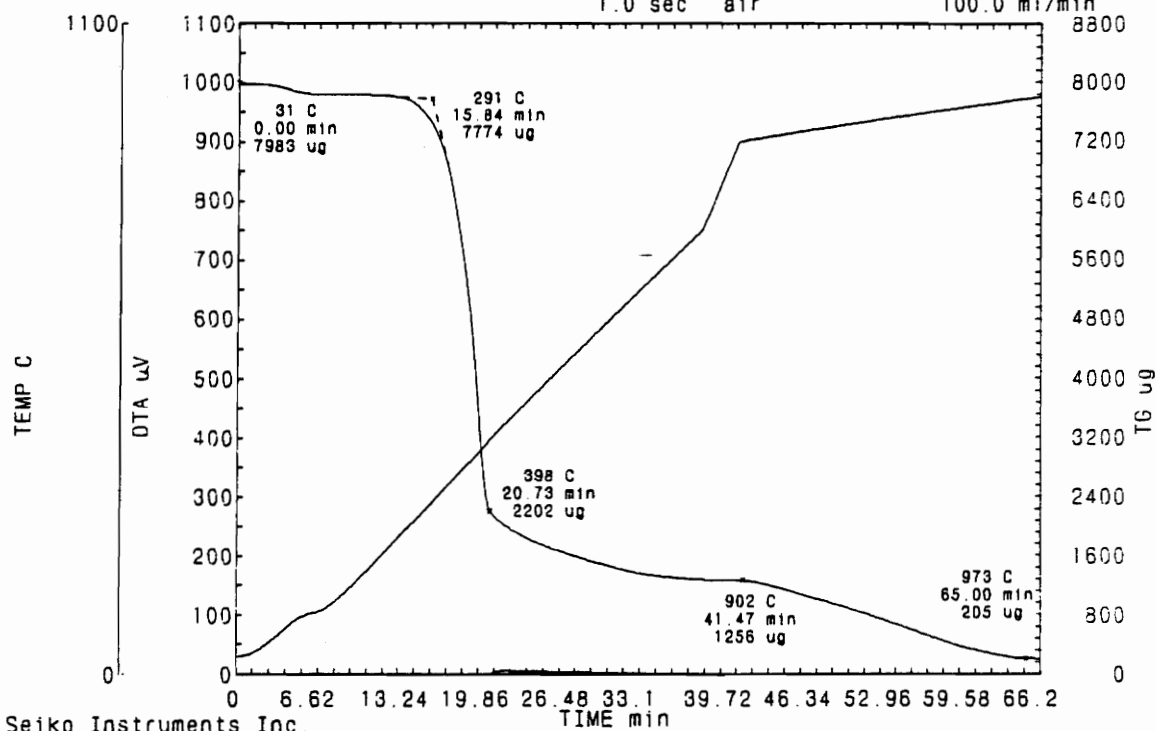


Figure 15. Thermogravimetric plot of Run 16: HTT 750°C.

TG/DTA

<Name>  
gas17.750  
<Date>  
92/04/16 01:14

<Sample>	<Comment>	<Temp.program(C)	[C/min]	[min]>
Doug. fir chips	HTT 750	1*	30.0- 110.0	20.00 2.00
8.066 mg	-----	2*	110.0- 750.0	20.00 0.00
( 8.066 mg)	-----	3*	750.0- 900.0	50.00 0.00
<Reference>	-----	4*	900.0- 975.0	3.00 0.00
-----	-----	<Gas>		
0.000 mg	<Sampling>	n2		100.0 ml/min
	1.0 sec	co2		100.0 ml/min

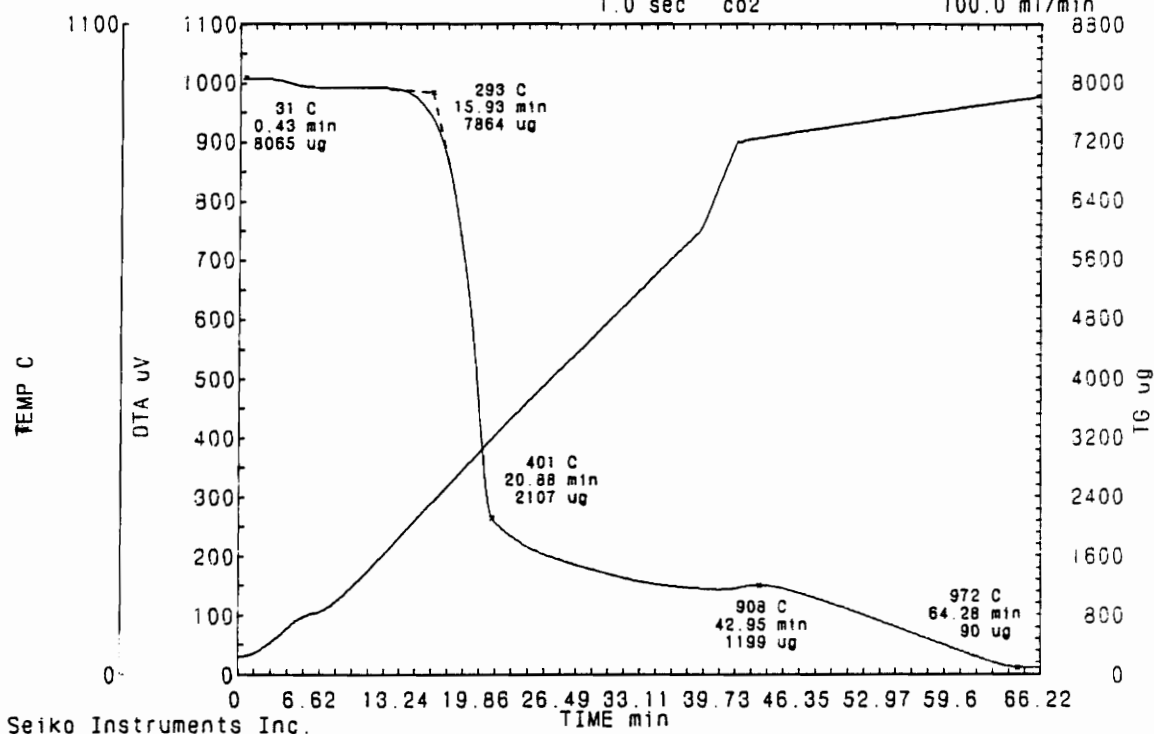


Figure 16. Thermogravimetric plot of Run 17: HTT 750°C.

TG/DTA

<Name>  
gas18.600  
<Date>  
92/04/16 10:57

<Sample>	<Comment>	<Temp.program(C)	(C/min)	(min)
Doug. fir chips	HTT 600	1*	30.0- 110.0	20.00 2.00
8.009 mg	-----	2*	110.0- 600.0	20.00 0.00
( 8.009 mg)	-----	3*	600.0- 900.0	50.00 0.00
<Reference>	-----	4*	900.0- 975.0	3.00 0.00
0.000 mg	<Sampling>	<Gas>		
	1.0 sec	n2	100.0 ml/min	
		co2	100.0 ml/min	

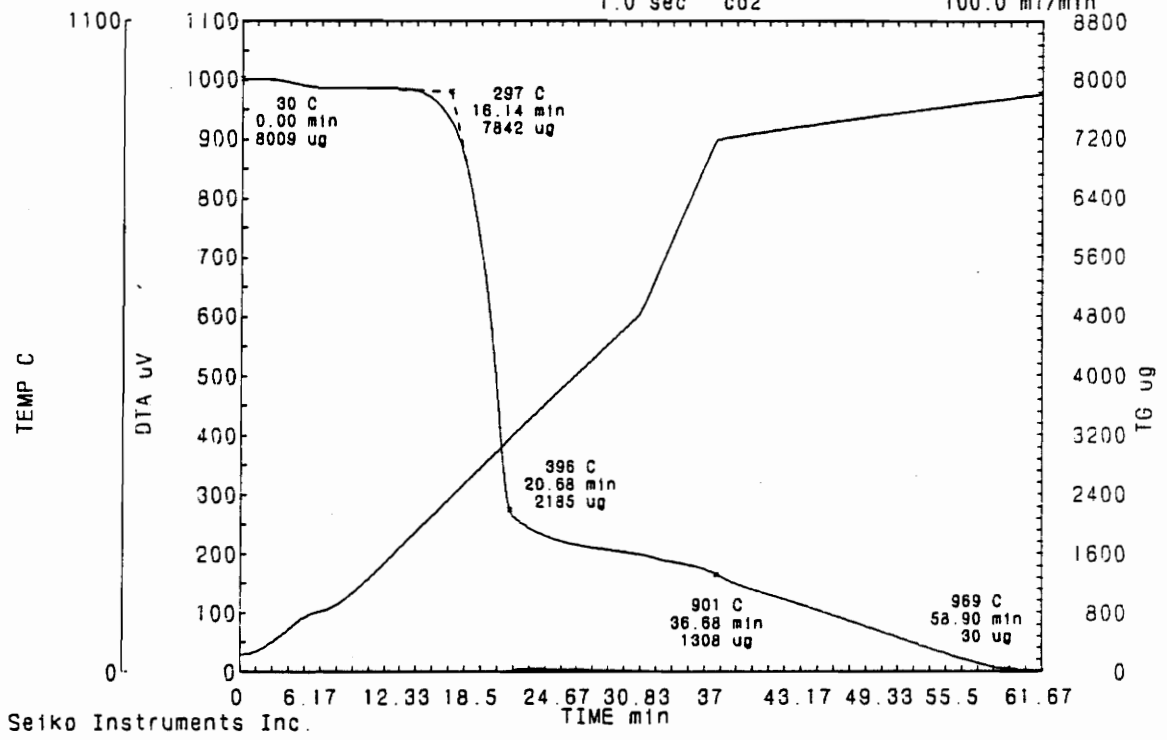


Figure 17. Thermogravimetric plot of Run 18: HTT 600°C.

TG/DTA

<Name>	<Sample>	<Comment>	<Temp.program(C)	[C/min]	[min]
gas19.600	Doug. fir chips	HTT 600	1*	30.0- 110.0	20.00 2.00
<Date>	7.940 mg	-----	2*	110.0- 600.0	20.00 0.00
92/04/16 16:56	( 7.940 mg)	-----	3*	600.0- 900.0	50.00 0.00
	<Reference>	-----	4*	900.0- 985.0	3.00 0.00
	0.000 mg	<Sampling>	<Gas>		
		1.0 sec	n2	100.0 ml/min	
			co2	100.0 ml/min	

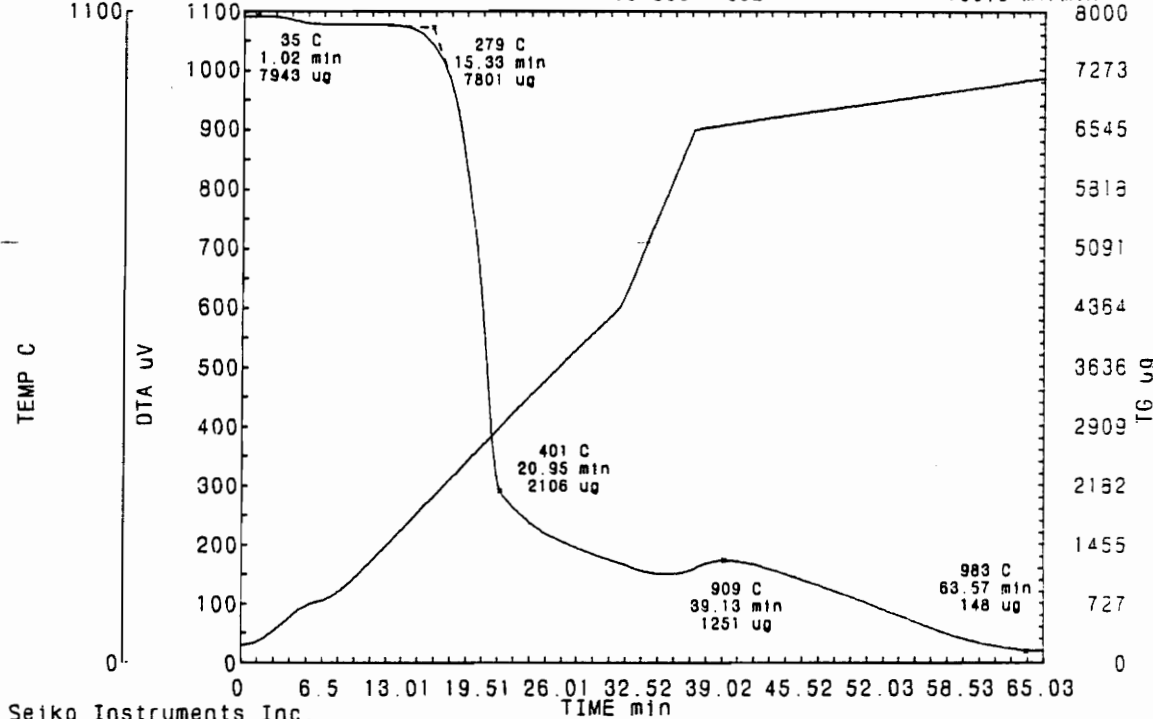


Figure 18. Thermogravimetric plot of Run 19: HTT 600°C.

TG/DTA

<Name>  
gas20.600  
<Date>  
92/04/17 01:34

<Sample>	<Comment>	<Temp.program(C)	(C/min)	(min)
Doug. fir chips	HTT 600	1*	30.0- 110.0	20.00 2.00
7.918 mg	-----	2*	110.0- 600.0	20.00 0.00
( 7.918 mg)	-----	3*	600.0- 900.0	50.00 0.00
<Reference>	-----	4*	900.0- 990.0	3.00 0.00
-----	-----	<Gas>		
0.000 mg	<Sampling>	n2	100.0 ml/min	
	1.0 sec	co2	100.0 ml/min	

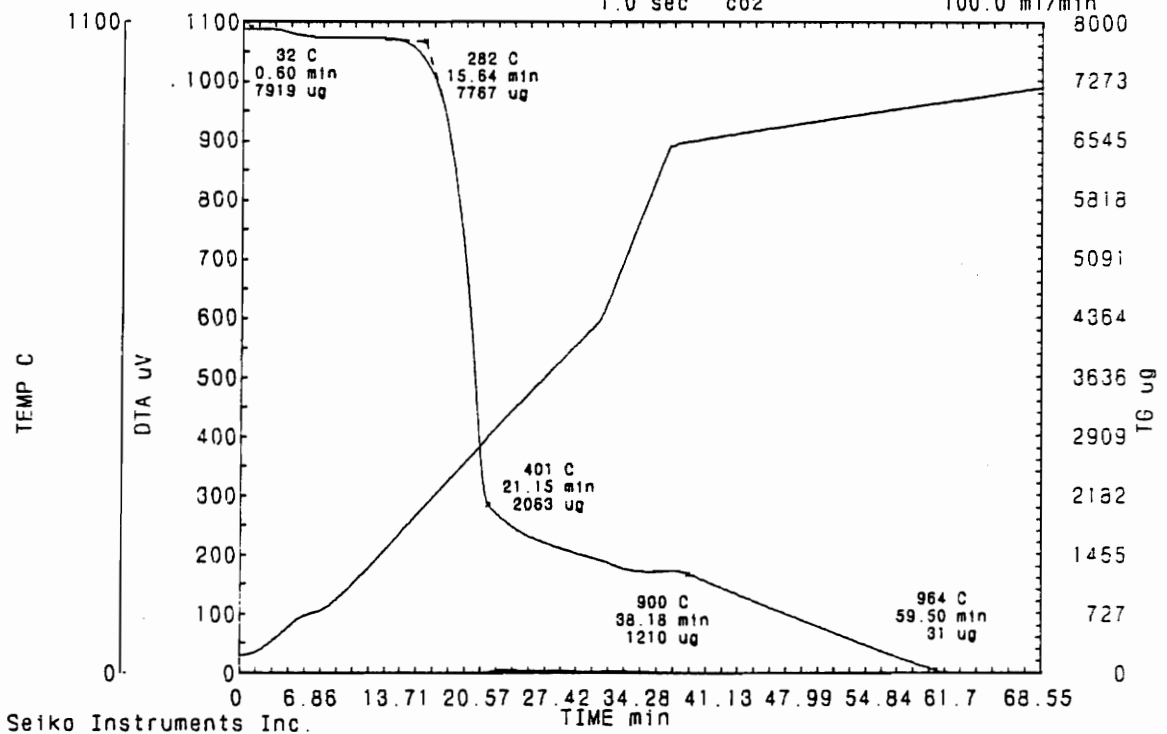


Figure 19. Thermogravimetric plot of Run 20: HTT 600°C.

TG/DTA

<Name>  
gas21.600  
<Date>  
92/04/17 12:02

<Sample>	<Comment>	<Temp.program(C)	[C/min]	[min]
Doug. fir chips	HTT 600	1*	30.0- 110.0	20.00 2.00
7.985 mg	-----	2*	110.0- 600.0	20.00 0.00
( 7.985 mg)	-----	3*	600.0- 900.0	50.00 0.00
<Reference>	-----	4*	900.0-1000.0	3.00 0.00
0.000 mg	<Sampling>	<Gas>		
	1.0 sec	n2	100.0 ml/min	
		co2	100.0 ml/min	

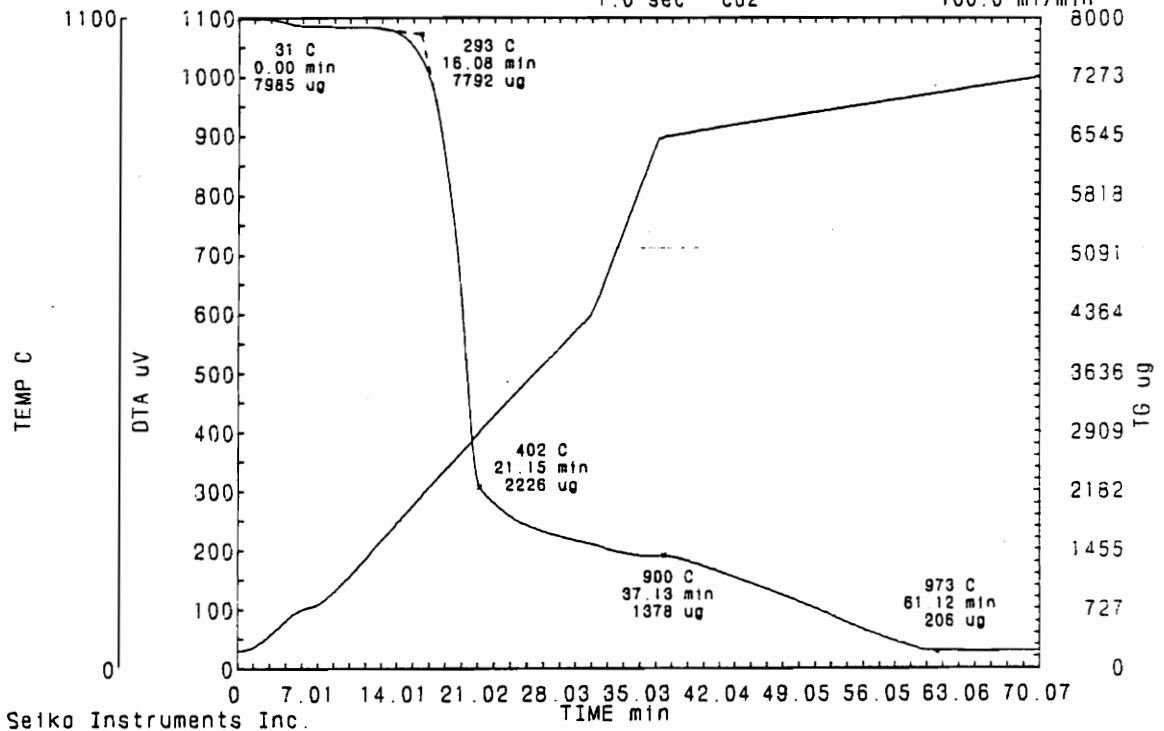


Figure 20. Thermogravimetric plot of Run 21: HTT 600°C.

TG/DTA	<Sample>	<Comment>	<Temp.program(C) [C/min] [min]>
<Name>	Doug. fir chips	HTT 600	1* 30.0- 110.0 20.00 2.00
gas22.900	8.032 mg	-----	2* 110.0- 900.0 20.00 0.00
<Date>	( 8.032 mg)	-----	3* 900.0- 900.0 50.00 0.00
92/04/18 01:23	<Reference>	-----	4* 900.0- 973.0 3.00 0.00
	0.000 mg	<Sampling>	<Gas>
		1.0 sec	n2 100.0 ml/min
			co2 100.0 ml/min

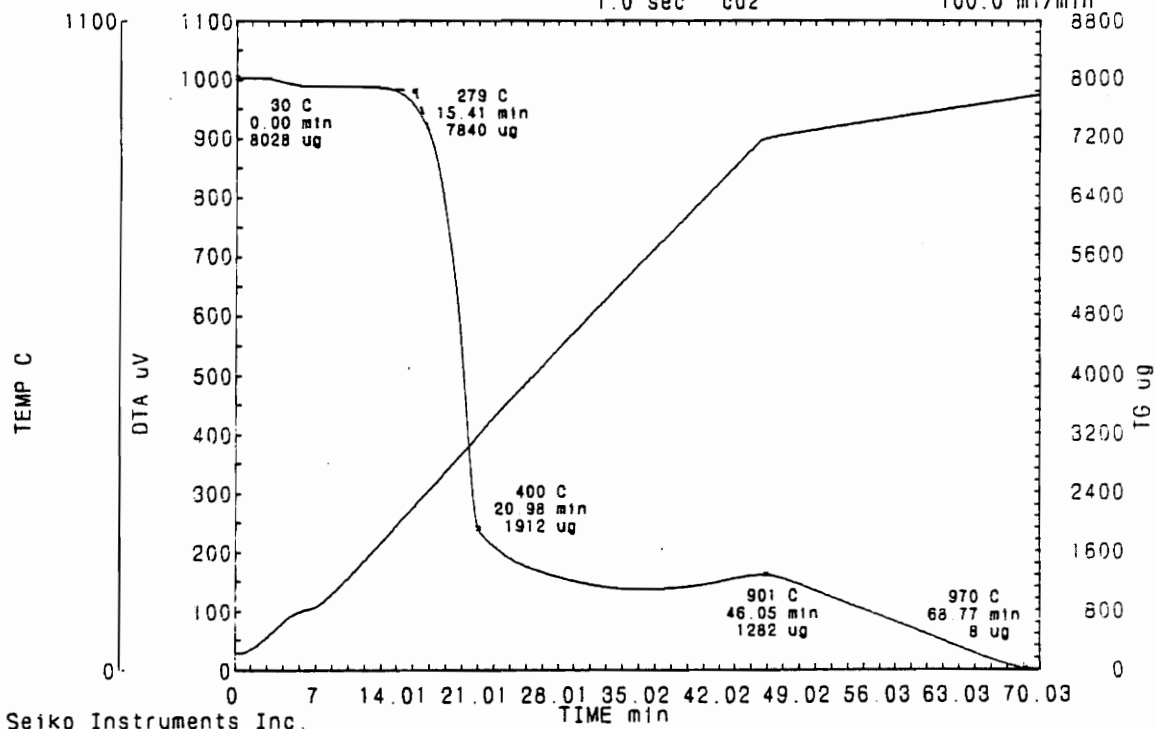
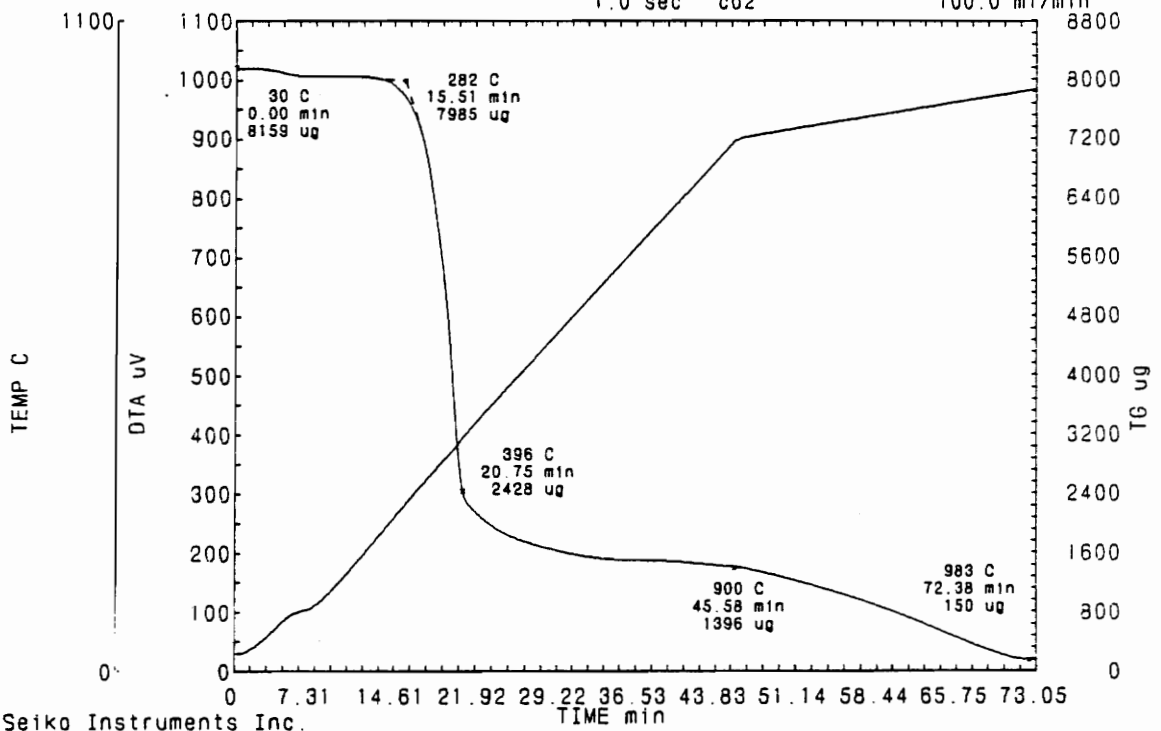


Figure 21. Thermogravimetric plot of Run 22: HTT 900°C.

TG/DTA

<Name>  
gas23.900  
<Date>  
92/04/19 02:38

<Sample>	<Comment>	<Temp.program(C) [C/min] [min]>	
Doug. fir chips	HTT 600	1* 30.0- 110.0	20.00 2.00
8.160 mg	-----	2* 110.0- 900.0	20.00 0.00
( 8.160 mg)	-----	3* 900.0- 900.0	50.00 0.00
<Reference>	-----	4* 900.0- 982.0	3.00 0.00
0.000 mg	<Sampling>	<Gas>	
	1.0 sec	n2	100.0 ml/min
		co2	100.0 ml/min



Seiko Instruments Inc.

Figure 22. Thermogravimetric plot of Run 23: HTT 900°C.

TG/DTA

<Name>  
gas24.900  
<Date>  
92/04/21 02:05

<Sample>	<Comment>	<Temp.program[C]>	[C/min]	[min]
Doug. fir chips	HTT 900	1*	31.0- 110.0	20.00 2.00
8.072 mg	-----	2*	110.0- 900.0	20.00 0.00
( 8.072 mg)	-----	3*	900.0- 900.0	50.00 0.00
<Reference>	-----	4*	900.0- 980.0	3.00 0.00
0.000 mg	<Sampling>	<Gas>		
	1.0 sec	n2	100.0 ml/min	
		co2	100.0 ml/min	

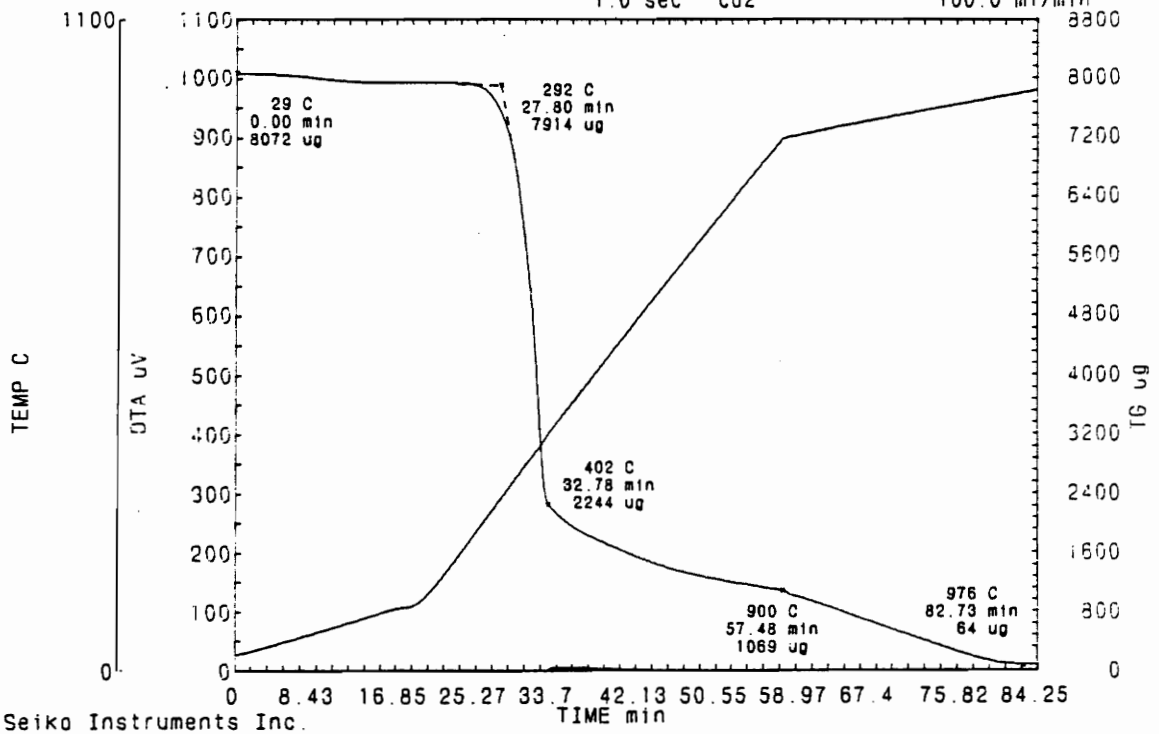


Figure 23. Thermogravimetric plot of Run 24: HTT 900°C.

TG/DTA

<Name>	<Sample>	<Comment>	<Temp.program[C]>	[C/min]	[min]
after.1	pinus radiata	-----	1*	30.0- 110.0	20.00 2.00
<Date>	7.913 mg	-----	2*	110.0- 900.0	20.00 0.00
92/06/22 19:59	( 7.913 mg)	-----	3*	900.0- 950.0	3.00 0.00
	<Reference>	-----	4*	950.0-1000.0	20.00 0.00
	0.000 mg	<Sampling>	<Gas>		
		1.0 sec	n2	100.0 ml/min	
			co2	100.0 ml/min	

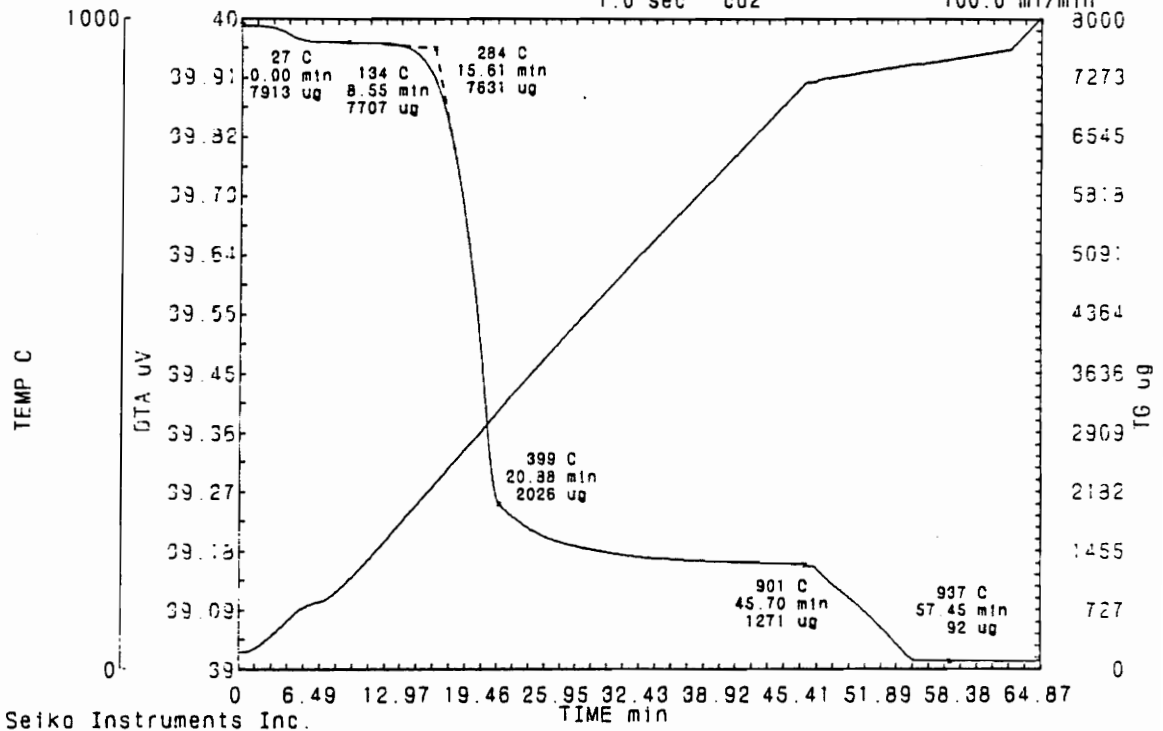


Figure 24. Thermogravimetric plot of Run A1: HTT 900°C.

TG/DTA  
 <Name>  
 after.2  
 <Date>  
 92/06/23 15:51

<Sample>	<Comment>	<Temp.program[C]	[C/min]	(min)
pinus radiata	Monterey pine	1*	30.0-110.0	20.00 2.00
8.132 mg	-----	2*	110.0-900.0	20.00 0.00
( 8.132 mg)	-----	3*	900.0-950.0	3.00 0.00
<Reference>	-----	4*	950.0-1000.0	20.00 0.00
0.000 mg	<Sampling>	<Gas>		
	1.0 sec	n2	100.0 ml/min	
		co2	100.0 ml/min	

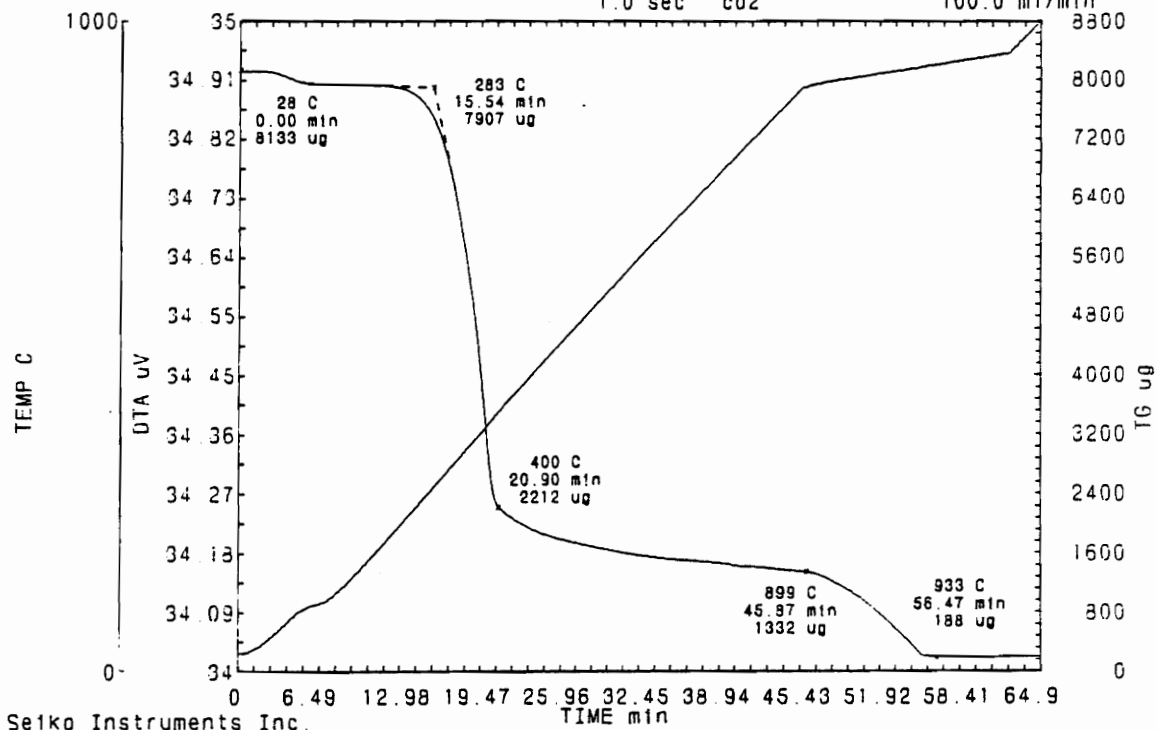


Figure 25. Thermogravimetric plot of Run A2: HTT 900°C.

TG/DTA

<Name>  
after.3  
<Date>  
92/06/24 14:41

<Sample>	<Comment>	<Temp.program[C]>	[C/min]	[min]
pinus radiata	Monterey pine	1*	30.0- 110.0	20.00 2.00
8.042 mg	-----	2*	110.0- 900.0	20.00 0.00
( 8.042 mg)	-----	3*	900.0- 950.0	3.00 0.00
<Reference>	-----	4*	950.0-1000.0	20.00 0.00
0.000 mg	<Sampling>	<Gas>		
	1.0 sec	n2	100.0 ml/min	
		co2	100.0 ml/min	

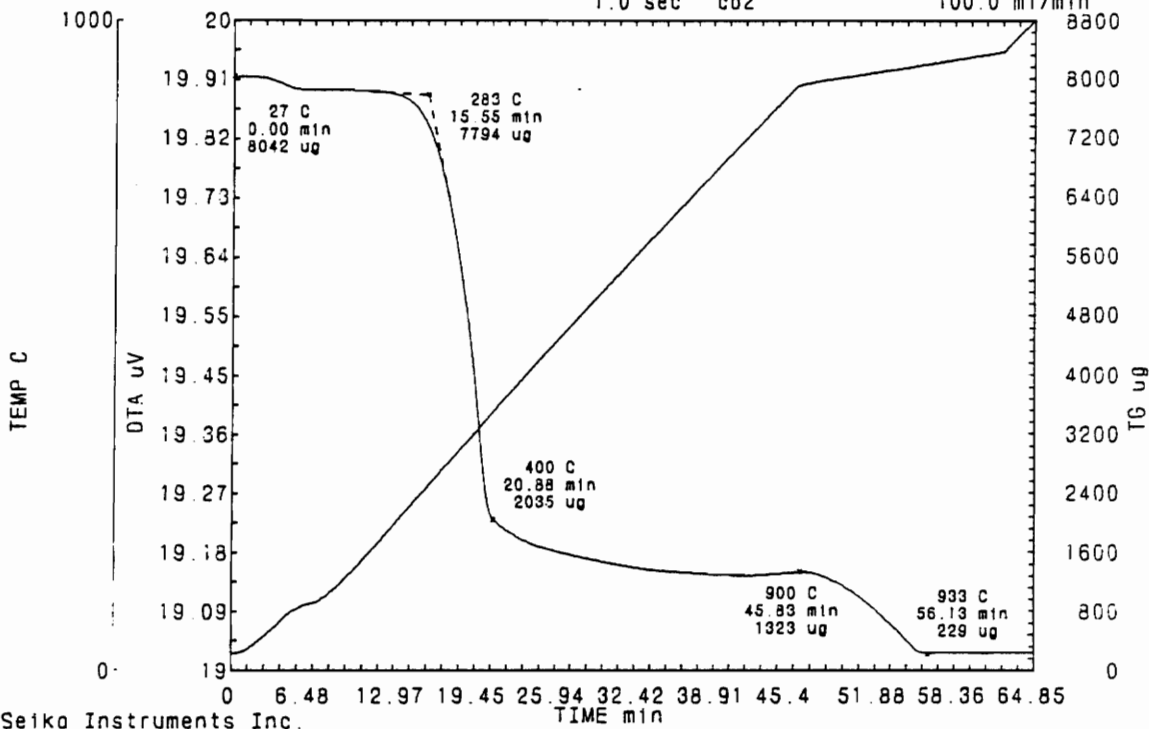


Figure 26. Thermogravimetric plot of Run A3: HTT 900°C.

TG/DTA

<Name>  
after.4  
<Date>  
92/06/24 20:31

<Sample>	<Comment>	<Temp.program(C)>	[C/min]	[min]
pinus radiata	Monterey pine	1*	30.0- 110.0	20.00 2.00
7.978 mg	-----	2*	110.0- 900.0	20.00 0.00
( 7.978 mg)	-----	3*	900.0- 950.0	3.00 0.00
<Reference>	-----	4*	950.0-1000.0	20.00 0.00
0.000 mg	<Sampling>	<Gas>		
	1.0 sec	n2	100.0 ml/min	
		co2	100.0 ml/min	

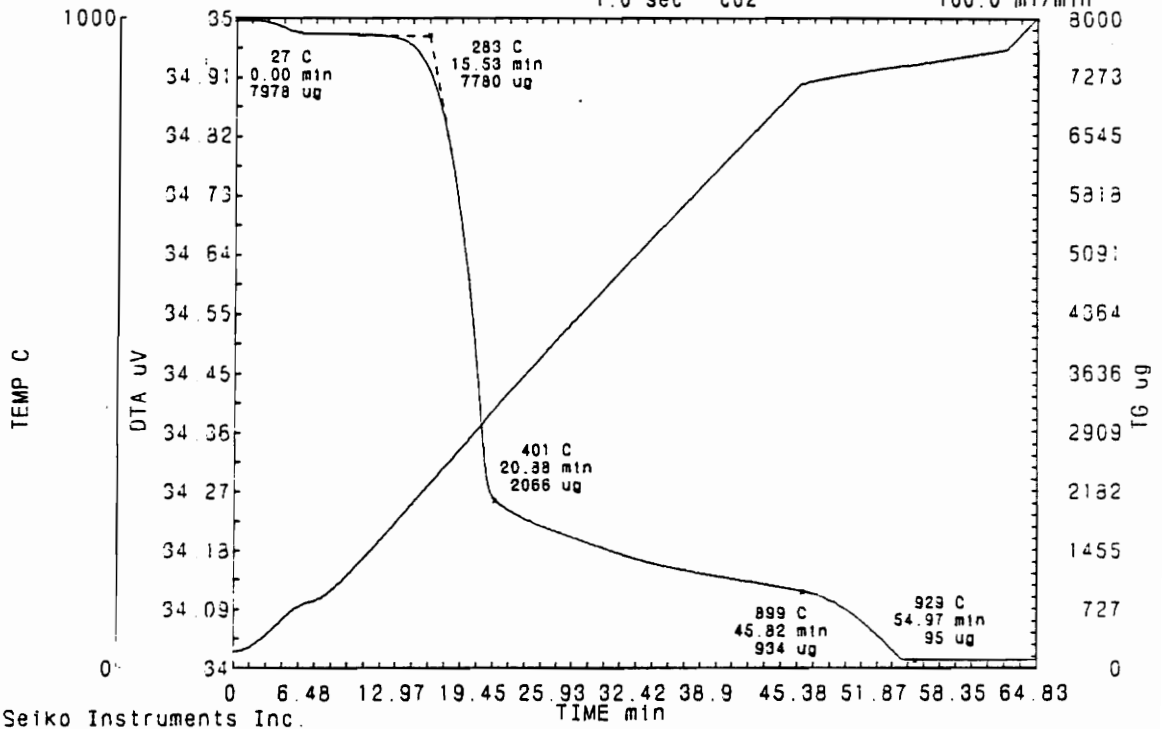
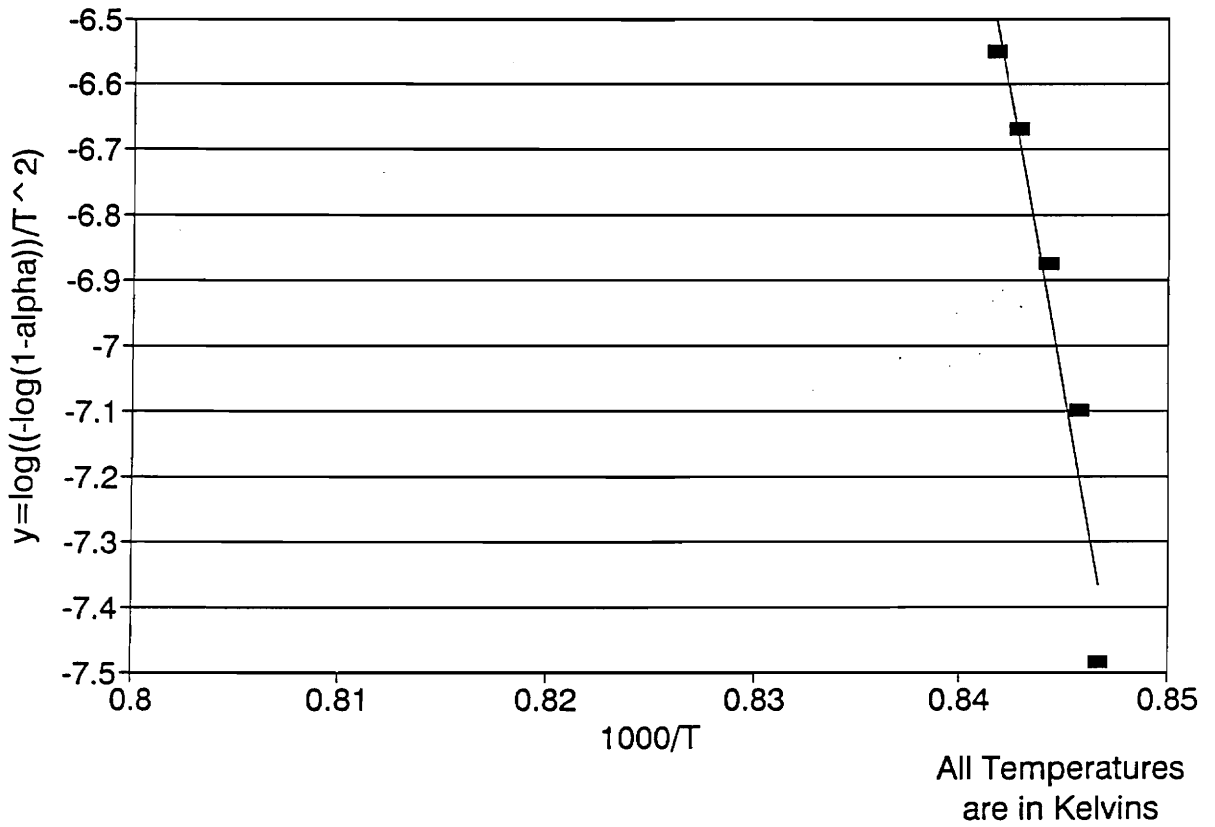


Figure 27. Thermogravimetric plot of Run A4: HTT 900°C.

## Appendix B. Coats-Redfern Kinetic Plots

This appendix presents the Coats-Redfern kinetic plots for Runs 9-11, 13, 15-22, 24, and A1-A4 from which the slope and y-intercept was used to calculate the activation energies and preexponential constants. The curves with an "A" are runs that used Monterey pine instead of Douglas fir. They are all presented over the same range of values for comparison.



**Figure 28. Coats-Redfern kinetic plot of Run 9: HTT 900°C.**

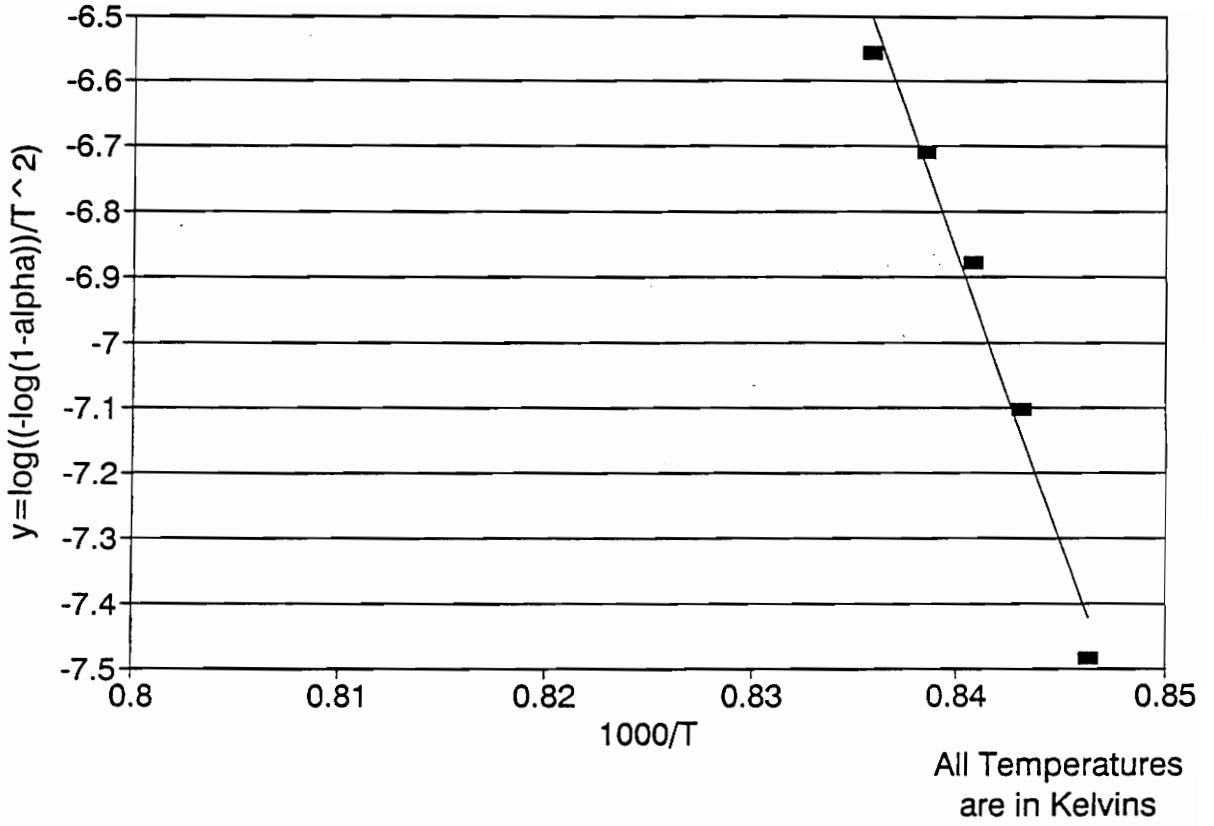


**Figure 29. Coats-Redfern kinetic plot of Run 10: HTT 900°C.**

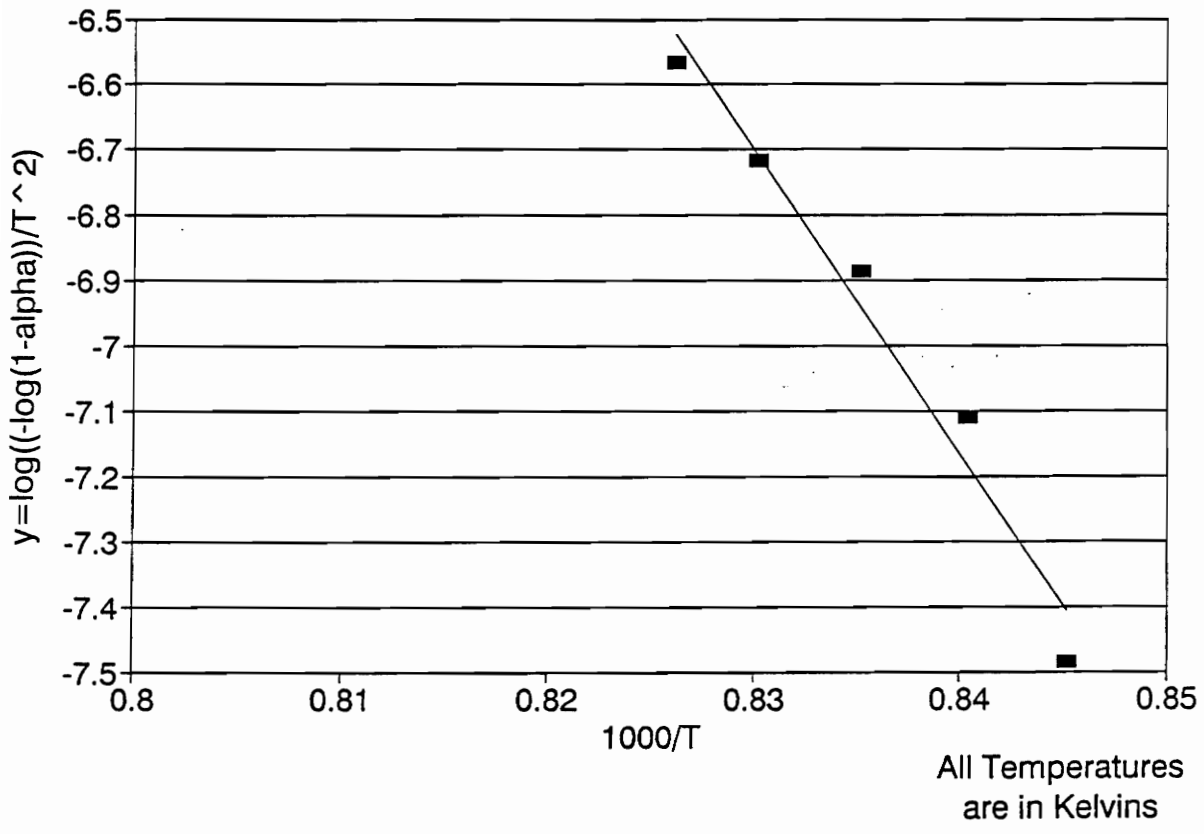


**Figure 30. Coats-Redfern kinetic plot of Run 11: HTT 900°C.**

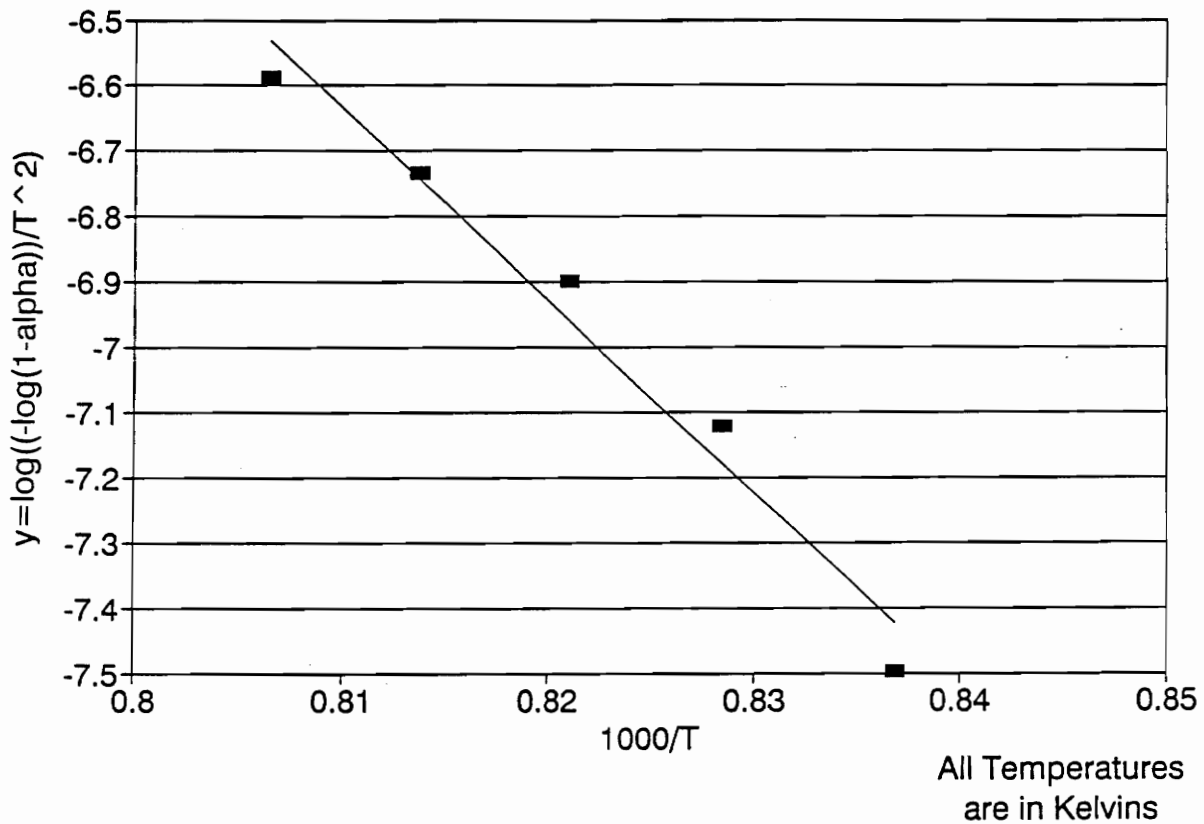
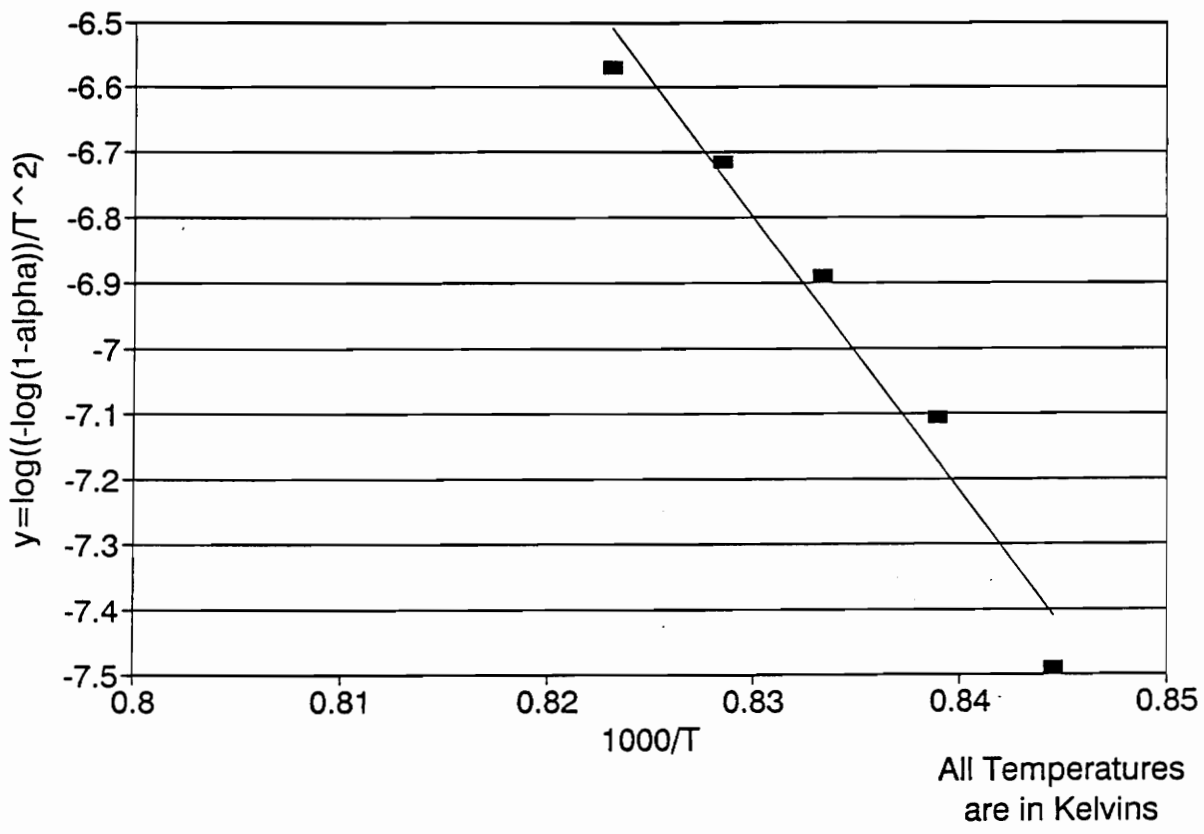
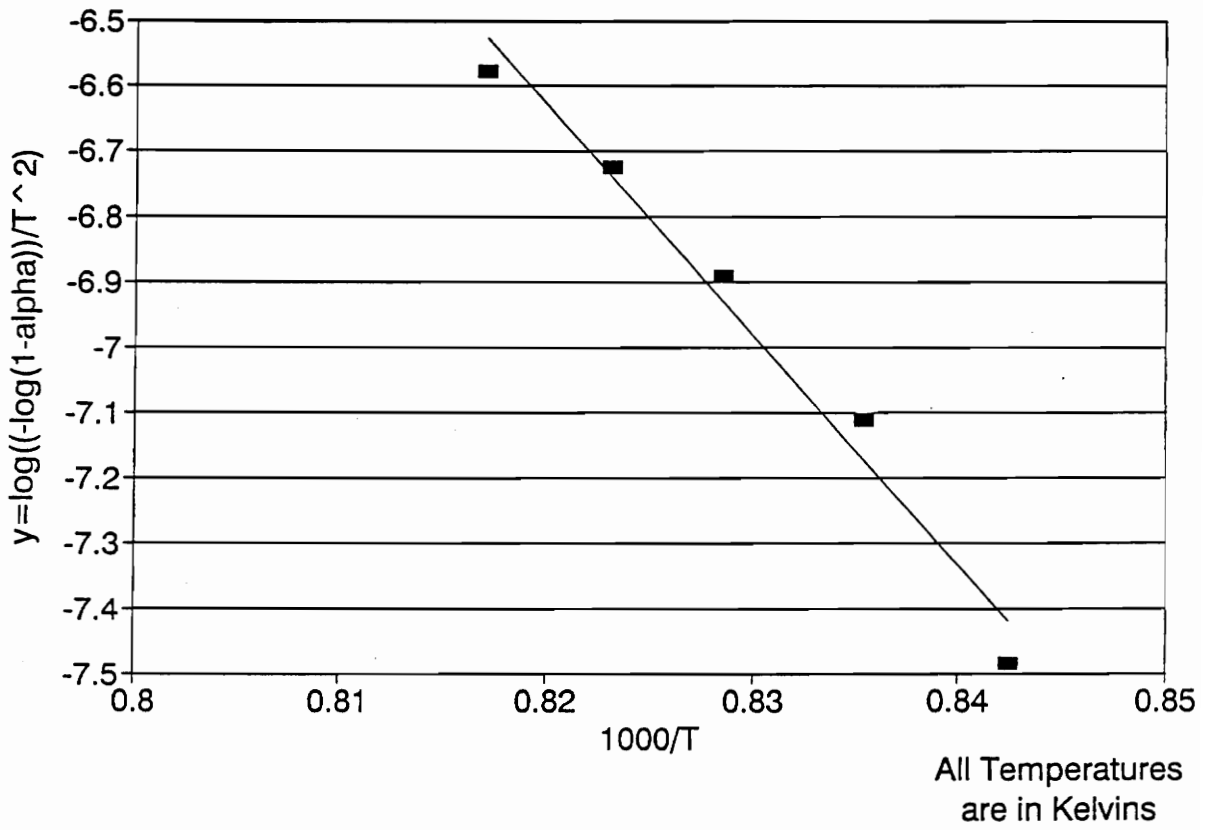


Figure 31. Coats-Redfern kinetic plot of Run 13: HTT 750°C.



**Figure 32. Coats-Redfern kinetic plot of Run 15: HTT 750°C.**



**Figure 33. Coats-Redfern kinetic plot of Run 16: HTT 750°C.**

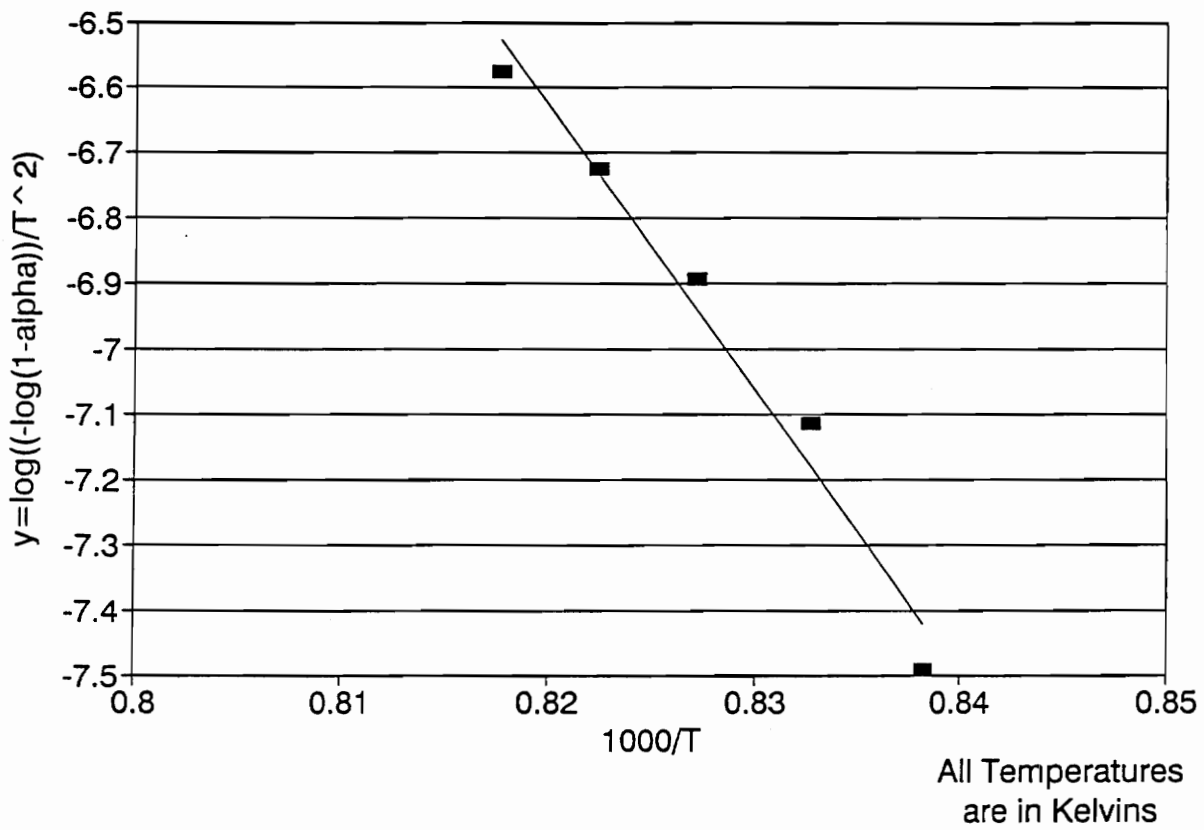


**Figure 34. Coats-Redfern kinetic plot of Run 17: HTT 750°C.**

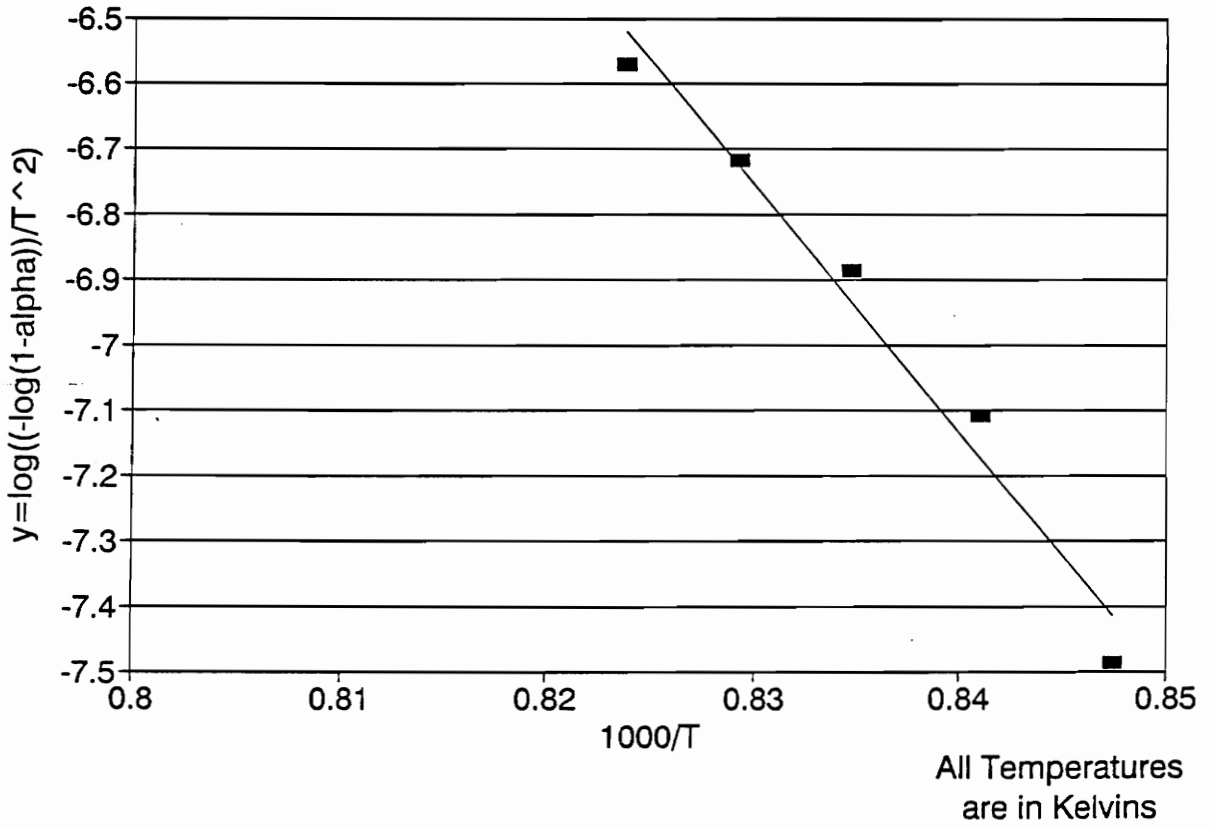


**Figure 35. Coats-Redfern kinetic plot of Run 18: HTT 600°C.**

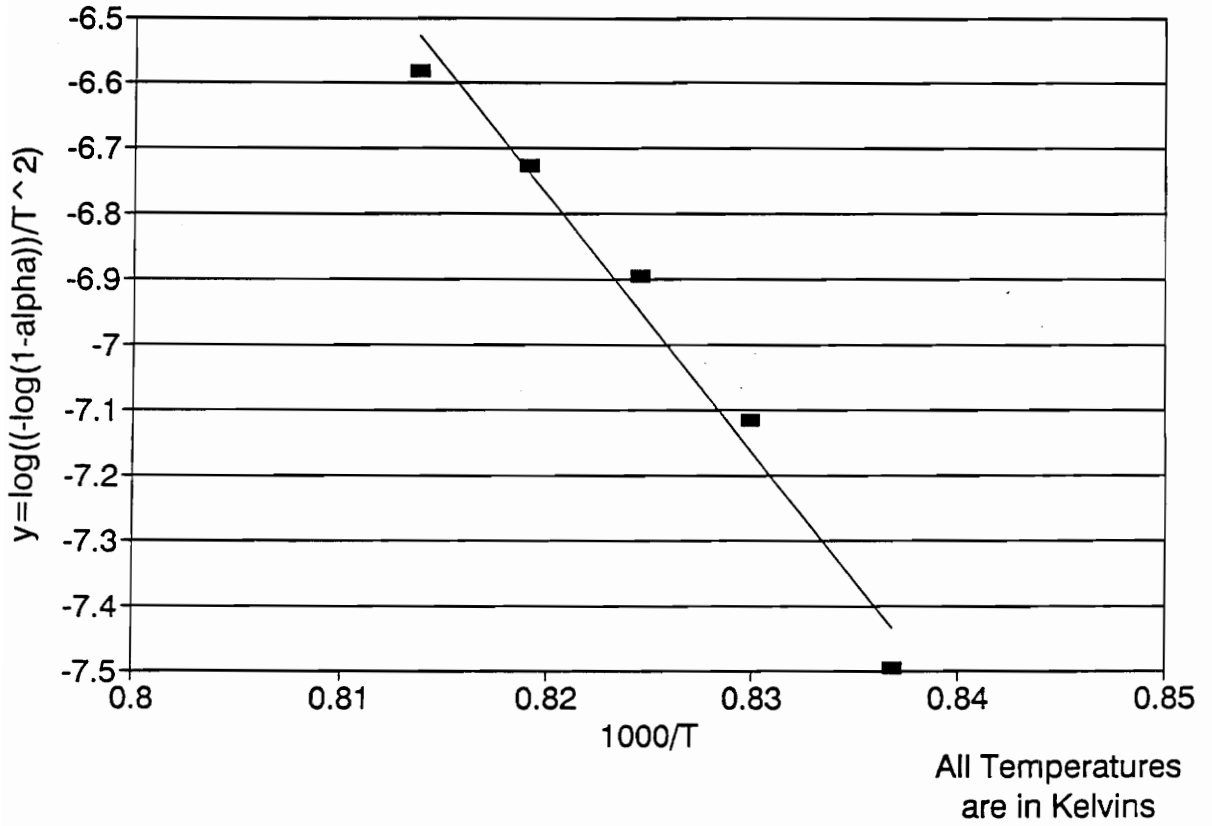


**Figure 36. Coats-Redfern kinetic plot of Run 19: HTT 600°C.**

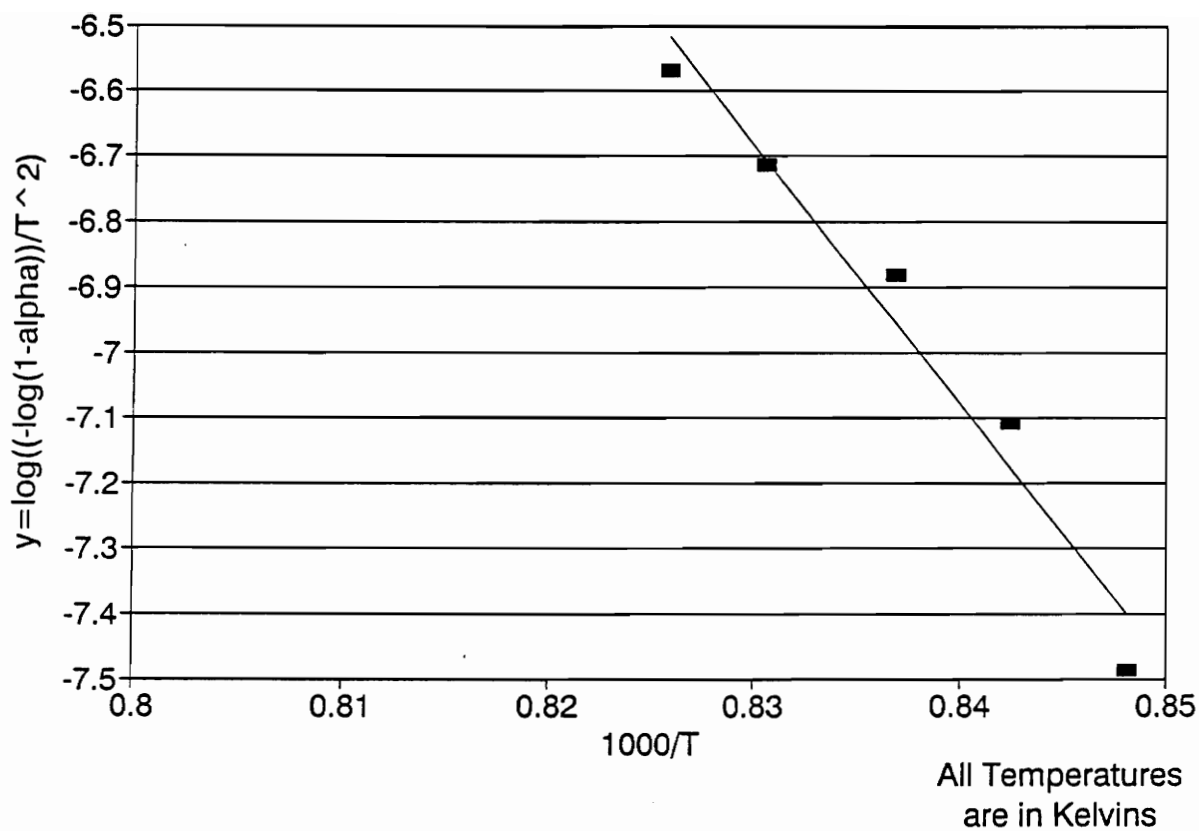


**Figure 37. Coats-Redfern kinetic plot of Run 20: HTT 600°C.**

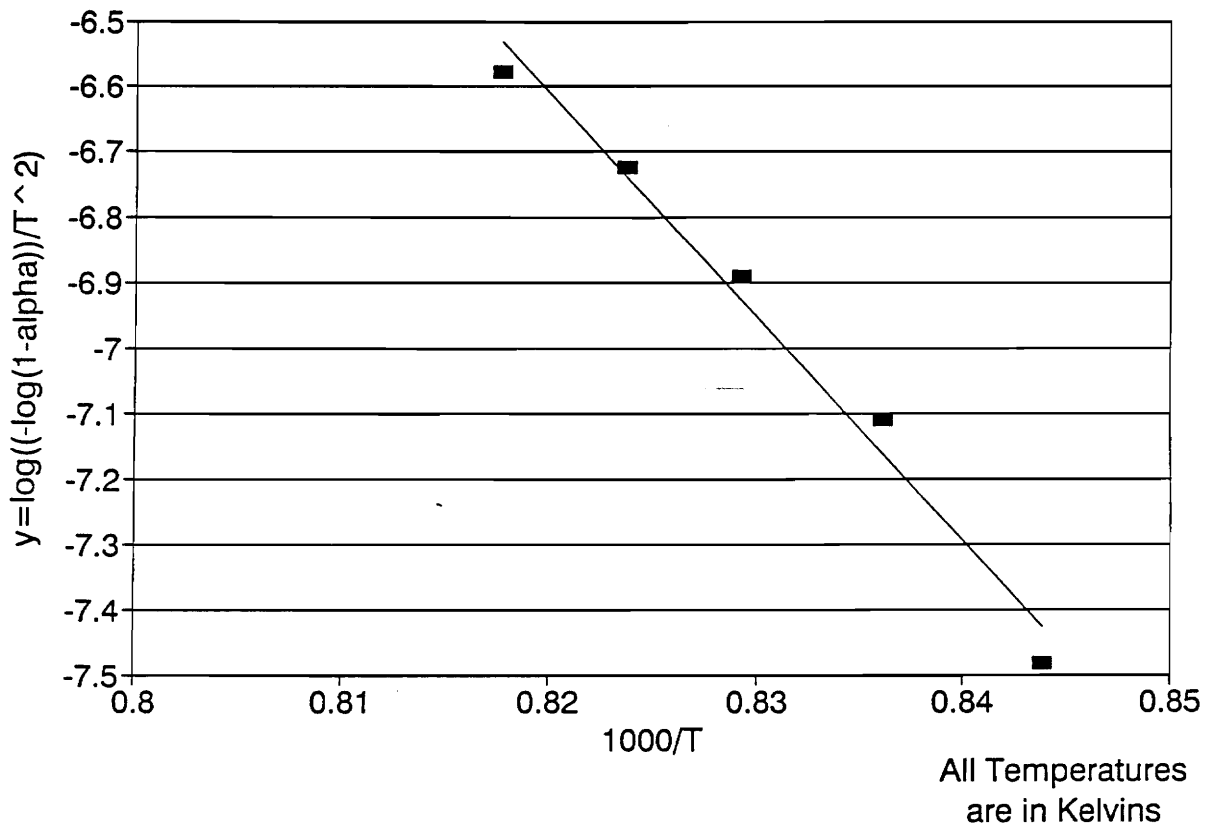
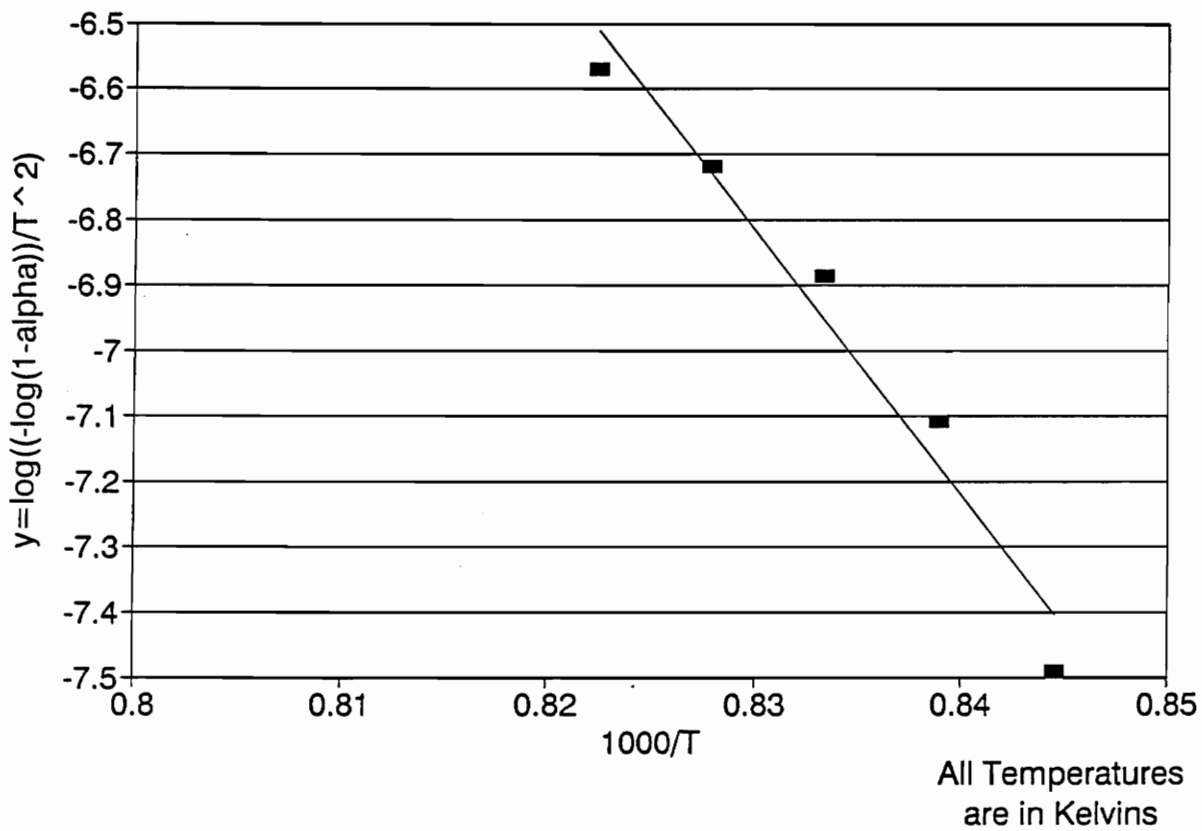
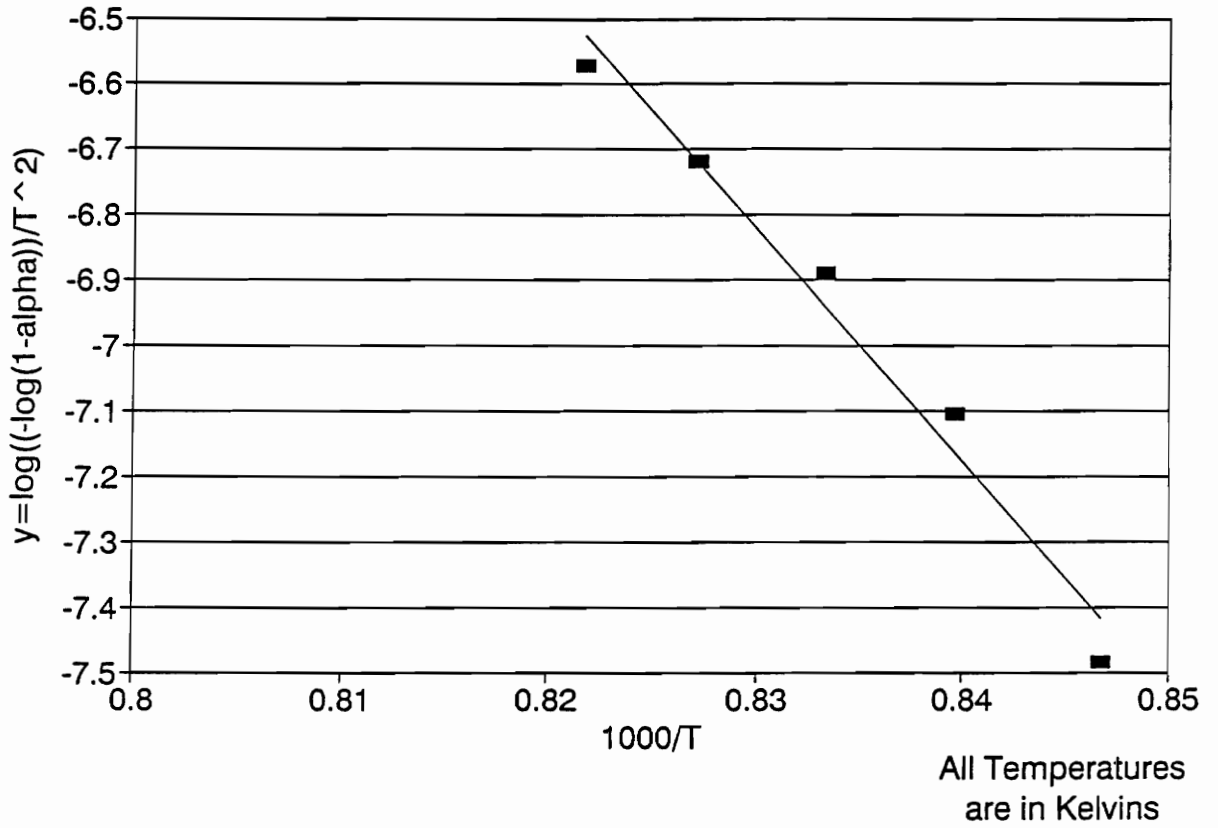


Figure 38. Coats-Redfern kinetic plot of Run 21: HTT 600°C.



**Figure 39. Coats-Redfern kinetic plot of Run 22: HTT 900°C.**



**Figure 40. Coats-Redfern kinetic plot of Run 24: HTT 900°C.**

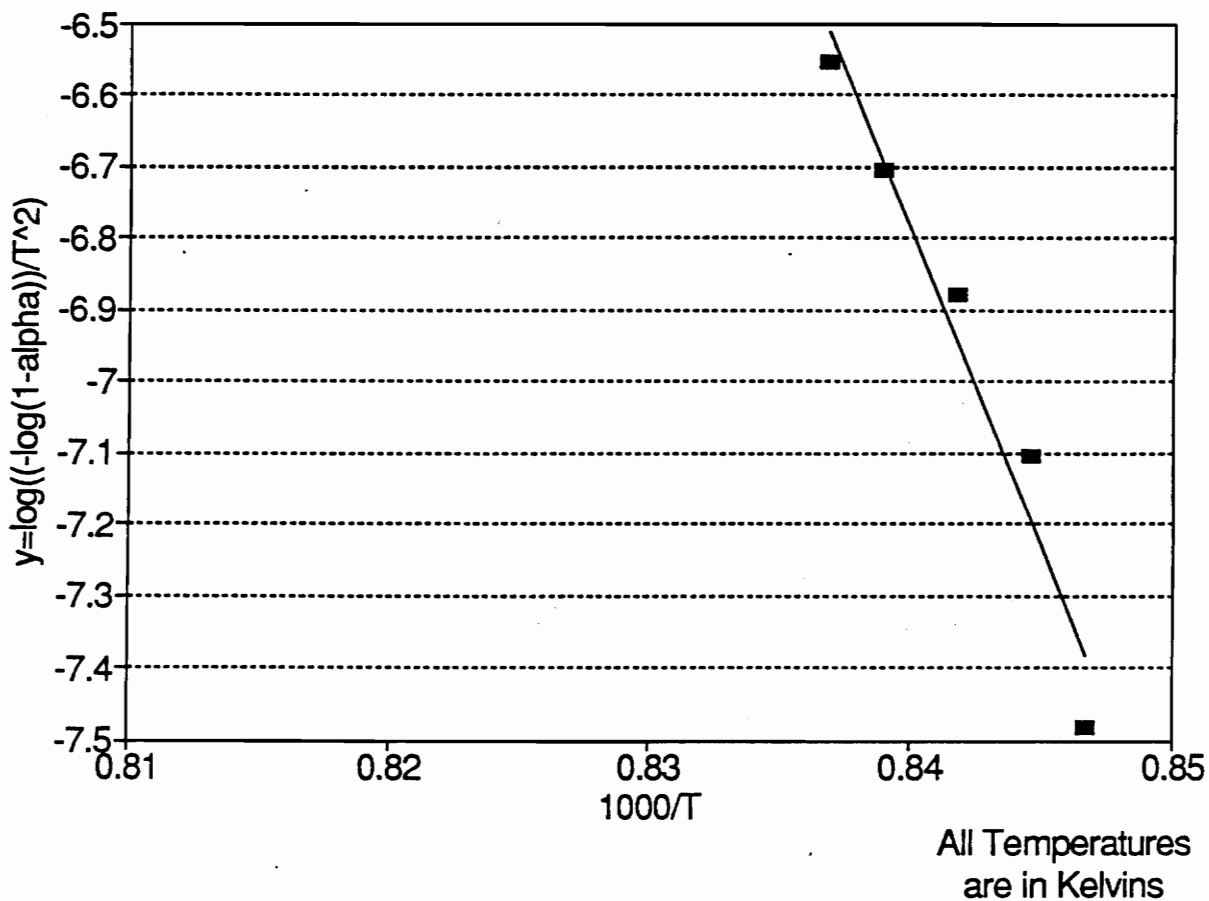


**Figure 41. Coats-Redfern kinetic plot of Run A1: HTT 900°C.**

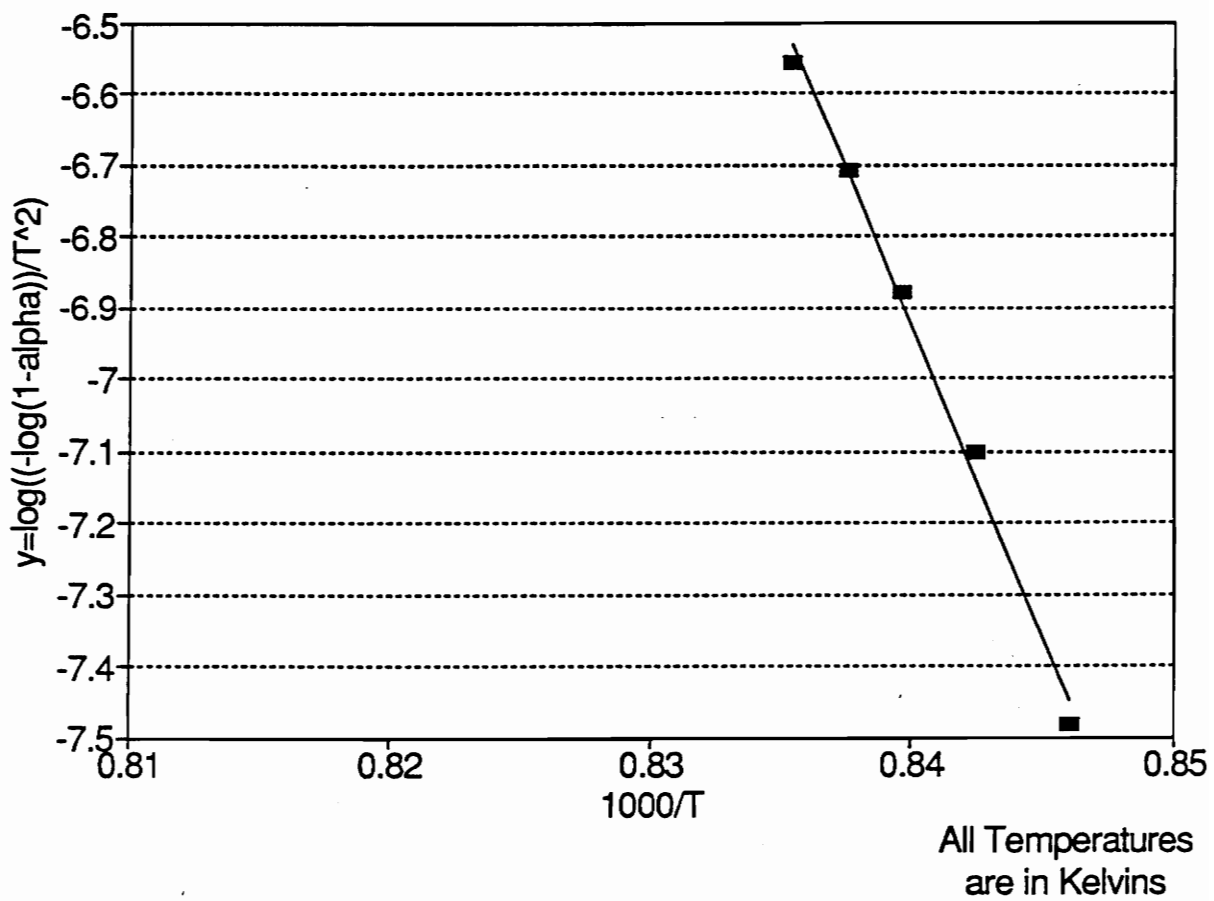


**Figure 42. Coats-Redfern kinetic plot of Run A2: HTT 900°C.**

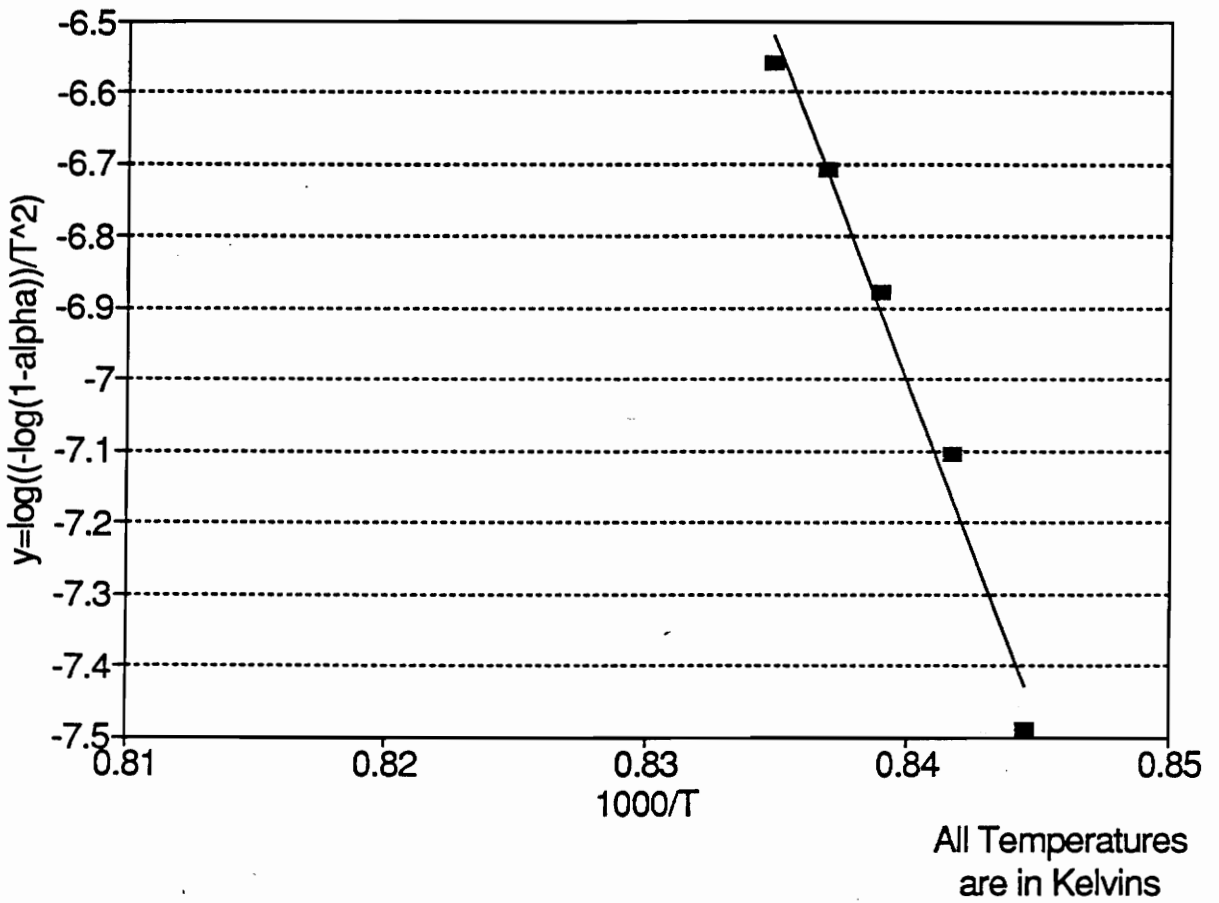
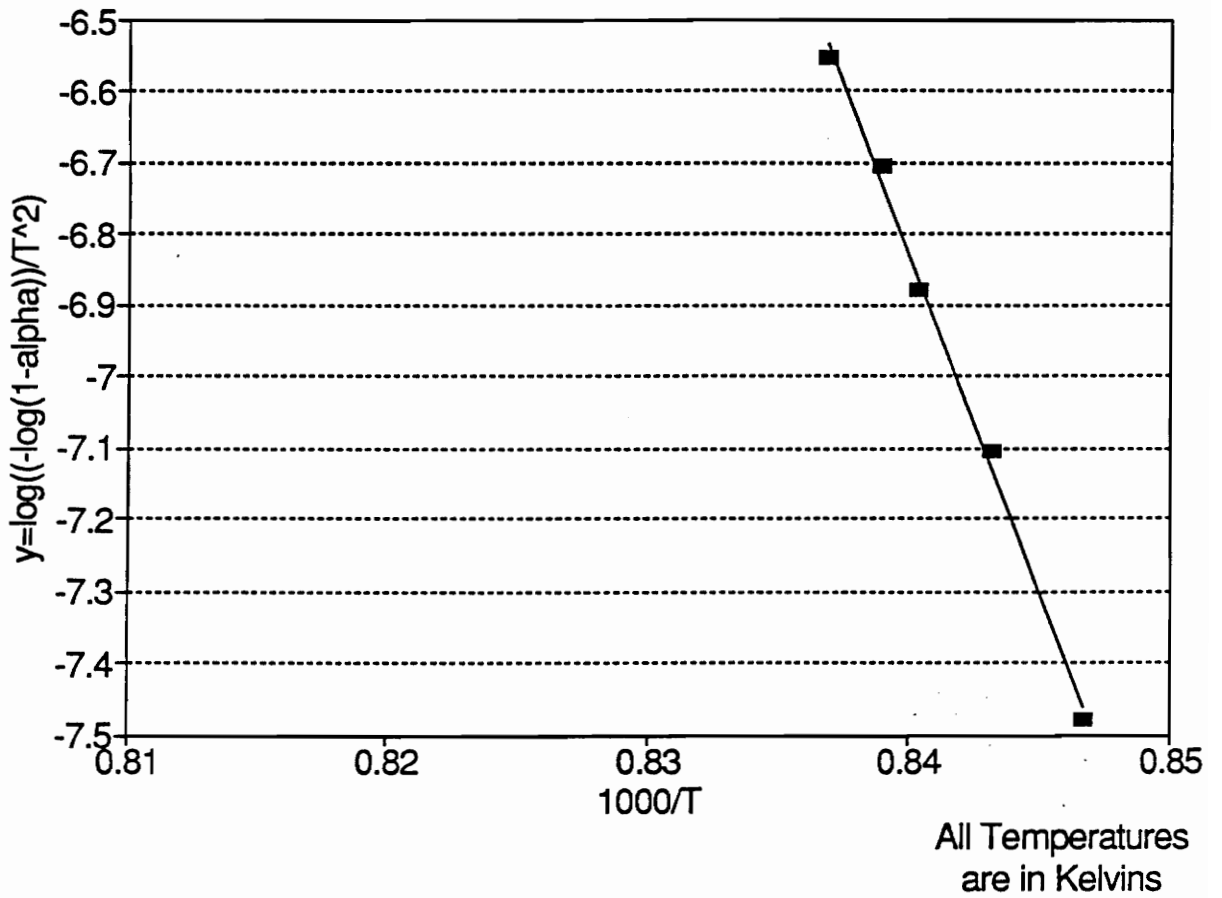


Figure 43. Coats-Redfern kinetic plot of Run A3: HTT 900°C.



**Figure 44. Coats-Redfern kinetic plot of Run A4: HTT 900°C.**

## Appendix C. Numerical Data

This appendix contains the data obtained from each run and used to calculate apparent activation energies. At the end of the data are four runs labeled with an "A," which used Monterey pine instead of Douglas fir. A sample calculation of the apparent activation energy and preexponential factor for one run follows the data.

### Char HTT 600°C

Run #	Weight Fraction Decomposed	Temperature (K)	Activation Energy (kJ/mole)	ln A
18	0.0994	1180		
	0.2248	1189		
	0.3494	1198		
	0.4748	1206		
	0.5994	1214	721.2	69.0
19	0.0999	1195		
	0.2262	1205		
	0.3509	1213		
	0.4764	1221		
	0.5995	1229	748.6	70.8
20	0.0992	1179		
	0.2240	1187		
	0.3512	1195		
	0.4760	1204		
	0.5992	1211	753.3	72.4

**Char HTT 600°C (cont.)**

Run #	Weight Fraction Decomposed	Temperature (K)	Activation Energy (kJ/mole)	ln A
21	0.1009	1185	654.0	61.7
	0.2257	1196		
	0.3505	1206		
	0.4739	1214		
	0.5980	1223		

**Char HTT 750°C**

13	0.0993	1195	562.4	51.8
	0.2245	1207		
	0.3510	1218		
	0.4750	1229		
	0.6009	1240		
15	0.0992	1184	800.7	77.0
	0.2263	1192		
	0.3490	1200		
	0.4761	1207		
	0.6005	1215		
16	0.1011	1187	669.8	63.3
	0.2253	1197		
	0.3503	1207		
	0.4745	1215		
	0.5995	1224		
17	0.1001	1193	832.4	79.6
	0.2260	1201		
	0.3503	1209		
	0.4746	1216		
	0.5997	1223		

**Char HTT 900°C**

9	0.1001	1181	3410	345
	0.2265	1182		
	0.3506	1185		
	0.5019	1187		
	0.6005	1188		
10	0.1002	1182	1667	166
	0.2258	1186		
	0.3506	1189		
	0.4736	1192		
	0.5993	1197		

Char HTT 900°C (cont.)

Run #	Weight Fraction Decomposed	Temperature (K)	Activation Energy (kJ/mole)	ln A
11	0.1001	1183	882.7	85.5
	0.2238	1190		
	0.3494	1197		
	0.4744	1205		
	0.6008	1211		
22	0.0991	1184	769.3	73.7
	0.2254	1192		
	0.3510	1200		
	0.4743	1208		
	0.6006	1216		
23	0.0996	1188	601.8	56.2
	0.2249	1201		
	0.3510	1212		
	0.4756	1221		
	0.6017	1230		
24	0.1001	1181	680.5	64.7
	0.2264	1191		
	0.3489	1200		
	0.4752	1209		
	0.5996	1217		
A1	0.0999	1181	1682	167
	0.2242	1184		
	0.3485	1188		
	0.4752	1192		
	0.5995	1195		
A2	0.1006	1182	1658	165
	0.2230	1187		
	0.3514	1191		
	0.4745	1194		
	0.5999	1197		
A3	0.0998	1184	1764	176
	0.2245	1188		
	0.3515	1192		
	0.4747	1195		
	0.5994	1198		
A4	0.1006	1181	1793	179
	0.2248	1186		
	0.3501	1190		
	0.4764	1192		
	0.5996	1195		

What follows is a sample calculation of the activation energy and preexponential factor for Run 24 using the temperature and weight fraction decomposed data given above. First, the data must be changed to  $x$  and  $y$  coordinates using the equations from the Coats-Redfern analysis method,

$$y = \log \left\{ \frac{-\log(1 - \alpha)}{T^n} \right\} \quad (n = 1) \quad [2.2.10]$$

$$x = \frac{1}{T} \quad [2.2.11]$$

where  $\alpha$  is the weight fraction decomposed,  $T$  is the temperature, and  $n$  is the reaction order (1 for all cases in this study). These points are assumed to lie along a line described by  $y = mx + b$ . A least-squares fit to a line is used to find the slope ( $m$ ) and the y-intercept ( $b$ ), where

$$m = \frac{N \sum x_i y_i - \sum x_i \sum y_i}{\Delta} \quad [C.1]$$

$$b = \frac{\sum x_i^2 \sum y_i - \sum x_i \sum x_i y_i}{\Delta} \quad [C.2]$$

where  $N$  is the number of data points (5 for all cases in this study), and

$$\Delta = N \sum x_i^2 - [\sum x_i]^2 \quad [C.3]$$

Calculating the needed values from the  $x$  and  $y$  values,

$$\sum x_i = 0.004169$$

$$\sum x_i^2 = 3.48 \times 10^{-6}$$

$$\sum y_i = -34.77$$

$$\sum x_i y_i = -0.029$$

$$\Delta = 1.994 \times 10^{-9}$$

Using these values to calculate the slope and y-intercept of a line that fits the points using Equations C.1 and C.2.

$$m = -35582.3$$

$$b = 22.712$$

In order to determine how well the  $x$  and  $y$  values fit a straight line, the linear correlation coefficient,  $r$ , can be found,

$$r = \frac{\sum (x_i - \bar{x})(y_i - \bar{y})}{\sqrt{\sum (x_i - \bar{x})^2 \sum (y_i - \bar{y})^2}}$$

where  $\bar{x}$  and  $\bar{y}$  are the mean values. The closer the linear correlation coefficient is to one or negative one, the better the fit. In this case  $r$  is found to be 0.987, which indicates a good fit.

Now the apparent activation energy and preexponential factor can be calculated. The apparent activation energy is given by:

$$m = \frac{-E}{2.3R} \quad [2.2.12]$$

where  $E$  is the activation energy and  $R$  is the universal gas constant (8.315 kJ/kmol K in this study). Solving for the activation energy,

$$E = -2.3mR$$

and substituting the known values gives an apparent activation energy of 680.5 kJ/mole. The pre-exponential factor,  $A$  is given by

$$b = \log \left\{ \frac{AR}{aE} \left[ 1 - \frac{2RT}{E} \right] \right\} \quad [2.2.13]$$

where  $a$  is the rate of temperature increase (3°C/min in this study), and  $T$  is the average of the temperature range in Kelvins. Solving this for  $A$ ,

$$A = \frac{10^b aE}{R \left[ 1 - \frac{2RT}{E} \right]}$$

and substituting, gives a preexponential factor of  $1.26 \times 10^{28}$ . For ease of reporting it is customary to present the natural log of the preexponential factor, which in this case is 64.7.

## Appendix D. Effect of Reaction Order on Kinetic Parameters

This appendix presents the effect of changing the assumed reaction order on the activation energy and natural log of the preexponential factor. The parameters were calculated using a reaction order of  $2/3$  and  $1/2$  in the same manner as those using a reaction order of one, as shown in Appendix C. However, the  $y$  values for the kinetic analysis were calculated using Equation 2.2.9 (for reaction orders other than one) instead of Equation 2.2.10 (for reaction orders of one). Typical Coats-Redfern plots for reaction orders of  $2/3$  and  $1/2$  are also presented.

**Table 3. Effect of Reaction Order on Kinetic Parameters.**

Run #	E (kJ/mole)			ln A		
	Reaction Order			Reaction Order		
	1	2/3	1/2	1	2/3	1/2
9	3410	3193	3089	345	323	313
10	1667	1564	1515	166	156	151
11	883	827	801	85	81	78
13	562	527	509	52	49	47
15	801	750	726	77	73	70
16	670	627	607	63	60	58
17	832	780	755	80	75	72
18	721	676	654	69	65	63
19	749	702	679	71	67	65
20	753	706	683	72	68	66
21	654	612	593	62	58	56
22	769	721	697	74	70	67
23	602	564	546	56	53	51
24	680	638	617	65	61	59
<b>% Change:</b>		-6.28	-5.66		-9.31	-8.91

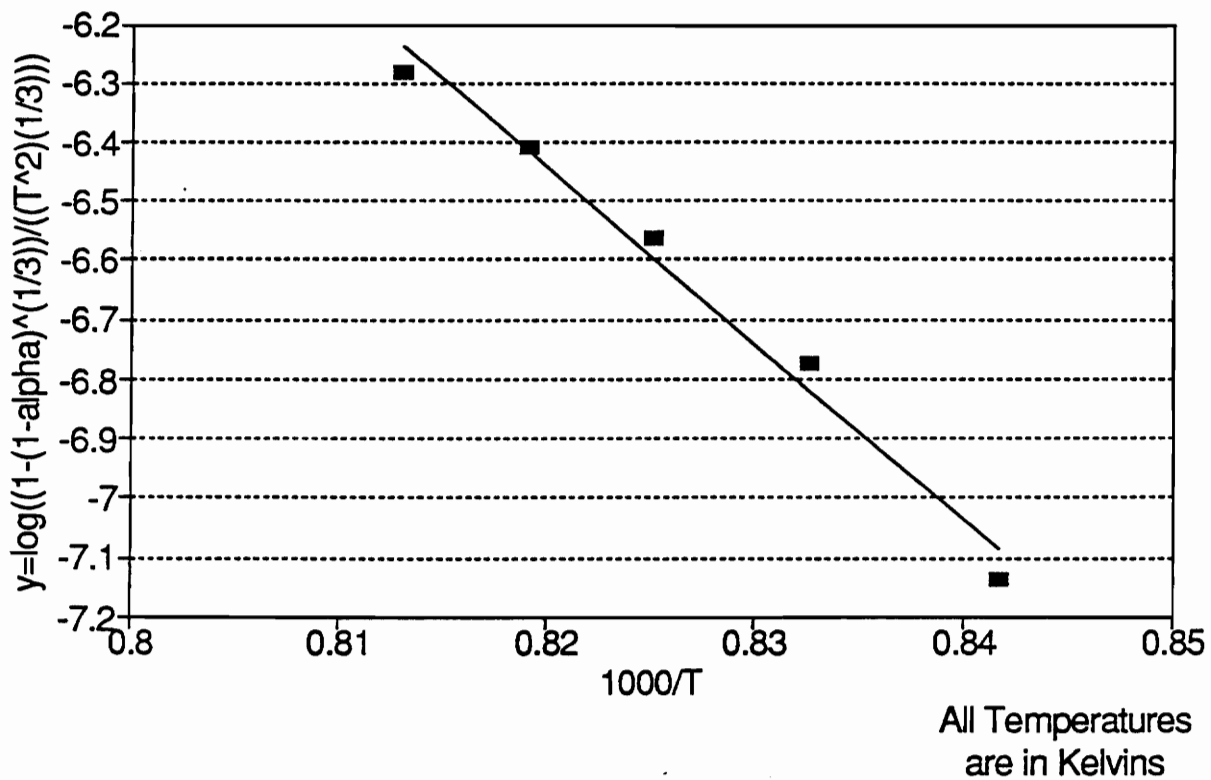


Figure 45. Coats-Redfern plot of Run 23 (reaction order of 2/3): HTT 900°C.

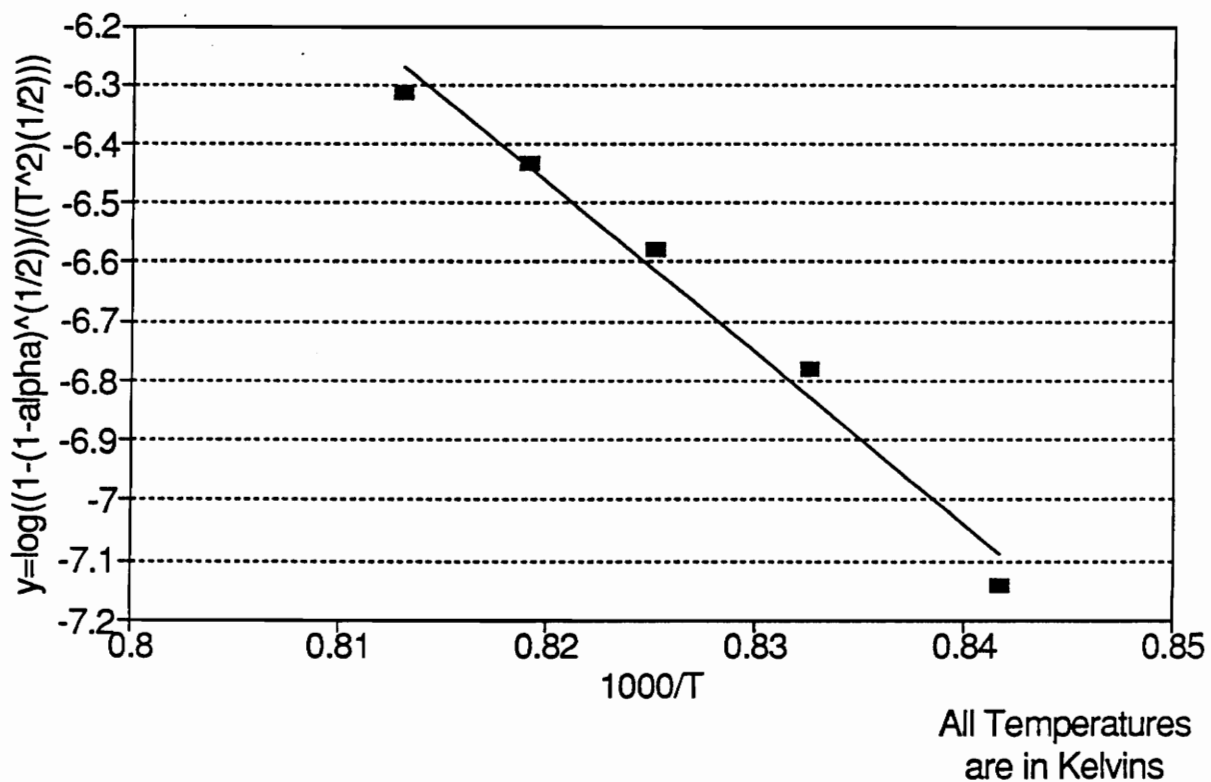


Figure 46. Coats-Redfern plot of Run 23 (reaction order of 1/2): HTT 900°C.

## Appendix E. Verification of TGA

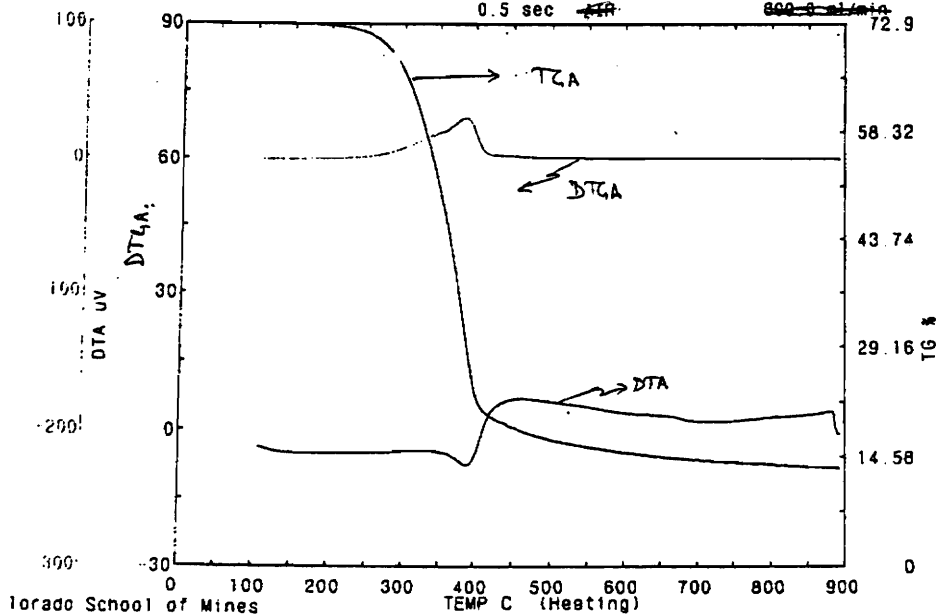
This appendix presents the thermograms of the pyrolysis of Monterey pine under nitrogen performed by another laboratory and using the TGA of this study. The thermogram from Dr. T.B. Reed's laboratory at the Colorado School of Mines is shown in Figure 47, and the thermogram from the TGA used in this study is shown in Figure 48. The difference in weight percent remaining when the initial pyrolysis begins is probably a result of different amounts of moisture initially present in the sample.

TG/DTA  
 <Name> PINUSR.1A  
 <Date> 92/02/08 11:57

<Sample>	<Comment>	<Temp. program(C) (C/min) (min)>
10.000 mg		1- 25.0- 105.0 40.00 6.00
( 10.000 mg)		2- 105.0- 900.0 40.00 6.00
		3- 900.0- 900.0 1.00 10.00
		4- 900.0- 50.0 100.00 0.00
		5- 50.0- 50.0 100.00 0.00

<Reference> 0.000 mg  
 <Sampling> 0.5 sec  
 <Gas> N2 300.0 ml/min  
 800.0 ml/min

*Operating conditions*  
 only Nitrogen used in the area



Colorado School of Mines

JUN-23-92 TUE 13:49

P.02

Figure 47. Pyrolysis of Monterey pine: (Colorado School of Mines).

TG/DTA

<Name>  
verify  
<Date>

92/06/25 20:40

<Sample>	<Comment>	<Temp.program(C)	[C/min]	[min]
pinus radiata	Monterey pine	1*	25.0- 105.0	40.00 6.00
10.160 mg	-----	2*	105.0- 900.0	40.00 6.00
( 10.160 mg)	-----	3*	900.0- 900.0	1.00 10.00
<Reference>	-----	<Gas>		
0.000 mg	<Sampling>	n2	100.0 ml/min	
	1.0 sec	co2	100.0 ml/min	

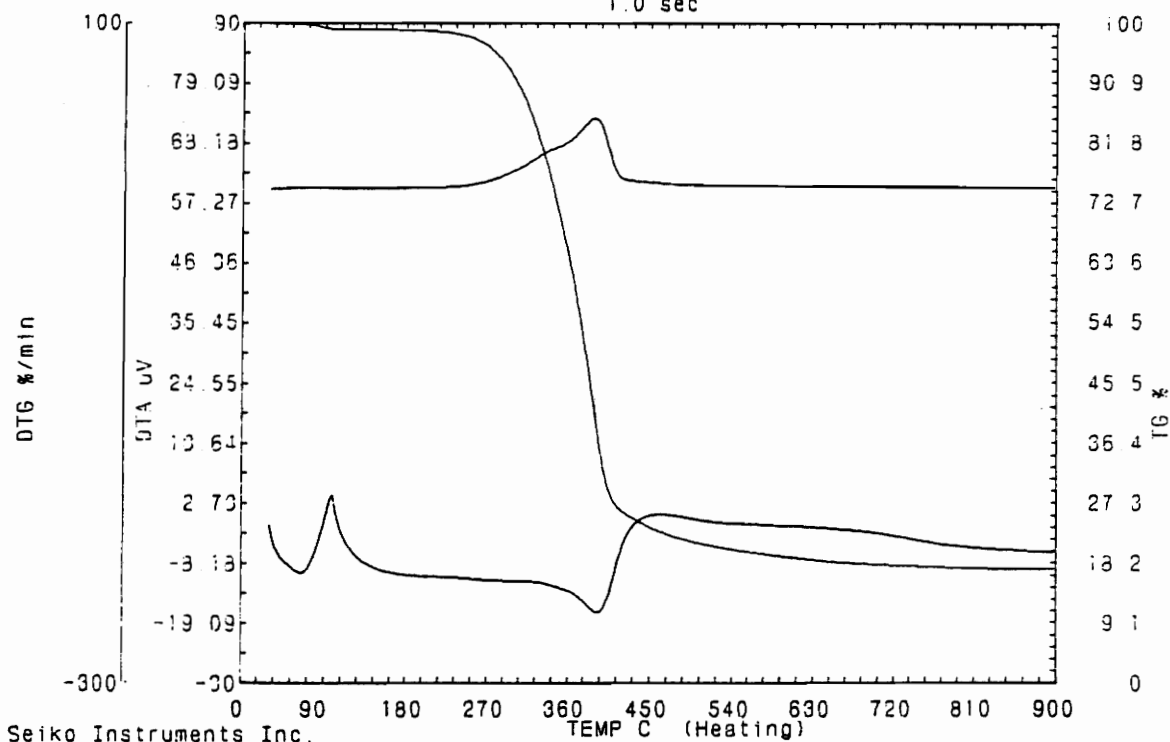


Figure 48. Pyrolysis of Monterey pine: (This study).

## Appendix F. Approximate Kinetic Analysis

This appendix presents the approximate kinetic analysis method used for comparison with the Coats-Redfern kinetic analysis method. The approximate method is derived from the Arrhenius equation as is the Coats-Redfern method. Starting with Equation 2.2.5, using a reaction order ( $n$ ) of one, and substituting  $\beta$  (the weight fraction of sample remaining at a particular temperature) for the expression  $(1 - \alpha)$  gives

$$-a \frac{d\beta}{dT} = A e^{-E/RT} \beta \quad [F.1]$$

Rearranging results in

$$- \frac{d \ln \beta}{dT} = \frac{A}{a} e^{-E/RT} \quad [F.2]$$

Taking the natural log of both sides,

$$\ln \left[ - \frac{d \ln \beta}{dT} \right] = - \frac{E}{RT} + \ln \left( \frac{A}{a} \right) \quad [F.3]$$

This results in an equation of the form  $y = mx + b$ . The derivative on the left-hand side of Equation F.3 can be approximated by

$$\ln \left[ - \frac{\Delta \ln \beta}{\Delta T} \right] \quad [F.4]$$

Taking the natural log of local slopes from a plot of  $\ln \beta$  versus temperature gives the  $y$  values and the inverse of the temperature ( $1/T$ , in Kelvins) gives the  $x$  values for two lines which have the same slope ( $m$ ) and  $y$ -intercept ( $b$ ). Subtracting the two linear equations and rearranging leaves the slope as the only unknown:

$$m = \frac{y_2 - y_1}{x_2 - x_1} \quad [F.5]$$

From Equation F.3, the slope is the negative activation energy ( $E$ ) divided by the universal gas constant ( $R = 8.315 \text{ kJ/kmole K}$ ), which can be rearranged to give the activation energy explicitly

$$E = - mR \quad [F.6]$$

From a plot of  $\beta$  versus temperature, two pairs of points two degrees apart, one set around  $\beta = 0.9$  and the other around  $\beta = 0.4$ , were selected. The natural log of each point was taken and then the slope between both pairs of points was found by

$$\frac{\ln \beta_2 - \ln \beta_1}{T_2 - T_1} \quad [F.7]$$

The natural log of the negative of these slopes gives the  $y$  values and the inverse of the average temperature between the points gives the  $x$  values used to find the slope ( $m$ ) of Equation F.5. This slope is then used to calculate the approximate apparent activation energy using Equation F.6. The apparent activation energies found using both the Coats-Redfern and the approximate method and the percentage difference are shown in Table 4.

**Table 4. Comparison of Apparent Activation Energies from Approximate and C-R Analysis Methods.**

Run #	E (kJ/mole)		% Change
	C-R	Approx.	
9	3410	531	-84
10	1667	966	-42
11	883	516	-42
13	562	140	-75
15	801	374	-53
16	670	370	-45
17	832	402	-52
18	721	179	-75
19	749	474	-37
20	753	353	-53
21	654	325	-50
22	769	315	-59
23	602	420	-30
24	681	354	-48
A1	1682	661	-61
A2	1658	1276	-23
A3	1764	1248	-29
A4	1793	1333	-26
		<b>Average</b>	<b>-49</b>

## Vita

Eric Victor Barner Albright was born in Lynchburg, Virginia on December 21, 1966. He lived in Iran, Pennsylvania, and Egypt (in that order), earning a high school diploma from Cairo American College in Ma'adi, Egypt in June 1984. Eric graduated with a Bachelor of Science degree in Mechanical Engineering from Virginia Polytechnic Institute and State University in May of 1989. He then continued his studies there in pursuit of a Master of Science degree in Mechanical Engineering. The degree was completed in June 1992.

*Eric V. B. Albright*